

THE EFFECT OF FLOW RATE, NEEDLE DESIGN, AND NEEDLE PLACEMENT ON  
APICAL PRESSURE AND IRRIGANT EXCHANGE IN AN *IN VITRO* TOOTH MODEL

by

Ellen Park

B.Sc. (Hons), The University of Toronto, 2002

DDS, The University of Western Ontario, 2006

A THESIS SUBMITTED IN PARTIAL FULFILLMENT OF

THE REQUIREMENTS FOR THE DEGREE OF

MASTER OF SCIENCE

in

THE FACULTY OF GRADUATE STUDIES

(Craniofacial Science)

THE UNIVERSITY OF BRITISH COLUMBIA

(Vancouver)

July 2012

© Ellen Park, 2012

## **Abstract**

Heavy irrigation forces in a root canal can lead to irrigant extrusion accidents, causing negative sequelae for patients. There are no guidelines for a safe and optimal irrigation flow rate and little data on the apical pressures generated during irrigation. This study aimed to measure the pressure generated during positive and negative pressure irrigation at the periapex of an *in vitro* tooth model using a novel method of measurement, investigating the effect of flow rate, depth of needle placement, and needle design. Apical pressure was correlated with extent of dye clearance from the end of a needle tip in a similar model. A mandibular molar was prepared and placed into a chamber coupled to a pressure transducer. Irrigation was performed using a digital peristaltic pump using flow rates from 1-15 ml/min with irrigation needles of different size and design. A similar plastic root canal model filled with dye was used to measure the extent of dye clearance beyond the needle tip using the same irrigation conditions.

Positive pressure irrigation revealed a flow rate dependent and depth of needle placement dependent increase in apical pressure ( $P < 0.05$ ). Needle designs with safety features yielded statistically significant lower apical pressures than needles without safety features ( $P < 0.05$ ).

There was no further increase in dye clearance from the end of the needle tip in a root canal model at flow rates higher than 4 ml/min. During negative pressure irrigation, no positive apical pressures were generated even when the needle was placed at 1 mm from working length while certain needle designs demonstrated superior clearance of dye.

Apical pressure is dependent upon flow rate, depth of needle placement, needle design, and positive or negative pressure irrigation. The apical pressure at high irrigation flow rates

can be several times higher than at low flow rates, yet there is no further clearance of dye above 4 ml/min. If apical clearance of dye beyond the needle tip is a measure of irrigation effectiveness, then maximum effectiveness can be gained at specifically determined flow rates using specific needle tip designs with safe apical pressures.

## **Preface**

All of the work presented in this thesis was performed by Dr. Ellen Park. The relative contribution of the collaborators in this project was: Dr. Ellen Park 60%, Dr. Markus Haapasalo 20%, Dr. Ya Shen 20%. UBC Clinical Research Ethics Board approval was obtained (H12-00745).

## Table of Contents

<b>Abstract .....</b>	<b>ii</b>
<b>Preface .....</b>	<b>iv</b>
<b>Table of Contents.....</b>	<b>v</b>
<b>List of Tables.....</b>	<b>vii</b>
<b>List of Figures .....</b>	<b>xi</b>
<b>List of Abbreviations.....</b>	<b>xiii</b>
<b>Acknowledgements .....</b>	<b>xiv</b>
<b>Dedication.....</b>	<b>xv</b>
<b>Chapter 1: Literature Review.....</b>	<b>1</b>
1.1 Introduction.....	1
1.2 Mechanical instrumentation.....	2
1.3 Endodontic irrigation.....	6
1.3.1 Irrigation research: 1970s .....	7
1.3.2 Irrigation research: 1980s and 1990s.....	9
1.3.3 Contemporary irrigation research.....	10
1.3.4 Fluid dynamics .....	11
1.3.5 Agitation during irrigation.....	13
1.3.6 Current irrigation recommendations.....	16
1.3.7 Positive pressure irrigation .....	16
1.3.8 Negative pressure irrigation.....	19
1.3.9 Apical pressure measurement .....	21

<b>Chapter 2: Rationale and Hypothesis</b> .....	<b>24</b>
<b>Chapter 3: Materials and Methods</b> .....	<b>25</b>
3.1 Dye clearance measurement .....	25
3.2 Apical pressure measurement .....	26
3.3 Statistical analysis.....	28
<b>Chapter 4: Results</b> .....	<b>33</b>
4.1 Dye clearance measurement using positive pressure irrigation.....	33
4.2 Dye clearance measurement using negative pressure irrigation.....	45
4.3 Apical pressure measurement using positive pressure irrigation.....	57
4.4 Apical pressure measurement using negative pressure irrigation.....	74
<b>Chapter 5: Discussion</b> .....	<b>89</b>
<b>Chapter 6: Conclusion</b> .....	<b>97</b>
<b>References</b> .....	<b>99</b>

## List of Tables

Table 4.1	Two-way ANOVA for dye clearance during PPI 5 mm from the apex using 5 different irrigation needle tips for flow rates 1 - 8 ml/min.....	37
Table 4.2	Two-way ANOVA for dye clearance during PPI 5 mm from the apex using 5 different irrigation needle tips for flow rates 1 - 4 ml/min.....	37
Table 4.3	Two-way ANOVA for dye clearance during PPI 5 mm from the apex using 5 different irrigation needle tips for flow rates 5 - 8 ml/min.....	37
Table 4.4	Two-way ANOVA for dye clearance during PPI 3 mm from the apex using 5 different irrigation needle tips for flow rates 1 - 8 ml/min.....	39
Table 4.5	Two-way ANOVA for dye clearance during PPI 3 mm from the apex using 5 different irrigation needle tips for flow rates 1 - 4 ml/min.....	39
Table 4.6	Two-way ANOVA for dye clearance during PPI 3 mm from the apex using 5 different irrigation needle tips for flow rates 5 - 8 ml/min.....	39
Table 4.7	Two-way ANOVA for dye clearance during PPI 5 mm and 3 mm from the apex with a 25 ga blunt open-ended (FlexiGlide) needle.....	40
Table 4.8	Two-way ANOVA for dye clearance during PPI 5 mm and 3 mm from the apex with a 30 ga blunt open-ended (FlexiGlide) needle.....	41
Table 4.9	Two-way ANOVA for dye clearance during PPI 5 mm and 3 mm from the apex with a 27 ga slotted open-ended (Monoject) needle.....	42
Table 4.10	Two-way ANOVA for dye clearance during PPI 5 mm and 3 mm from the apex with a 30 ga side-vented closed-ended (ProRinse) needle.....	43
Table 4.11	Two-way ANOVA for dye clearance during PPI 5 mm and 3 mm from the apex with an ISO 32 closed-ended needle with multiple perforations (EndoVac).....	44

Table 4.12	Two-way ANOVA for dye clearance during NPI 5 mm from the apex using 4 different irrigation needle tips (excludes 30 ga ProRinse) for 1 - 8 ml/min....	49
Table 4.13	Two-way ANOVA for dye clearance during NPI 5 mm from the apex using 2 different irrigation needle tips (25 ga, 30 ga FlexiGlide) for 1 - 4 ml/min.....	49
Table 4.14	Two-way ANOVA for dye clearance during NPI 5 mm from the apex using 2 different irrigation needle tips (25 ga, 30 ga FlexiGlide) for 4 - 8 ml/min.....	49
Table 4.15	Two-way ANOVA for dye clearance during NPI 3 mm from the apex using 4 different irrigation needle tips (excludes 30 ga ProRinse) for all flow rates...	51
Table 4.16	Two-way ANOVA for dye clearance during NPI 3 mm from the apex using 2 different irrigation needle tips (25 ga, 30 ga FlexiGlide) for 1 - 4 ml/min.....	51
Table 4.17	Two-way ANOVA for dye clearance during NPI 3 mm from the apex using 2 different irrigation needle tips (25 ga, 30 ga FlexiGlide) for 4 - 8 ml/min.....	51
Table 4.18	Two-way ANOVA for dye clearance during NPI 5 mm and 3 mm from the apex with a 25 ga blunt open-ended (FlexiGlide) needle.....	52
Table 4.19	Two-way ANOVA for dye clearance during NPI 5 mm and 3 mm from the apex with a 30 ga blunt open-ended (FlexiGlide) needle.....	53
Table 4.20	Two-way ANOVA for dye clearance during NPI 5 mm and 3 mm from the apex with a 27 ga slotted open-ended (Monoject) needle.....	54
Table 4.21	Two-way ANOVA for dye clearance during NPI 5 mm and 3 mm from the apex with a 30 ga side-vented closed-ended (ProRinse) needle.....	55
Table 4.22	Two-way ANOVA for dye clearance during NPI 5 mm and 3 mm from the apex with an ISO 32 closed-ended needle with multiple perforations (EndoVac).....	56
Table 4.23	Two-way ANOVA for apical pressure during PPI 5 mm from the apex with 25 ga FlexiGlide, 30 ga FlexiGlide, 27 ga Monoject, and 25 ga Max-I-Probe for the flow rate range 1 - 12 ml/min.....	61

Table 4.24	Two-way ANOVA for apical pressure during PPI 3 mm from the apex with 25 ga FlexiGlide, 30 ga FlexiGlide, 27 ga Monoject, and 25 ga Max-I-Probe for the flow rate range 1 - 12 ml/min.....	63
Table 4.25	Two-way ANOVA for apical pressure during PPI 1 mm from the apex for the flow rate range 1 - 8 ml/min.....	65
Table 4.26	Two-way ANOVA for apical pressure during PPI 5 mm and 3 mm from the apex with a 25 ga blunt open-ended (FlexiGlide) needle.....	66
Table 4.27	Two-way ANOVA for apical pressure during PPI 5 mm and 3 mm from the apex with a 25 ga side-vented closed-ended (Max-I-Probe) needle.....	67
Table 4.28	Two-way ANOVA for apical pressure during PPI 5 mm and 3 mm from the apex with a 27 ga slotted open-ended (Monoject) needle.....	68
Table 4.29	Two-way ANOVA for apical pressure during PPI 5 mm and 3 mm from the apex with a 27 ga side-vented closed-ended (VistaProbe) needle.....	69
Table 4.30	Two-way ANOVA for apical pressure during PPI 5 , 3, and 1 mm from the apex with a 30 ga side-vented closed-ended (ProRinse) needle.....	70
Table 4.31	Two-way ANOVA for apical pressure during PPI 5 , 3, and 1 mm from the apex with a 30 ga blunt open-ended (FlexiGlide) needle.....	72
Table 4.32	Two-way ANOVA for apical pressure during PPI 5, 3, and 1 mm from the apex with an ISO 32 EndoVac needle.....	73
Table 4.33	Two-way ANOVA for apical pressure during NPI 5 mm from the apex with 5 irrigation needles (excludes 30 ga ProRinse, 27 ga VistaProbe) for the flow rate range 1 - 9 ml/min.....	77
Table 4.34	Two-way ANOVA for apical pressure during NPI 3 mm from the apex with 5 irrigation needles (excludes 30 ga ProRinse, 27 ga VistaProbe) for the flow rate range 1 - 9 ml/min.....	79
Table 4.35	Two-way ANOVA for apical pressure during NPI 1 mm from the apex with 2 irrigation needles (excludes 30 ga ProRinse) for the flow rate range 1 - 9 ml/min .....	81

Table 4.36	Two-way ANOVA for apical pressure during NPI at 5 mm and 3 mm from the apex with a 25 ga blunt open-ended (FlexiGlide)needle.....	82
Table 4.37	Two-way ANOVA for apical pressure during NPI at 5 mm and 3 mm from the apex with a 25 ga side-vented closed-ended (Max-I-Probe) needle.....	83
Table 4.38	Two-way ANOVA for apical pressure during NPI at 5 mm and 3 mm from the apex with a 27 ga slotted open-ended (Monoject) needle.....	84
Table 4.39	Two-way ANOVA for apical pressure during NPI at 5 mm and 3 mm from the apex with a 27 ga side-vented closed-ended (VistaProbe) needle.....	85
Table 4.40	Two-way ANOVA for apical pressure during NPI at 5 mm and 3 mm from the apex with a 30 ga side-vented closed-ended (ProRinse) needle.....	86
Table 4.41	Two-way ANOVA for apical pressure during NPI at 5 mm, 3 mm, and 1 mm from the apex with a 30 ga blunt open-ended (FlexiGlide) needle.....	87
Table 4.42	Two-way ANOVA for apical pressure during NPI at 5 mm, 3 mm, and 1 mm from the apex with an ISO 32 EndoVac needle.....	88

## List of Figures

Figure 3.1	Irrigation needle types used.....	30
Figure 3.2	Radiograph and CBCT images of mandibular molar used in the study.....	31
Figure 3.3	Diagrammatic representation of dye clearance measurement set-up.....	32
Figure 3.4	Diagrammatic representation of apical pressure measurement set-up.....	32
Figure 4.1	Dye clearance during PPI at 5 mm from the apex.....	36
Figure 4.2	Dye clearance during PPI at 3 mm from the apex.....	38
Figure 4.3	Dye clearance during PPI with a 25 ga blunt open-ended needle.....	40
Figure 4.4	Dye clearance during PPI with a 30 ga blunt open-ended needle.....	41
Figure 4.5	Dye clearance during PPI with a 27 ga slotted open-ended needle.....	42
Figure 4.6	Dye clearance during PPI with a 30 ga side-vented closed-ended needle.....	43
Figure 4.7	Dye clearance during PPI with an ISO 32 EndoVac needle.....	44
Figure 4.8	Dye clearance during NPI at 5 mm from the apex.....	48
Figure 4.9	Dye clearance during NPI at 3 mm from the apex.....	50
Figure 4.10	Dye clearance during NPI with a 25 ga blunt open-ended needle.....	52
Figure 4.11	Dye clearance during NPI with a 30 ga blunt open-ended needle.....	53
Figure 4.12	Dye clearance during NPI with a 27 ga slotted open-ended needle.....	54
Figure 4.13	Dye clearance during NPI with a 30 ga side-vented closed-ended needle.....	55
Figure 4.14	Dye clearance during NPI with an ISO 32 EndoVac needle.....	56
Figure 4.15	Apical pressure during PPI at 5 mm from the apex.....	60
Figure 4.16	Apical pressure during PPI at 3 mm from the apex.....	62
Figure 4.17	Apical pressure during PPI at 1 mm from the apex.....	64

Figure 4.18	Apical pressure during PPI with a 25 ga blunt open-ended needle .....	66
Figure 4.19	Apical pressure during PPI with a 25 ga side-vented closed-ended needle.....	67
Figure 4.20	Apical pressure during PPI with a 27 ga slotted open-ended needle .....	68
Figure 4.21	Apical pressure during PPI with a 27 ga side-vented closed-ended needle .....	69
Figure 4.22	Apical pressure during PPI with a 30 ga side-vented closed-ended needle .....	70
Figure 4.23	Apical pressure during PPI with a 30 ga blunt open-ended needle .....	71
Figure 4.24	Apical pressure during PPI with an ISO 32 EndoVac needle.....	73
Figure 4.25	Apical pressure during NPI at 5 mm from the apex.....	76
Figure 4.26	Apical pressure during NPI at 3 mm from the apex.....	78
Figure 4.27	Apical pressure during NPI at 1 mm from the apex.....	80
Figure 4.28	Apical pressure during NPI with a 25 ga blunt open-ended needle .....	82
Figure 4.29	Apical pressure during NPI with a 25 ga side-vented closed-ended needle.....	83
Figure 4.30	Apical pressure during NPI with a 27 ga slotted open-ended needle.....	84
Figure 4.31	Apical pressure during NPI with a 27 ga side-vented closed-ended needle.....	85
Figure 4.32	Apical pressure during NPI with a 30 ga side-vented closed-ended needle.....	86
Figure 4.33	Apical pressure during NPI with a 30 ga blunt open-ended needle .....	87
Figure 4.34	Apical pressure during NPI with an ISO 32 EndoVac needle .....	88

## List of Abbreviations

CBCT.....	cone beam computed tomography
CFD.....	computational fluid dynamics
ga.....	gauge
NPI.....	negative pressure irrigation
PPI.....	positive pressure irrigation
ISO.....	International Organization for Standardization

## **Acknowledgements**

I am thankful to the faculty, staff and my fellow students at UBC, who have supported me and have become previous friends during my time of study. I offer my enduring gratitude to Dr. Markus Haapasalo and Dr. Ya Shen, who both model dedication, creativity, patience, and perseverance in research and teaching. It was often hard to believe I was doing research with giants in the endodontic community, because your encouragement, kindness, and humor are so unlike giants of fable lore, and more akin to the temperament of extraordinary friends.

I wish to thank Dr. Jeffrey Coil for his adventurous reflection and thoughtful feedback on all things related to endodontics. Your sense of curiosity, exploration, and duty toward education has colored our program with bold strokes of innovation, camaraderie, and great expectations. I consider you to be an exceptional mentor, and I am grateful to have been a part of the program with you at the helm.

I wish to thank my committee members for their valuable input on this study: Dr. Fernanda Almeida and Dr. Jeffrey Coil.

## **Dedication**

This dedication is for my parents, my brother, and my husband and his family, who have supported me throughout my education. I am humbled once and then humbled again by your love and care as each day passes, such that in every still and ordinary moment, halos of your strength course through the curtains, through the thread.

# **Chapter 1: Literature Review**

## **1.1 Introduction**

The challenge in achieving successful endodontic treatment lies in the variety of factors that impact upon a clinician's ability to reduce the bacterial load inside the complex root canal system to a threshold beyond which the number of bacterial cells is insufficient to sustain or induce apical periodontitis (Siqueira & Rôças, 2008). It is well established that bacteria are required for the development of periapical disease (Kakehashiet al., 1965; Bergenholtz, 1974). The precise number of bacterial cells remaining in the root canal system compatible with healing is not known but complete elimination of microbes is regarded as ideal. There is a positive correlation between a negative culture from the root canal before obturation and periapical healing; in a study of 55 patients, complete periapical healing occurred in 94% of patients with a negative culture before obturation, and healing in 68% of patients with a positive culture before obturation (Sjögren et al., 1997). The goal of endodontic treatment, then, is the removal of vital and necrotic pulp remnants, microorganisms, and microbial toxins primarily through mechanical preparation of the root canal through contemporary methods of instrumentation using hand and rotary files, and chemical disinfection, by means of copious irrigation (Haapasalo et al., 2010; Sirén et al., 2004). The combined process of mechanical preparation and chemical disinfection can be referred to as chemomechanical preparation, as both components are necessary for successful endodontic treatment and are generally performed together. However, they will be discussed separately, with a particularly in-depth literature review of contemporary methods of chemical disinfection.

## **1.2 Mechanical instrumentation**

Root canal shaping instruments have a relatively long history. With the first rotary endodontic handpiece for root canal treatment developed in 1889 and the first K-file introduced in 1915, the next several decades made significant improvements on these initial designs (Peters & Dummer, 2005). In addition to the hand instruments available for manual instrumentation, there are currently many engine-driven systems available for use, including conventional systems using rotation or reciprocal rotation, as well as sonic and ultrasonic systems. These systems have been widely researched in order to compare and improve the efficacy of mechanical debridement. The results of such studies have been ambivalent; one study reports manual instrumentation to result in superior canal enlargement, more planed walls, and less remaining pre-dentin and debris than with the use of sonic or ultrasonic instrumentation (Reynolds et al., 1987), while another study reports that ultrasonic instrumentation results in greater canal cleanliness than with sonic or hand instrumentation (Stamos et al., 1987).

The use of nickel-titanium in endodontics, first in the form of a hand file (Walia & Brantley, 1988) and subsequently used for many iterations of rotary file systems, is also a subject of comparative study for the purpose of improving mechanical debridement. Again, existing research remains inconclusive when comparing the mechanical debridement efficacy of different rotary file systems. Dalton et al. (1998) reported no advantage of rotary instrumentation over manual instrumentation with respect to reduction of intracanal bacteria; neither technique could predictably render the canal free of bacteria in this study but there was substantial bacterial reduction after instrumentation and irrigation with only saline.

Peters and Barbakow (2000) compared two different rotary instrument systems, and found that neither system was better in removing debris, but surmised that a larger canal preparation would result in greater canal cleanliness. In fact, several factors possibly influencing canal cleanliness aside from mechanical instrumentation have been put forward, such as apical size of instrumentation, canal length, irrigant volume, and depth of penetration of the irrigation needle (Usman et al., 2004).

The shortcoming of current rotary and hand instrumentation lies in the anatomical complexity of a root canal system. Canal morphology studies have revealed that root canals are rarely perfectly conical or straight, and have lateral canals, apical deltas, fins, webs, and transverse anastomoses which are part of the inherent variation of teeth (Vertucci, 1984).

Thus, uninstrumented recesses in oval canals of mandibular incisors can be present in up to 65% of teeth even after balanced force instrumentation of canals (Wesselink, 2001), and 65.2% - 74.4% of the apical 4 mm of the distal roots of mandibular molars can remain untouched by instruments after mechanical debridement has been completed (Paqué et al., 2010). In those root canal systems where mechanically prepared canals harbor areas where endodontic files have never touched, the solvent action of an irrigant such as sodium hypochlorite is effective in dissolving pulp tissue (Senia, Marshall, & Rosen, 1971) and in killing of bacteria (Rôças & Siqueira, 2011). Thus, the role of root canal instrumentation shifts from that of debridement to radicular access for irrigants (Gulabivala et al., 2005). Irrigation is thus an essential component of the chemomechanical removal of pulpal and dentinal debris, given the inability of metal instruments to directly plane the walls of complex root canals. It is important, then, for clinicians to be able to consistently deliver

irrigants to the full length of the root canal in order to achieve bacterial biofilm and debris removal. Mechanical instrumentation alone without any irrigation has been shown to result in 75% more debris in the canal than when irrigation is used (Baker et al., 1975). Dentin debris can also accumulate in isthmus areas, despite the use of irrigation, preventing sealer and filler material from entering this kind of anatomical irregularity and possibly allowing bacterial survival (Endal et al., 2011). With the advent of a new paradigm of instrument design, the self-adjusting file is one that adapts to the cross-section of a canal while simultaneously delivering irrigant through the file, and has been shown to result in better canal cleanliness and shaping than rotary files, leaving little canal surface uninstrumented in ovoid and irregularly shaped canals (Metzger et al., 2010; Peters et al., 2010). This appears to represent a great new advantage in mechanical instrumentation, but in addition to planing as much of the dentin wall as possible, chemical disinfection still remains an important component of root canal treatment, especially in the most apical portion of the root canal (Peters & Dummer, 2005).

Mechanical instrumentation coupled with saline as an irrigant has been shown to significantly reduce the number of bacteria in the root canal. Bystrom and Sundqvist (1981) studied the presence of bacteria in 17 single-rooted teeth with periapical lesions, which were irrigated with physiologic saline solution during instrumentation. Mechanical manual instrumentation reduced the number of bacteria from  $10^4 - 10^6$  bacterial cells to  $10^2 - 10^3$  fewer bacterial cells. Bacteria were not detected from the root canals of 8 teeth but bacteria persisted in 7 teeth despite treatment on five successive occasions. However, when an antimicrobial irrigant such as 0.5% sodium hypochlorite was used in place of saline, the

antibacterial effect was much more effective, with no recoverable bacteria in 12 out of 15 teeth after five appointments (Byström & Sundqvist, 1983). Neutral irrigants such as saline are not able to adequately debride canals free of pulp tissue, debris, or bacteria. Similarly, rotary instrumentation was able to significantly reduce the number of bacteria in an infected canal when irrigated with saline only (Dalton et al., 1998), but there was a significantly greater reduction of bacteria when rotary instrumentation was coupled with 1% sodium hypochlorite irrigation (Shuping et al., 2000). Even with sodium hypochlorite irrigation, it was reported from this study that it was impossible to render the canals consistently free of bacteria. This is supported by an *in vivo* study where root canal treatment was provided for sixteen patients with primary apical periodontitis (Nair et al., 2005). The apical portion of the root of each tooth was surgically removed and examined, the specimen prepared, and examined by transmission light microscopy. They found that 14 of the 16 specimens showed residual bacterial biofilm in the uninstrumented recesses of the root canal. Despite this glum fact, it is apparent that both instrumentation and irrigation are required to cause a significant decrease in the number of bacteria in a root canal. Just as mechanical instrumentation continues to see technological and ideological advancements such as with the self-adjusting file system, chemical disinfection has expanded into the field of irrigation fluid dynamics, which, coupled with the use and invention of effective irrigants, may translate to optimal irrigation conditions.

### **1.3 Endodontic irrigation**

This review of chemical disinfection will focus on the evolution of irrigation studies, fluid dynamics, techniques for delivery of irrigation and apical pressure measurement. For a review of specific irrigants and their properties, please see the excellent review by Haapasalo et al. (2010). In the late 19<sup>th</sup> century, Willoughby Dayton Miller published a paper describing the microflora of more than 250 infected pulps, thus making an association between bacterial and periapical disease; as a result, he was the first to recommend an aseptic approach to endodontic treatment (Sedgley, 2004). Studies such as this and the acceptance of the germ theory of disease during the 19<sup>th</sup> century influenced the development of endodontic irrigation. Heat cautery and destruction of the pulp through the use of explosive mixtures of potassium and sodium metal mixtures soon gave way to syringing of root canals with hydrogen peroxide in the early 20<sup>th</sup> century, as hydrogen peroxide was a known antiseptic (Sedgley, 2004).

However, Henry Drysdale Dakin apparently regarded hydrogen peroxide as an ineffective antiseptic, and had introduced the use of a dilute solution of sodium hypochlorite to treat the wounds of soldiers during World War I (Sedgley, 2004). It was subsequently shown in 1941 that chlorinated soda solution (sodium hypochlorite and sodium chloride mixture containing at least 5% of available chlorine) had the ability to dissolve human pulp tissue in less than two hours, which was much more effective and faster than other tested solutions, such as 30% hydrochloric acid and 20% sodium hydroxide (Grossman, 1982). The superior tissue dissolving capacity of 1% sodium hypochlorite has also been demonstrated in comparison to contemporary endodontic irrigants, such as 10% chlorhexidine, 30% hydrogen

peroxide, and 10% citric acid (Naenni et al., 2004). In addition, it has been shown that increased temperature, higher concentration, continuous agitation, and the inclusion of surfactant increases the tissue dissolving action of sodium hypochlorite (Stojicic, et al., 2010). The superior antibacterial efficacy of sodium hypochlorite has also been demonstrated in planktonic situations (Marshall & Rosen, 1970) and on bacteria in biofilm (Stojicic et al., 2011).

### **1.3.1 Irrigation research: 1970s**

Despite the efficacy of sodium hypochlorite on pulp tissue dissolution and bacterial killing, an early study published in 1971 investigating the solvent action of sodium hypochlorite described the presence of pulp tissue in the mesial canals of lower mandibular molars despite instrumentation and application of sodium hypochlorite for 15 minutes and 30 minutes, especially in the apical 1 mm and in the isthmuses (Senia et al., 1971). This paper went on to describe challenges and to identify variables in irrigation that still remain as challenges and variables to address today. The authors identified limited surface contact, volume of irrigation, and limited exchange of solution as factors that limit irrigation efficacy. The authors noted in particular the difficulty in exchanging solution in the limited space and confining geometry of the apical region of the root canal. Part of this difficulty is also attributed to the entrapment of air in the apical 0-2 mm of a pointed root canal, which is referred to as the vapor lock phenomenon (Tay et al., 2010). The authors also made reference to the inadequacy of the large irrigation needles available at the time and the method in which clinicians were accustomed to delivering irrigant - where irrigation needles seldom

entered the narrow canals, resulting in limited circulation of the irrigant (Senia et al., 1971). Similarly, other studies from this decade were focused on measuring the remaining debris in the canal after chemomechanical preparation with various concentrations of sodium hypochlorite, but there are scant details on the irrigation conditions used, such as depth of needle placement, flow rate, volume of irrigant used, time of irrigation application, taper of the preparation and apical preparation size. 23 gauge irrigation needles were commonly used, which are much larger than the needle sizes generally used for root canal irrigation today. The method of scoring remaining debris also varied, involving section microscopy, scanning electro microscopy, or chemical analysis. As a result, the results from these studies are inconclusive, and state that the use of sodium hypochlorite either results in less canal debris or no difference when compared with saline (Svec & Harrison, 1977; Trepagnier et al., 1977; Baker et al., 1975). However, one important result of the studies from the 1970s is the possible requirement for a minimum apical size in order for irrigant to be able to reach the most apical portion of the root canal. Salzgeber and Brilliant (1977) visualized the apical penetration of irrigant using radiography through the use of a radiopaque liquid in patients and concluded that an apical preparation ISO size of 30 (0.3 mm) was required for irrigant to reach the apical part of the root canal. Ram (1977), using a similar protocol in extracted teeth, concluded that an apical preparation ISO size of at least 40 (0.4 mm), and ideally, ISO size 60 (0.6 mm) was required in order to consistently irrigate the entire root canal; this study placed the irrigation needle in the coronal third of the root. This study also concluded that irrigating with more hand pressure did not substantially change the efficacy of irrigation; this was an important conclusion as one of the earliest cases of the negative sequelae when

injection sodium hypochlorite beyond the root apex was also published in this decade (Becker et al., 1974).

### **1.3.2 Irrigation research: 1980s and 1990s**

The studies of the 1970s were an important foundation for the studies of 1980s and 1990s. With the identification of factors limiting irrigation efficacy, the later studies started to provide greater detail such as the flow rate used or size of canal preparation, and investigated one or more of these factors using different study models. Abou-Rass and Piccinino (1982) used a radiographic method in extracted teeth to examine the efficacy of irrigation using four different irrigation methods. The main conclusions from this study was that in order for irrigation to be effective, the irrigation needle needed to be placed close to the apical region, and that a smaller gauge needle, such as a 30 gauge needle, was more effective than a larger gauge needle. One of the first studies to report the extent of flushing of irrigation beyond the needle tip used a standardized glass root canal and small particle beads ranging from 10 - 40  $\mu\text{m}$  in size, stained with ink (Chow, 1983). After irrigation, the remaining column of stained particles was measured. This study concluded that irrigation effectiveness was a function of the apical placement of the needle tip in the canal and the use of smaller needle sizes, and that larger canals were more effectively irrigated than smaller canals. These were similar conclusions to other studies published during this time (Kahn et al., 1995; Druttman & Stock, 1989). However, the interesting observation was made that there was very limited flushing or displacement of these particle beads beyond the needle tip, and this result would be a harbinger of future studies modelling irrigation fluid dynamics using computer software.

### **1.3.3 Contemporary irrigation research**

More contemporary studies of irrigation have examined the variables associated with irrigation efficiency, but unlike the irrigation studies of the previous decades, have used novel experimental models. One study used thermal image analysis to record the fluid dynamic distribution during irrigation in extracted teeth (Hsieh et al., 2007). They found that a size 27 gauge needle should be placed 3 mm from the apical stop in order to achieve successful irrigation when the canal was prepared to ISO size 30 (0.3 mm). When the needle tip was placed 6 mm from the apical stop, successful irrigation was seen only when the root canal was prepared to at least ISO size 50 (0.5 mm). So, this study demonstrated that irrigation was improved by apical placement of the needle tip and size of canal preparation. Another study confirmed that irrigation is affected by the depth of placement of the needle tip by using real-time imaging of bioluminescent bacteria inoculated into a root canal. Emission of bioluminescence was imaged before and after irrigation (Sedgley et al., 2005). The same technique was used to show that increased canal curvature negatively affected irrigation effectiveness (Nguy & Sedgley, 2006). A study by Huang et al. (2007) was able to rank the importance of different factors influencing the removal of a stained collagen bio-molecular film in extracted teeth. The collagen bio-molecular film thickness approximated the thickness of bacterial biofilm. The percentage of canal surface covered with stained collagen was quantified before and after irrigation. The authors found that, in order of decreasing priority, the depth of placement of the needle tip, the apical size and taper of the canal preparation, and the use of dynamic or static irrigation were factors influencing the removal of a collagen film in a root canal (Huang & Gulabivala, 2008).

What these studies demonstrate is that irrigation effectiveness is multi-factorial, and that efficacy can be measured through specific outcomes such as the dissolving ability of an irrigant, bacterial viability, or canal cleanliness, but it is difficult to delineate what the impact is of the flushing action of the irrigant inside the root canal, or any other factor, as they are difficult to singly isolate in a study. Taken as a whole, irrigation seems to be variably effective. Comparison of these different studies is also difficult due to the range in experimental models used and experimental conditions. It is unlikely that simply measuring the aforementioned study outcomes will help to determine exactly what processes enable effective irrigation. Thus, it becomes apparent that a greater understanding of fluid dynamics inside the root canal will aid and advance the purpose of irrigation.

#### **1.3.4 Fluid dynamics**

The application of engineering and physical science to endodontic irrigation is helping to understand the nature of the fluid flow field in the root canal system. Some techniques for this approach include scaled laboratory experiments, CFD and analytical modelling (Gulabivala et al., 2010).

These types of studies have confirmed the existence of a stagnation plane beyond which irrigant will not penetrate from the end of the needle tip. The further the stagnation plane is from the end of the needle tip is an indication of better irrigant penetration; ideally, one would want the stagnation plane to be coincident with the root apex. The presence of the stagnation plane has been shown in a previously described *ex vivo* study measuring the efficacy of replacing radioopaque solution in extracted teeth syringe irrigation

(Ram, 1977). It was found that the apical half of the radioopaque solution was undisturbed in small canals after irrigation. This phenomenon has been also shown through CFD modelling; it is of course beneficial to have *in vitro* or *ex vivo* studies validate the results of theoretical models. The results of one CFD analysis of fluid flow during endodontic irrigation by Gao et al. (2009) shows the existence of a 2.3 mm long cleared zone beyond the needle tip, beyond which is the “dead water” zone. The length of cleared zone as computed by CFD was shown to be dependent upon needle design also, with a notched, or slotted needle showing almost 3 mm of cleared zone beyond the needle tip, while a side-vented closed-ended needle demonstrated poorer penetration of irrigant (Shen et al., 2010). Another CFD study also identifies the limit of irrigant replacement beyond the needle tip as 1 - 1.5 mm, regardless of the flow rate used, which included very high, and possibly, clinically irrelevant, flow rates of over 15 ml/min (Boutsioukis et al., 2009). The distance of the stagnation plane from the end of the needle tip can also be predicted through distinct mathematical formulae, formulae which in turn depend on variables such as irrigant velocity, viscosity, and density. This kind of modelling is able to predict that flat open-ended needles are likely to have better irrigant penetration than closed-ended needle designs (Gulabivala et al., 2010). Thus, factors that are known mathematically to affect the calculation of the distance of the stagnation plane to the end of the needle tip such as flow rate and needle tip design can be investigated in order to minimize the existence of the stagnation plane.

The concept of the Reynolds number is particularly important, as it describes the ratio of inertial forces to viscous forces, and is again determined by a mathematical formula. A fluid flow with a low Reynolds number is characterized as being laminar, as it is dominated by

viscous forces. A fluid flow with a high Reynolds number is characterized as being turbulent, as the inertial forces dominate. It is known that the root canal represents a system with a low Reynolds number. This means that fluid moves very slowly against the canal walls, tending to be a laminar type of fluid flow (as opposed to chaotic and turbulent). As a result, in order to achieve irrigation replenishment, it is predicted that fresh irrigant would reach the walls largely through diffusion, requiring irrigation of approximately 100 times the volume of the root canal in order to achieve effective replenishment - clinically, this translates to using at least 1 mL of irrigant at clinically relevant flow rates (Gulabivala et al., 2010). It is hoped that understanding the principles of fluid dynamics as applied to root canal geometry through these models, such as the aforementioned examples, can translate into palpable objectives for root canal research such as devising needle tip designs or irrigation methods that would avoid the development of a stagnation plane, and establish clinically relevant guidelines for irrigation, such as the probable requirement for irrigation with at least 1 mL of irrigant in order to achieve effective replenishment.

### **1.3.5 Agitation during irrigation**

It should be mentioned that there are important irrigation technologies and methodologies that are able to overcome the limitations of laminar flow during conventional syringe irrigation - as mentioned in the previous sub-section, the limitations of syringe irrigation include the presence of the stagnation plane and concomitant difficulty in irrigant penetration, and the shortcomings of laminar flow in being able to exert shear stresses on the canals walls in order to flush out debris and bacterial biofilm (Gulabivala et al., 2010). An *in*

*vitro* radiographic study assessing the penetration of irrigant in mandibular molars with root curvature compared syringe irrigation and mechanical manual activation of the irrigant with a well-fitting gutta percha cone (Bronnec et al., 2010). The results showed that agitation of the irrigant using the gutta percha cone, specifically with three short vertical strokes with a 5 mm amplitude, resulted in 100% penetration of the irrigant in all samples. Although syringe irrigation showed very effective penetration, especially when the needle was placed at 3 mm from working length, complete replacement of the irrigant could not be achieved consistently. It is theorized that agitation using a well-fitting gutta percha cone is effective because it forces irrigant to be pushed down toward the apical region, and if the irrigant is not extruded into the periapical area, the irrigant moves back into the canal between the canal wall and the gutta percha cone, creating mixing (Gulabivala et al., 2010). So, agitation can be achieved in endodontics through manual vertical stroke motions with a well-fitting gutta percha cone as in the previous example, or sometimes an endodontic file. Another study also reports on the efficacy of the Endovage syringe, a syringe that automatically aspirates following irrigation, when pressure on the plunger is released; the results show that at the 1 mm level in the mesial roots of extracted molars, this system created superior canal cleanliness than other conventional syringe irrigation needles (Sinanan et al., 1983). Agitation of the irrigant is also achieved through the application of sonic and ultrasonic oscillations. The physical process behind the principle of using sonic and ultrasonic agitation is the phenomenon of acoustic micro-streaming. In one study, the streaming field was visualized under light microscope and direction of flow of the eddies intimately described, with smaller files exhibiting more rapid streaming, and an increase in power increasing the

size and velocity of the eddies (Ahmad & Ford, 1987). Ultrasonic agitation of irrigant has been shown to be much more effective than syringe irrigation with respect to irrigant flushing and penetration (Teplitsky et al., 1987) and also in debris removal from canals (Jiang et al., 2010) and narrow isthmuses (Susin et al., 2010). Ultrasonic activation was also shown to result in superior tissue dissolution in comparison to sonic activation in a simulated canal filled with necrotic bovine tissue (Al-Jadaa et al., 2009). In comparison to agitation of an irrigant with a K-file, gutta-percha, sonic activation, or a polymer rotary finishing file, ultrasonic activation resulted in greater penetration of irrigant into dentinal tubules, even at 1 mm from working length (Paragliola et al., 2010). In contrast, both sonic and ultrasonic activation were shown to allow better penetration of irrigant into lateral canals than syringe irrigation (de Gregorio et al., 2009), and also better smear layer removal in the apical third of a curved root canal (Blank-Gonçalves et al., 2011). In a multispecies biofilm model, sonic and ultrasonic activation of chlorhexidine irrigant containing wetting agents and surface modifiers was seen to cause a significantly higher bactericidal effect than in non-agitation conditions (Shen et al., 2011). However, the existing literature is inconclusive when it comes to comparing the irrigation efficacy of ultrasonic, sonic and syringe irrigation methods. For instance, there was no significant difference in the mean percentage of dye clearance after irrigation of plastic root canal models when comparing syringe, ultrasonic, and sonic irrigation methods (Kahn et al., 1995), and also no significant difference when comparing the same three irrigation methods for their antibacterial efficacy against *Enterococcus faecalis* in root canals (Tardivo et al., 2010). Some recent literature has found sonic activation to be more effective than ultrasonic activation in removing debris in instrumented and extracted

teeth at all levels in the canal (Kanter et al., 2011), while a newer method of irrigant agitation that is able to transfer pulsed laser energy to fluids, termed photon-initiated photoacoustic streaming, was significantly more effective in reducing bacterial counts in a root canal in comparison to ultrasonic activation (Peters et al., 2011). Despite the inconclusive nature of the existing literature on the comparative efficacy of different agitation methods, it becomes increasingly clear that irrigation optimization might require the use of supplementary methods of irrigation, for example, syringe irrigation in addition to agitation methods, in order to achieve optimal disinfection (Alves et al., 2011).

### **1.3.6 Current irrigation recommendations**

Current irrigation protocol recommendations, based on the body of research that is available and has been examined in the previous sections, suggest that clinicians should use a small gauge needle with a side vented or closed end design, and the needle should be placed 1 mm from working length or at least in the apical third (Zehnder, 2006; Boutsoukis et al., 2010b; Shen et al., 2010).

### **1.3.7 Positive pressure irrigation**

The most common way that irrigant has been introduced into the root canal has been through a needle connected to a syringe by a luer lock connection. Finger pressure is placed on the barrel of the syringe which pushes irrigant through the needle, and this is known as positive pressure irrigation. In terms of needle tip size, it is common to use 27 gauge and 30 gauge needles for endodontic irrigation. These needle sizes allow the needle a better opportunity to

deliver irrigant to the apex of the tooth with the current range of canal preparation sizes. Needle designs have been modified in an attempt to provide patient safety during treatment; needles that are open-ended have been discouraged for use due to the possible risk of irrigant extrusion past the root apex into the periapical region from the generation of high irrigation pressures (Gulabivala et al., 2010). A side-vented or closed-ended needle design is preferred in order to minimize safety risks, possibly by reducing any high pressures generated during irrigation and by deflecting the irrigant laterally, not toward the periapical region. It is theorized that high pressure or binding of the needle tip in the root canal leaving no pathway for the irrigant to exit the canal coronally may lead to the extrusion of irrigant (Hülsmann & Hahn, 2000). It is unknown to what extent a high irrigation flow rate contributes to such an accident. There is a lack of any evidence based guideline for what irrigation flow rate is the optimal flow rate to use during irrigation while maintaining patient safety. The available irrigation research uses a wide range of irrigation flow rates. When measuring the range of flow rates endodontists generate during the normal course of treatment, investigators found a very wide range, from 0.6 ml/min to 60 ml/min (Boutsioukis et al., 2007). The endodontists also delivered a significantly different volume of irrigant from each other, and placed significantly different pressures on the syringe barrel in comparison to each other. This is interesting information, as all of the variables studied in this particular paper are likely to impact upon the efficacy of irrigation, and despite any irrigation guideline that might exist, syringe irrigation is likely to be difficult to control from clinician to clinician. However, as new irrigation devices often involve a motorized pulp to deliver irrigant, an evidence-based recommendation for a safe and optimal irrigation flow rate becomes additionally important.

Although irrigants are routinely forced into the periapical region due to the piston-like motions of the instruments that are used (Brown et al., 1995), an accidental sodium hypochlorite extrusion accident results in the immediate development of extreme pain, as well as other signs such as hematoma and profuse hemorrhage from the canal (Hülsmann & Hahn, 2000). With proper management and patient assurance, healing from this type of event can be uneventful, however, there are reports of severe negative sequelae such as neurological complications, extensive necrosis and atrophy of tissues, and life threatening airway obstruction (Bowden et al., 2006; Witton et al., 2005). Sodium hypochlorite extrusion accidents do not seem to be a frequent occurrence, but a recent survey of diplomates of the American Board of Endodontics has revealed that 42% of respondents reported causing at least one sodium hypochlorite accident (Kleier et al., 2008). The respondents perception was that an open apex situation, wedging of the needle tip, or excessive syringe pressure was likely responsible for the occurrence of the extrusion accident.

Our desire for patient safety can seem at odds with the current recommendations for irrigation, especially with the apparent need for the needle tip to be placed within 1 mm of working length or at least in the apical third of the root canal and without any knowledge of the apical pressures generated when the needle is placed at this depth in the root canal.

However, our armamentarium for irrigation is not limited to positive pressure irrigation, and other irrigation modalities may represent an innovative way to ensure patient safety, yet achieve comparable disinfection.

### **1.3.8 Negative pressure irrigation**

A new technique of intracanal aspiration or apical negative pressure as a method of irrigation was first introduced in 2004, with publication by the same investigator in an English language journal in 2006 (Fukumoto et al., 2006). This technique addresses the limitations associated with positive pressure irrigation such as the difficulty in delivering and replenishing irrigant to all parts of the root canal, especially the apical third, due to limited space, gas entrapment, and also the safety issues that might occur when a needle is placed close to the root apex in trying to attempt effective delivery and replenishment. In this technique the irrigant was delivered into the root canal by tubing attached to a pump, positioned 12 mm from the root apex. Another needle was used for aspiration of the irrigant in the same root canal and was placed 2 mm and 4 mm short of the root end. Under the conditions of equal irrigation flow rate and volume, the investigators found that the intracanal aspiration technique removed smear layer more effectively than syringe irrigation, and produced limited extrusion of irrigant (Fukumoto et al., 2006).

This technique has been introduced to the commercial market as the EndoVac system (Schoeffel, 2007), and consists of a delivery tip which delivers irrigant into the pulp canal chamber, and a microcannula evacuation tip which is an ISO size 32 closed end metal needle with 12 small laterally positioned offset holes in 4 rows of 3. A larger plastic macrocannula tip has more recently become part of the system.

The ability of the EndoVac irrigation system to remove significantly more debris than conventional syringe irrigation has been reported in several studies. Some studies report no difference in debris removal at the 3 mm level but a significant difference at a 1 mm level

(Nielsen & Baumgartner, 2007; Siu & Baumgartner, 2010), while a different study reported significantly less debris at different levels in the root canal (Shin et al., 2010).

When comparing the EndoVac system to manual agitation using a well-fitting gutta percha cone in removal of debris in the isthmus region of mandibular molars, the EndoVac system removed more debris and produced cleaner canals (Susin et al., 2010). It is important to note that none of these studies reported the total removal of debris from canals.

The antimicrobial efficacy of the EndoVac system in comparison to conventional syringe irrigation and supplementary sonic agitation techniques has shown that these techniques are comparable and highly effective in bacterial reduction (Miller & Baumgartner, 2010; Brito et al., 2009). One study also reports the superior antimicrobial efficacy of the EndoVac system (Hockett et al., 2008), but these differences can be attributed to differences in bacterial sampling after irrigation.

The major benefit of the EndoVac system is the ability of apical negative pressure to prevent the apical extrusion of irrigant, even when placed very close to the root apex. This has been verified in several studies and tested in several different ways. In one study, agar was colored with a dye, and the amount of extrusion of irrigant evaluated by calculating the ratio of the area that had changed color due to contact with sodium hypochlorite to a standard area of evaluation (Fukumoto et al., 2006). In a similar study, the agar was colored with a chemical that reacts to a change in pH approximating the pH of sodium hypochlorite (Mitchell et al., 2011).

Finally, another study collected the volume of irrigant extruded during irrigation from the root end of teeth, and reported that the EndoVac microcannula and macrocannula did not

extrude any irrigant at all even when placed at full working length, in comparison to other techniques such as manual or ultrasonic activation (Desai & Himel, 2009). As an extension of the ability of apical negative pressure irrigation to prevent extrusion of irrigant yet deliver irrigant to full working length, one group has reported that the incidence of postoperative pain in patients where the EndoVac was used was significantly less than in those patients where conventional positive pressure syringe irrigation was used (Gondim et al., 2010). When assessing the ability of different irrigation techniques to deliver irrigant into simulated lateral canals, ultrasonic activation was superior in this aspect in comparison to sonic activation, EndoVac, and conventional syringe irrigation (de Gregorio et al., 2010). However, only EndoVac was able to deliver irrigant to full working length in all cases, while conventional syringe irrigation was not able to deliver irrigant to working length or penetrate any simulated canals in any number of extracted teeth. This particular study also reinforces the likely need for the synergistic use of several methods of irrigant delivery and activation in order to optimize disinfection.

### **1.3.9 Apical pressure measurement**

With the recent recommendations that irrigation needles should be placed approximately 1 mm from the working length, whether positive pressure or negative pressure irrigation methods are used, it becomes interesting to know what kind of apical pressures are generated when specific irrigation flow rates are used. As previously mentioned, clinicians use a wide range of irrigation flow rates, and commercial manufacturers of irrigation devices have started to recommend the use of specific flow rates with irrigation pump/delivery devices, yet

there is only very limited evidence for the apical pressures generated during irrigation at just a few selected flow rates. One *in vitro* study exists which measures the apical pressure at the end of a prepared root canal after delivering low pressure air at 5 p.s.i. - as if drying a canal - with various needle designs placed short of binding, and in a needle binding position (Bradford et al., 2002). The study concluded that when the needle was bound, higher pressures were registered. When the apical preparation size of the tooth was bigger, and when a larger gauge needle was used, higher apical air pressures were registered. Needle design had no apparent effect on apical air pressure. However, due to the wide variation seen in almost every group, the authors concluded that safety could not be assured when drying canals with pressurized air, and suggested that aspiration would be a safer way to dry root canals.

The other study method that has revealed some information on the apical pressures generated during irrigation are CFD studies. The published CFD studies are difficult to compare, as different simulated irrigation flow rates, a range of simulated needle designs and different canal preparation sizes were used. Also, the software algorithms used are potentially different. If we only compare similar needles, the apical pressure generated by a beveled needle tip at 3 mm from working length is reported to be 18 kPa by one group using a flow rate of 15.6 ml/min (Boutsioukis et al., 2010c), but 1.707 kPa by another group using an irrigation flow rate of 6 ml/min (Shen et al., 2010).

If we compare a side-vented closed end needle design, the apical pressure generated at 3 mm from working length is reported to be approximately 10 kPa by one group using a flow rate of 15.6 ml/min (Boutsioukis et al., 2010c), and 0.256 kPa by another group using a flow rate of 6 ml/min (Shen et al., 2010). These pressures differ by several orders of magnitude. In

order to compare the apical pressures reported to a reference point, although it may be premature to do so, one might choose average capillary pressure in the human body, which is 25 mmHg, or 3.3 kPa (Guyton and Hall, 2006).

To complement the existing research on conditions for irrigation efficacy, data on apical pressure during irrigation at a range of clinically relevant flow rates coupled with irrigant penetration studies for both positive pressure and negative pressure irrigation techniques would provide additional guidance for safe, yet effective irrigation flow rates.

## **Chapter 2: Rationale and Hypothesis**

A gap in the current body of research exists with respect to the most optimal and safe irrigation flow rate to use during endodontic treatment. This study aims to investigate optimal irrigation conditions by assessing the extent of irrigation replenishment that occurs in a clinically relevant range of flow rates. This study also aims to investigate safe irrigation characteristics by assessing the apical pressure generated by the irrigant using different needle designs and varying the needle placement in the root canal in a clinically relevant range of flow rates. The significant advantage in this study is the methodical use of incremental increases in irrigation flow rate.

During positive pressure irrigation, we hypothesize that the larger irrigation needle tips that lack modifications for patient safety, such as the blunt open-ended needles, will be able to achieve the greatest length of irrigant replenishment, yet will generate the highest apical pressures in the root canal. The corollary is that the smaller gauge needles with modifications for patient safety, such as the side-vented closed ended needle tips, may not replace irrigant to the same extent as the blunt open-ended needles, but will generate far less apical pressure in the root canal.

During negative pressure irrigation, we hypothesize that none of the irrigation needles will generate positive apical pressures, and that all of the needles will perform similarly with respect to the length of dye clearance, coinciding with the end of the needle tip. Thus, although positive pressure irrigation may place a patient's safety at some risk due to the generation of positive apical pressures, the efficacy of irrigation will be greater with positive pressure irrigation than with negative pressure irrigation, requiring the needle to be placed to the full extent of the canal for full efficacy during negative pressure irrigation.

## Chapter 3: Materials and Methods

### 3.1 Dye clearance measurement

A straight plastic root canal model (Dentsply Tulsa Dental, Tulsa, OK) was prepared to apical size 35 (0.35 mm), 6% taper (ProFile, Dentsply Tulsa Dental). A small, plastic cup-like reservoir for irrigant was affixed to the top of the plastic block using an epoxy resin to act as a chamber for the plastic root canal. After instrumentation and careful removal of any plastic debris within the prepared canal, crystal violet dye (BD Diagnostic Systems, Sparks, MD) was used to fill the canal, without air bubbles. Five irrigation needles were used (Figure 3.1):

- 25 gauge blunt open-ended needle with a flexible polyimide tubing tip (FlexiGlide, Vista Dental Products, Racine, WI)
- 30 gauge blunt open-ended needle with a flexible polyimide tubing tip (FlexiGlide, Vista Dental Products, Racine, WI)
- 27 gauge slotted open-ended needle (Monoject 471 Endodontic Irrigation Needle, Covidien, Mansfield, MA)
- 30 gauge side-vented closed-ended needle (ProRinse, Dentsply Tulsa Dental),
- ISO size 32 (0.32 mm) closed-ended needle with 12 laterally positioned offset holes within 0.7 mm of the needle tip (EndoVac microcannula, Discus Dental, Culver City, CA).

The needles were attached by a luer lock connection to 3-stop color-coded Tygon® ST tubing (Ismatec, Wertheim-Mondfeld, Germany) while the EndoVac needle was attached directly to 3-stop color-coded Tygon® ST tubing (Ismatec, Wertheim-Mondfeld, Germany) and secured in place with epoxy resin. A digital peristaltic pump (Reglo Digital MS-2/8, Ismatec,

Wertheim-Mondfeld, Germany) was used to deliver irrigant at precise flow rates.

The peristaltic pump was calibrated once at the start of the study with each irrigation needle to ensure accurate flow rate by measuring the weight of water delivered through the pump in a specified period of time, and the range of reproducible flow rates determined for each needle type. The needles were calibrated again with each set of irrigating conditions to ensure fidelity. A microscope (Global Surgical, St. Louis, MO) with a camcorder device (Sony HDR-XR520V, Tokyo, Japan) was used to record each irrigation sequence (Figure 3.3).

The plastic block was irrigated at 5 mm and 3 mm from the working length, and when possible without binding of the irrigation needle, 1 mm from the working length. The canal was irrigated for a minimum of 15 seconds at each flow rate and needle depth placement, using positive irrigation pressure, and subsequently, negative (aspiration) irrigation pressure by using the peristaltic pump in reverse mode. Each irrigation sequence was repeated in triplicate. A still image at the 10 second time point from each video was imported into ImageJ software (National Institute of Health, Bethesda, Maryland) for measurement of the length of dye cleared from the end of the irrigation needle; this was referred to as dye clearance. The numerical data was imported into a spreadsheet and statistical analysis performed.

### **3.2 Apical pressure measurement**

An extracted human mandibular molar with two separate mesial canals with independent apical foramina was chosen. The tooth was accessed and size 08 K-files were placed in the mesiobuccal and mesiolingual canals to confirm separate canal systems by radiographic

examination and cone beam computed tomography (CBCT) with 0.076 mm isotropic voxel size (Figure 3.2). The mesiobuccal canal of this mandibular molar was prepared to apical size 35 (0.35 mm) and 6% taper (ProFile, Dentsply Tulsa Dental) 1 mm short of the length at which an 08 K-file was seen under magnification at the apical foramen. The mesiolingual canal was uninstrumented. Copious irrigation with 3% sodium hypochlorite was used during instrumentation. Using a thin layer of nail varnish, the main mesiolingual and distal apical foramina were sealed in order to eliminate any effect of the presence of other foramina on apical pressure measurements. The mesiobuccal apical foramen remained patent. The tooth was placed into an air-tight custom fixture coupled to a pressure transducer (Endevco, San Juan Capistrano, CA). A strain gage signal conditioner (Vishay, Shelton, CT) connected to the pressure transducer relayed the pressure measurements to an oscilloscope (BK Precision, Yorba Linda, CA), providing 250 measurements per second (Figure 3.4).

Seven irrigation needles were used (Figure 3.1):

- 25 gauge blunt open-ended needle with a flexible polyimide tubing tip (FlexiGlide, Vista Dental Products)
- 30 gauge blunt open-ended needle with a flexible polyimide tubing tip (FlexiGlide, Vista Dental Products)
- 25 gauge side-vented closed-ended needle (Max-i-Probe, Dentsply Tulsa Dental)
- 27 gauge side-vented closed-ended needle (Vista-Probe, Vista Dental Products)
- 30 gauge side-vented closed-ended needle (ProRinse, Dentsply Tulsa Dental)
- 27 gauge slotted open-ended needle (Monoject 471 Endodontic Irrigation Needle, Covidien)

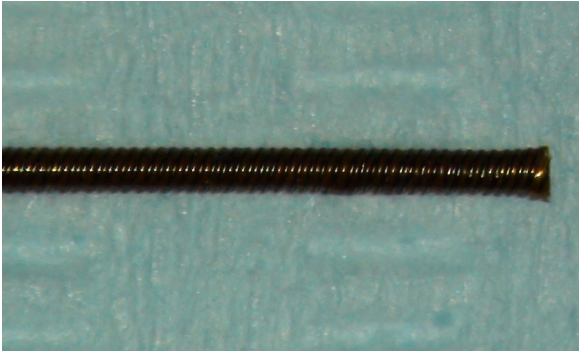
- ISO size 32 (0.32 mm) closed-ended needle with 12 laterally positioned offset holes within 0.7 mm of the needle tip (EndoVac microcannula, Discus Dental).

The needles were attached by a luer lock connection to 3-stop color-coded Tygon® ST tubing (Ismatec) while the EndoVac needle was attached directly to 3-stop color-coded Tygon® ST tubing (Ismatec) and secured in place with epoxy resin. A digital peristaltic pump (Reglo Digital MS-2/8, Ismatec) was used to deliver irrigant at precise flow rates. The peristaltic pump was calibrated once at the start of the study with each irrigation needle to ensure accurate flow rate by measuring the weight of water delivered through the pump in a specified period of time, and the range of reproducible flow rates determined for each needle type. The needles were calibrated again with each set of irrigating conditions to ensure fidelity. The mesiobuccal canal of the extracted mandibular molar was irrigated at 5 mm and 3 mm from the working length, and when possible without binding, 1 mm from the working length. The canal was irrigated for a minimum of 10 seconds at each flow rate and needle depth placement, using positive irrigation pressure, and subsequently, negative (aspiration) irrigation pressure by using the peristaltic pump in reverse mode. Each irrigation sequence was repeated in triplicate. The data from the oscilloscope was analyzed, and statistical analysis performed.

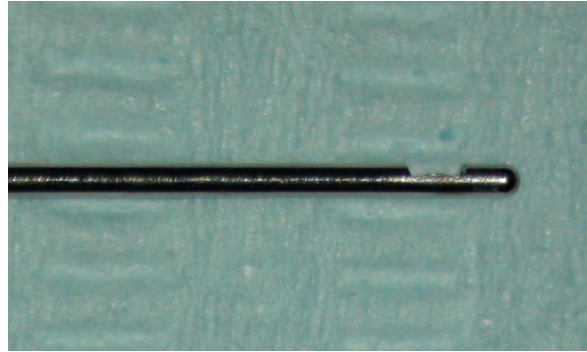
### **3.3 Statistical analysis**

Two-way ANOVA was used to determine the presence of any interaction between flow rate and needle design on the clearance of dye and apical pressure when comparing all or a selection of needle designs. Two-way ANOVA was also used to determine the presence of

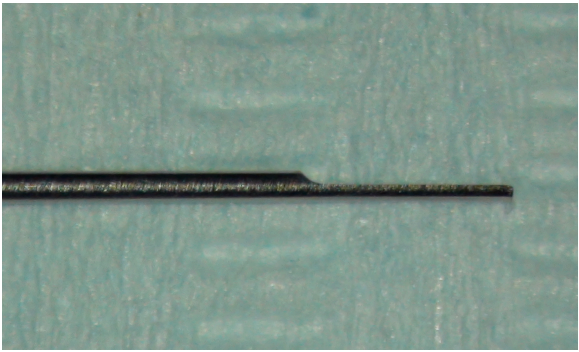
any interaction between flow rate and depth of needle placement on the clearance of dye and apical pressure when examining one needle design at a time. If the interaction from any two-way ANOVA analysis was statistically significant, a post hoc Bonferroni test was used. Subsequent two-way ANOVA analyses were performed on subgroups of the data set in order to investigate conditions for interaction. The P value threshold was  $P < 0.05$  for two-way ANOVA and post hoc Bonferroni analysis. Two-way ANOVA results are reported in table format for the majority of the data groups, but are omitted from the report in certain instances where the post hoc Bonferroni tests are reported in lieu. The results of post hoc Bonferroni analyses are shown graphically for the majority of results, and omitted where identification of statistical significance did not impact upon the importance of the overall study goals.



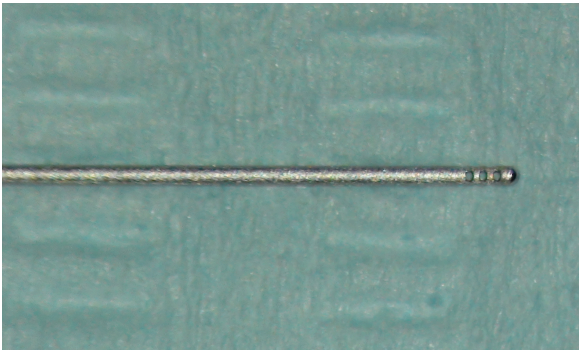
A. Blunt open-ended needle



B. Closed-ended side-vented needle



C. Open-ended slot tipped needle

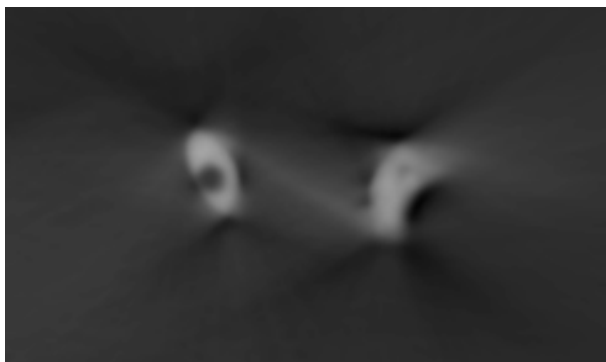
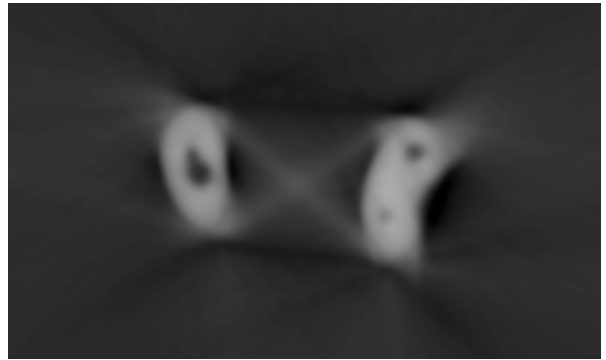
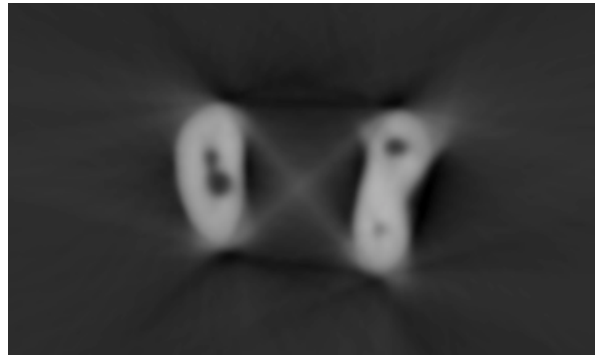


D. Closed-ended needle with 12 laterally positioned offset holes in the distal 0.7 mm

**Figure 3.1** A) Blunt open-ended needle (FlexiGlide) B) Side-vented closed-ended needle (ProRinse, Max-i-Probe) C) Slotted open-ended needle (Monoject) D) ISO 32 closed-ended needle with 12 laterally positioned offset holes in the distal 0.7mm (EndoVac).



**A.**



**B.**

**Figure 3.2** Radiograph (A) and CBCT images (B) from the mandibular molar used showing separate mesiobuccal (top right hand corner of image) and mesiolingual canals.

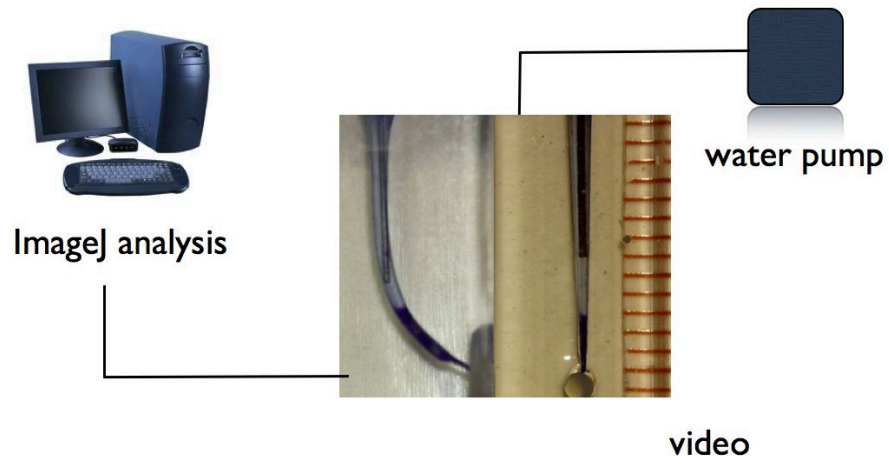


**Figure 3.3** Diagrammatic representation of dye clearance measurement set-up

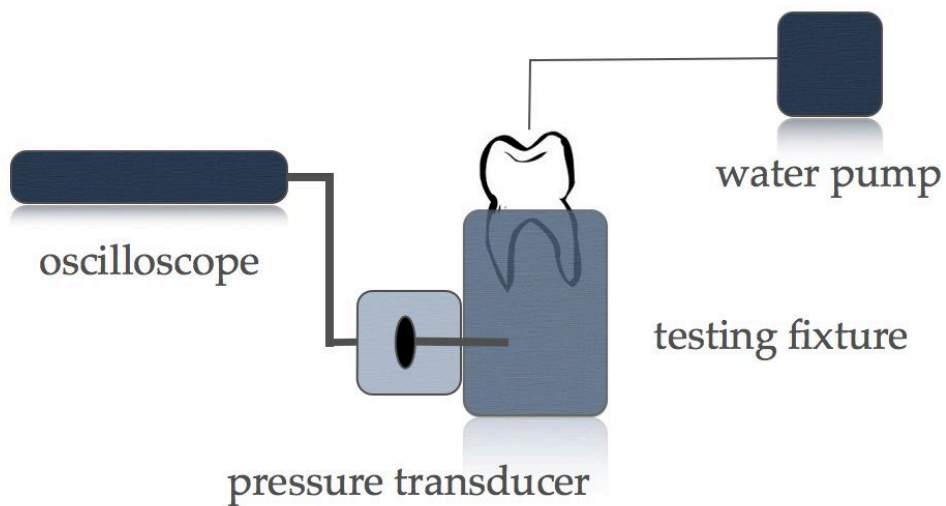


**Figure 3.4** Diagrammatic representation of apical pressure measurement set-up

## Chapter 4: Results

### 4.1 Dye clearance measurement using positive pressure irrigation

When measuring the clearance of dye beyond the end of the needle tip at 5 mm and 3 mm from the working length (Figure 4.1, 4.2), all five needles used showed a flow rate dependent increase in the length of dye cleared during irrigation that plateaued at flow rates beyond 4 ml/min. During positive pressure irrigation at 5 mm from the apex with all five needles (Figure 4.1), two-way ANOVA revealed significant interaction ( $P < 0.05$ ) (Table 4.1). The Bonferroni post hoc test demonstrated that the EndoVac microcannula cleared statistically significantly ( $P < 0.05$ ) less dye than all other needles at all flow rates, the 30 ga blunt open-ended (FlexiGlide) needle cleared more dye than the 30 ga side-vented closed-ended (ProRinse) needle ( $P < 0.05$ ), and the 27 ga slotted open-ended (Monoject) needle cleared more dye than the 25 ga blunt open-ended (FlexiGlide) needle ( $P < 0.05$ ) (Figure 4.1). Visual inspection of figure 4.1 showed interaction in the flow rate range of 1 - 4 ml/min, and a plateau in the length of dye cleared during irrigation beyond 4 ml/min. Thus, two-way ANOVA was repeated for two separate subsets of data: for all needles in the flow rate range of 1 - 4 ml/min (Table 4.2), and for all needles in the flow rate range of 5 - 8 ml/min (Table 4.3). Two-way ANOVA for data in the flow rate range of 1 - 4 ml/min showed significant interaction ( $P < 0.05$ ) as expected, with needle design comprising 52.91% of the total variance, and flow rate comprising 26.81% of the total variance. The effect of the needle design and flow rate were also statistically significant ( $P < 0.05$ ). Two-way ANOVA for data in the flow rate range of 5 - 8 ml/min showed significant interaction ( $P < 0.05$ ), with needle design comprising 93.21% of the total variance, and flow rate comprising 0.55% of the total

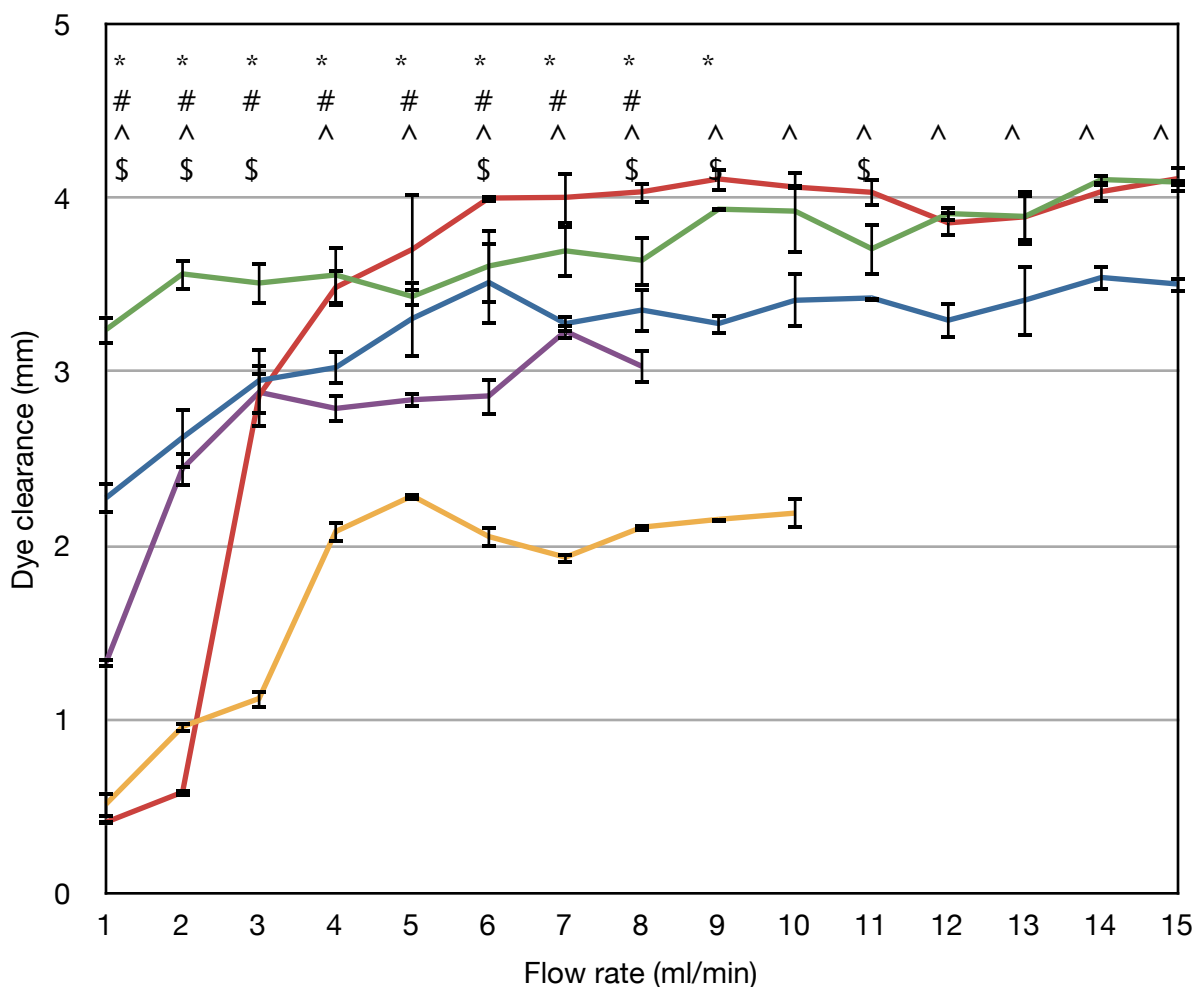
variance. Flow rate was not a significant source of variation in the flow rate range from 4 - 8 ml/min ( $P>0.05$ ).

During positive pressure irrigation at 3 mm from the apex with all five needles (Figure 4.2), two-way ANOVA revealed significant interaction ( $P<0.05$ ) (Table 4.4). The Bonferroni post hoc test demonstrated that the EndoVac microcannula cleared statistically significantly ( $P<0.05$ ) less dye than all other needles at all flow rates, the 30 ga blunt open-ended (FlexiGlide) needle cleared more dye than the 25 ga blunt open-ended (FlexiGlide) needle ( $P<0.05$ ), and the 27 ga slotted open-ended (Monoject) needle cleared more dye than the 25 ga blunt open-ended (FlexiGlide) needle ( $P<0.05$ ) (Figure 4.2). Visual inspection of figure 4.2 showed interaction in the flow rate range of 1 - 4 ml/min, and a plateau in the length of dye cleared during irrigation beyond 4 ml/min. Thus, two-way ANOVA was repeated for two separate subsets of data: for all needles in the flow rate range of 1 - 4 ml/min (Table 4.5), and for all needles in the flow rate range of 5 - 8 ml/min (Table 4.6). Two-way ANOVA for data in the flow rate range of 1 - 4 ml/min showed significant interaction ( $P<0.05$ ) as expected, with needle design comprising 61.51% of the total variance, and flow rate comprising 29.24% of the total variance. The effect of the needle design and flow rate were also statistically significant ( $P<0.05$ ). Two-way ANOVA for data in the flow rate range of 5 - 8 ml/min showed significant interaction ( $P<0.05$ ), with needle design comprising 91.85% of the total variance, and flow rate comprising 3.84% of the total variance. Flow rate was not a significant source of variation in the flow rate range from 5 - 8 ml/min.

For each individual needle except the 25 ga blunt open-ended (FlexiGlide) needle, two-way ANOVA revealed significant ( $P<0.05$ ) interaction for the independent variables depth of

placement of needle in the canal, and flow rate (Table 4.7 - 4.11). For the 25 ga blunt open-ended (FlexiGlide) needle, there was no significant interaction ( $P>0.05$ ) between the two independent variables, depth of needle placement, and flow rate. There was a statistically significant difference ( $P<0.05$ ) for all needles in the length of dye clearance when the needle was placed at 5 mm from working length and 3 mm from working length. For each individual needle, more length of dye was cleared when the needle was placed at 5 mm from working length. At both depths of needle placement the EndoVac microcannula cleared significantly less dye from the end of the needle tip than all other needle types used ( $P<0.05$ ). When the remaining four needle tips were placed at 5 mm from working length, approximately 3-4 mm of dye was cleared beyond the end of each needle tip at flow rates over 4 ml/min. When the remaining four needles were placed at 3 mm from working length, approximately 2-3 mm of dye was cleared from the end of the needle tip at flow rates beyond 4 ml/min. The ranking of needles from most effective to least effective in clearance of dye beyond the needle tip during positive pressure irrigation when placed at 5 mm and 3 mm from working length is: 30 ga blunt open-ended needle (FlexiGlide), 27 ga slotted open-ended needle (Monoject) > 25 ga blunt open-ended needle (FlexiGlide), 30 ga side-vented closed-ended needle (ProRinse) > ISO 32 EndoVac needle.

### Dye Clearance during PPI at 5 mm from the apex



- 25 ga blunt open-ended needle (FlexiGlide)
- 30 ga blunt open-ended needle (FlexiGlide)
- ISO size 32 closed-ended needle with 12 laterally positioned holes (EndoVac)
- 27 ga slotted open-ended needle (Monoject)
- 30 ga side-vented closed-ended needle (ProRinse)

\* statistically significant ( $P < 0.05$ ) difference between EndoVac and all other needle types (exception: 27 ga Monoject vs EndoVac at 1 ml/min)  
 # statistically significant ( $P < 0.05$ ) difference between 30 ga FlexiGlide and 30 ga ProRinse  
 ^ statistically significant ( $P < 0.05$ ) difference between 25 ga FlexiGlide and 27 ga Monoject  
 \$ statistically significant ( $P < 0.05$ ) difference between 30 ga FlexiGlide and 27 ga Monoject

**Figure 4.1 Dye clearance measurement during positive pressure irrigation at 5 mm from the apex using 5 different irrigation needle tips**

Source	df	Sum of Squares	Mean Square	F	Sig.	% of total variation
interaction	28	27.27	0.9740	59.00	<0.0001	23.10
needle	4	47.27	11.82	715.8	<0.0001	40.04
flow rate	7	42.19	6.027	365.0	<0.0001	35.74
error	80	1.321	0.01651			

**Table 4.1 Two-way ANOVA for dye clearance during PPI 5 mm from the apex using 5 different irrigation needle tips for all flow rates (1 - 8 ml/min)**

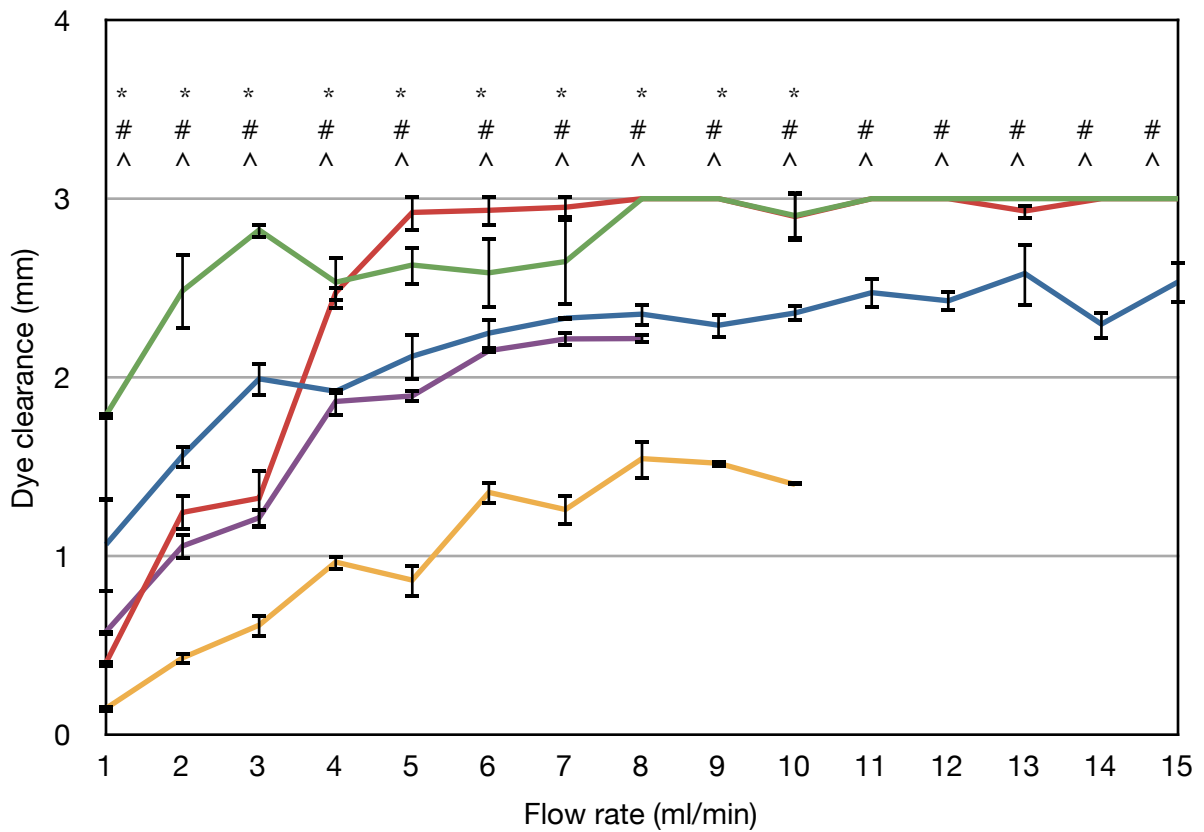
Source	df	Sum of Squares	Mean Square	F	Sig.	% of total variation
interaction	12	13.43	1.119	87.79	<0.0001	19.49
needle	4	36.46	9.114	715.0	<0.0001	52.91
flow rate	3	18.51	6.171	484.1	<0.0001	26.87
error	40	0.5099	0.01275			

**Table 4.2 Two-way ANOVA for dye clearance during PPI 5 mm from the apex using 5 different irrigation needle tips for flow rate range 1 - 4 ml/min**

Source	df	Sum of Squares	Mean Square	F	Sig.	% of total variation
interaction	12	0.7866	0.06555	3.234	0.0026	3.07
needle	4	23.87	5.967	294.3	<0.0001	93.21
flow rate	3	0.1403	0.04676	2.306	0.0913	0.55
error	40	0.8109	0.02027			

**Table 4.3 Two-way ANOVA for dye clearance during PPI 5 mm from the apex using 5 different irrigation needle tips for flow rate range 5 - 8 ml/min**

### Dye Clearance during PPI at 3 mm from the apex



- 25 ga blunt open-ended needle (FlexiGlide)
- 30 ga blunt open-ended needle (FlexiGlide)
- ISO size 32 closed-ended needle with 12 laterally positioned holes (EndoVac)
- 27 ga slotted open-ended needle (Monoject)
- 30 ga side-vented closed-ended needle (ProRinse)

\* statistically significant ( $P < 0.05$ ) difference between EndoVac and all other needle types  
 # statistically significant ( $P < 0.05$ ) difference between 30 ga FlexiGlide and 25 ga FlexiGlide  
 ^ statistically significant ( $P < 0.05$ ) difference between 27 ga Monoject and 25 ga FlexiGlide

**Figure 4.2** Dye clearance measurement during positive pressure irrigation at 3 mm from the apex using 5 different irrigation needle tips

Source	df	Sum of Squares	Mean Square	F	Sig.	% of total variation
interaction	28	8.924	0.3187	28.27	<0.0001	11.20
needle	4	37.37	9.342	828.7	<0.0001	46.89
flow rate	7	32.50	4.642	411.8	<0.0001	40.78
error	80	0.9019	0.01127			

**Table 4.4 Two-way ANOVA for dye clearance during PPI 3 mm from the apex using 5 different irrigation needle tips for all flow rates (1 - 8 ml/min)**

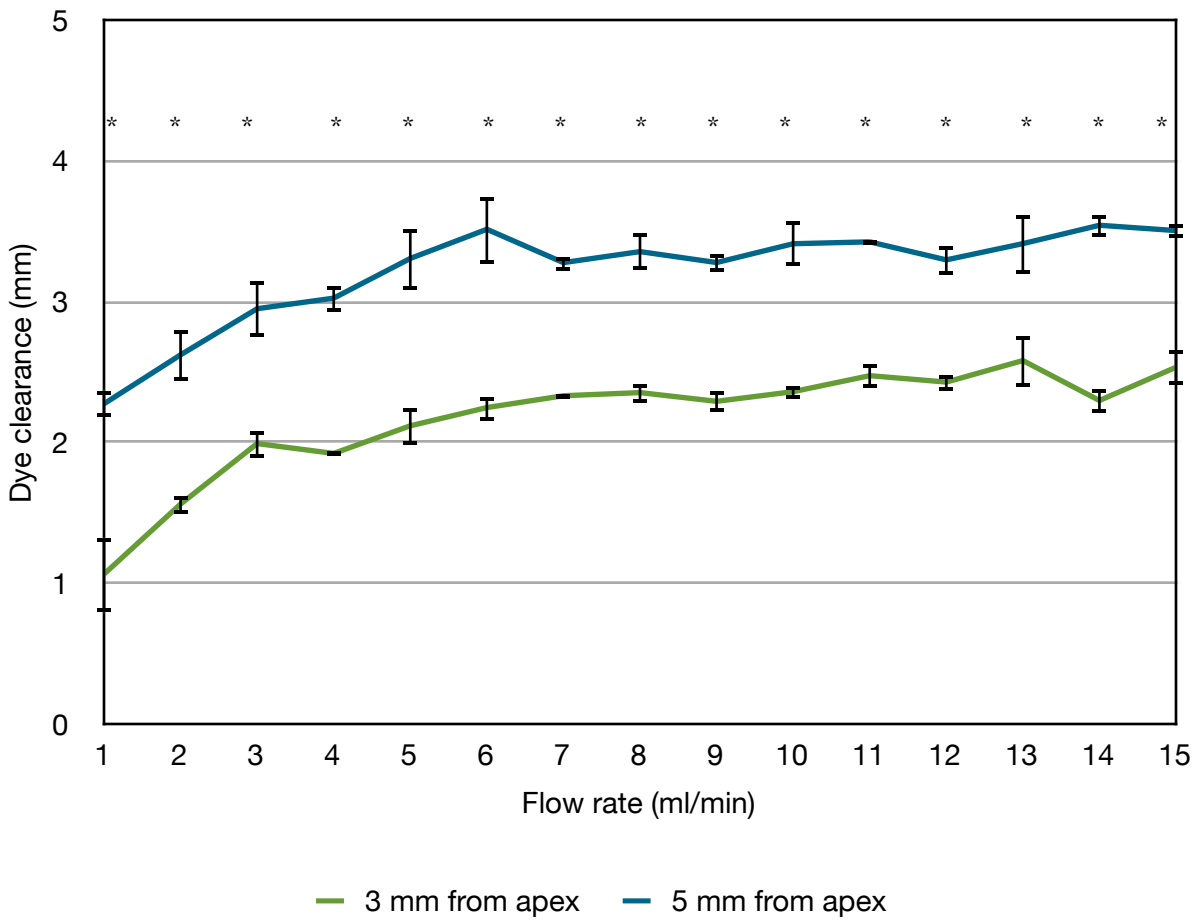
Source	df	Sum of Squares	Mean Square	F	Sig.	% of total variation
interaction	12	2.885	0.2404	20.53	<0.0001	7.95
needle	4	22.31	5.578	476.4	<0.0001	61.51
flow rate	3	3.546	3.536	302.0	<0.0001	29.24
error	40	0.01171	0.4684			

**Table 4.5 Two-way ANOVA for dye clearance during PPI 3 mm from the apex using 5 different irrigation needle tips for flow rate range 1 - 4 ml/min**

Source	df	Sum of Squares	Mean Square	F	Sig.	% of total variation
interaction	12	0.5308	0.04423	4.081	0.0004	2.37
needle	4	20.57	5.141	474.4	<0.0001	91.85
flow rate	3	0.8598	0.2866	26.44	<0.0001	3.84
error	40	0.4335	0.01084			

**Table 4.6 Two-way ANOVA for dye clearance during PPI 3 mm from the apex using 5 different irrigation needle tips for flow rate range 5 - 8 ml/min**

**Dye clearance during PPI with a 25 ga blunt open-ended needle**



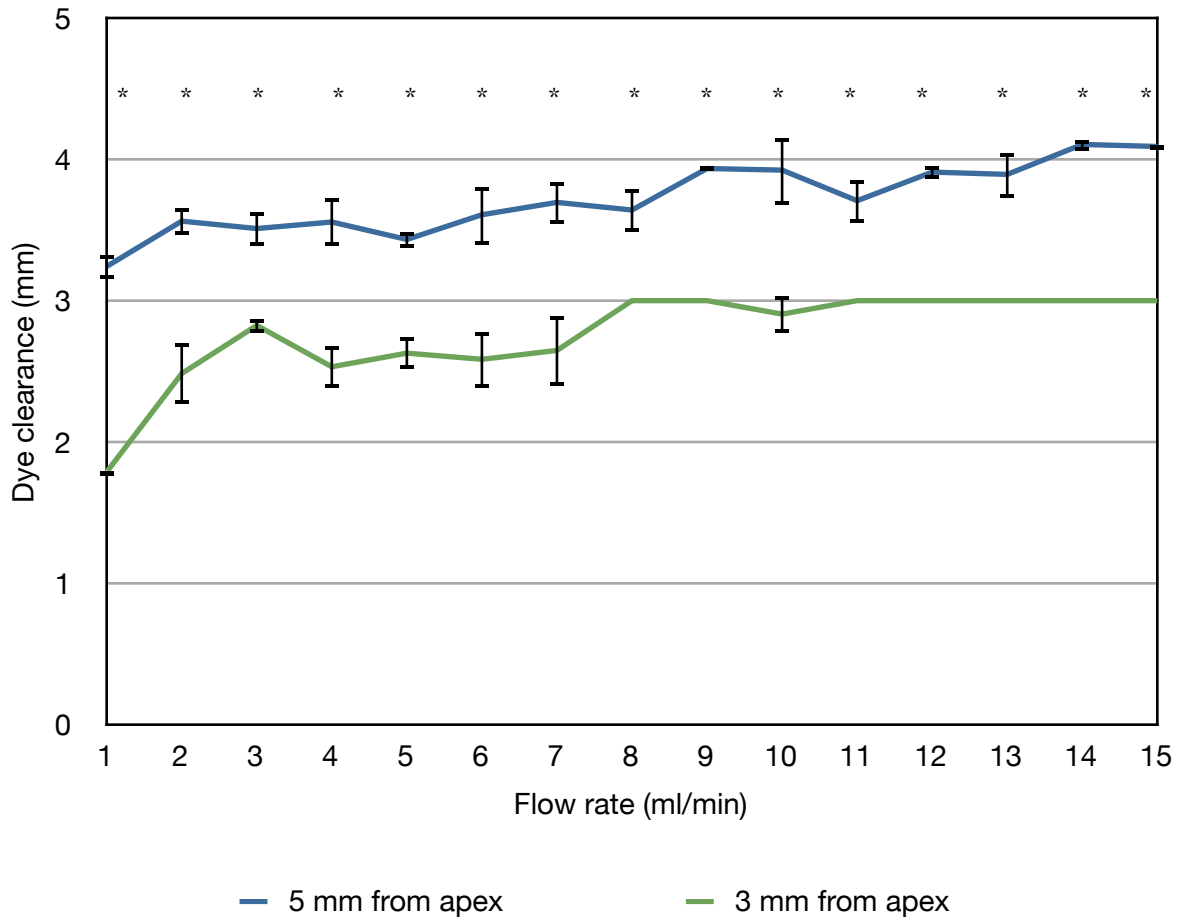
\* statistically significant (P<0.05) difference between placement at 5 mm and 3 mm

**Figure 4.3 Dye clearance during positive pressure irrigation with a 25 ga blunt open-ended (FlexiGlide) needle at 5 mm and 3 mm from the apex**

Source	df	Sum of Squares	Mean Square	F	Sig.	% of total variation
interaction	14	0.3822	0.02730	1.567	0.1157	1.01
depth	1	24.44	24.44	1403	<0.0001	64.84
flow rate	14	11.63	0.8446	48.49	<0.0001	31.38
error	60	1.045	0.01742			

**Table 4.7 Two-way ANOVA for dye clearance during PPI 5 mm and 3 mm from the apex with a 25 ga blunt open-ended (FlexiGlide) needle**

**Dye clearance during PPI with a 30 ga blunt open-ended needle**



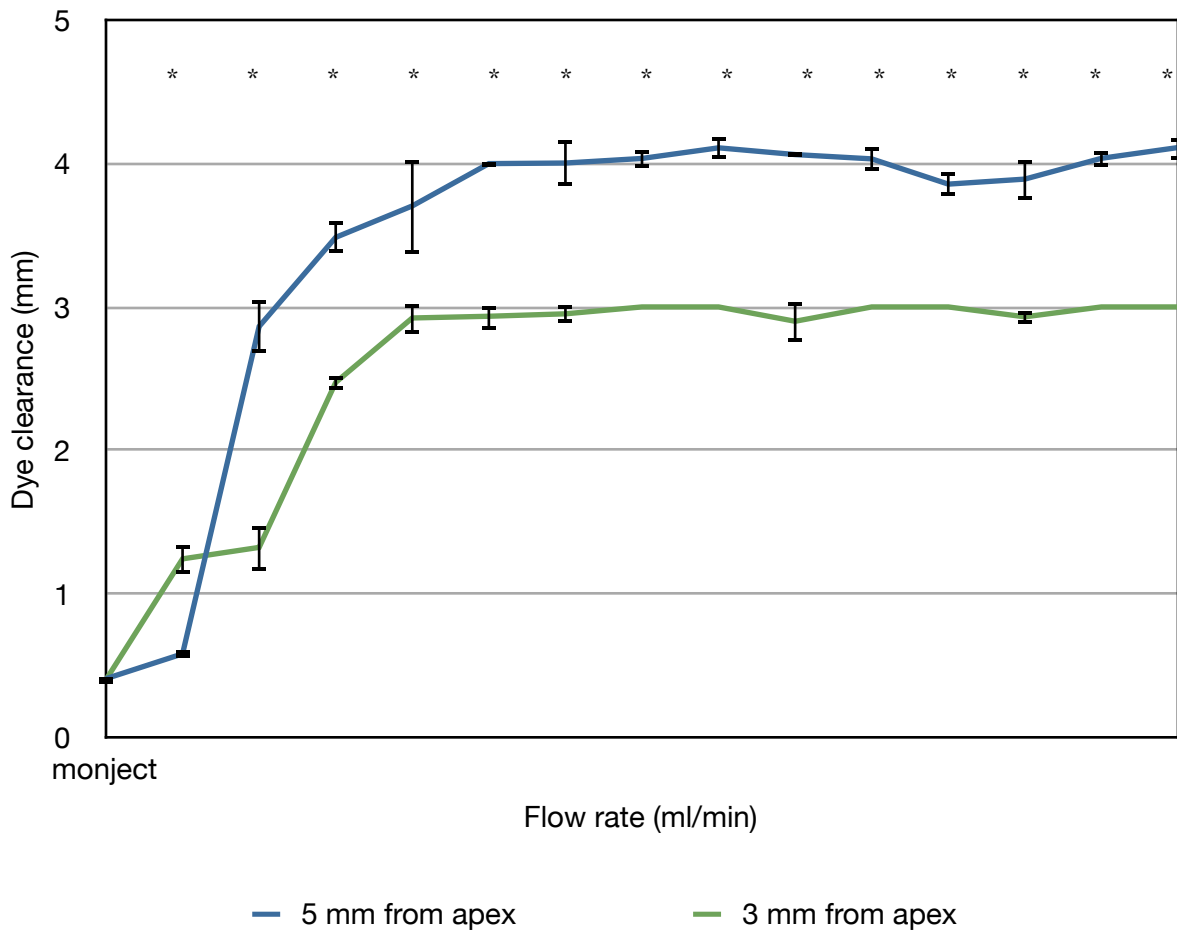
\* statistically significant ( $P < 0.05$ ) difference between placement at 5 mm and 3 mm

**Figure 4.4** Dye clearance during positive pressure irrigation with a 30 ga blunt open-ended (FlexiGlide) needle at 5 mm and 3 mm from the apex

Source	df	Sum of Squares	Mean Square	F	Sig.	% of total variation
interaction	14	0.8819	0.06300	3.884	0.0001	3.04
depth	1	20.79	20.79	1282	<0.0001	71.58
flow rate	14	6.399	0.4571	28.18	<0.0001	22.03
error	60	0.9730	0.01622			

**Table 4.8** Two-way ANOVA for dye clearance during PPI 5 mm and 3 mm from the apex with a 30 ga blunt open-ended (FlexiGlide) needle

### Dye clearance during PPI with a 27 ga slotted open-ended needle



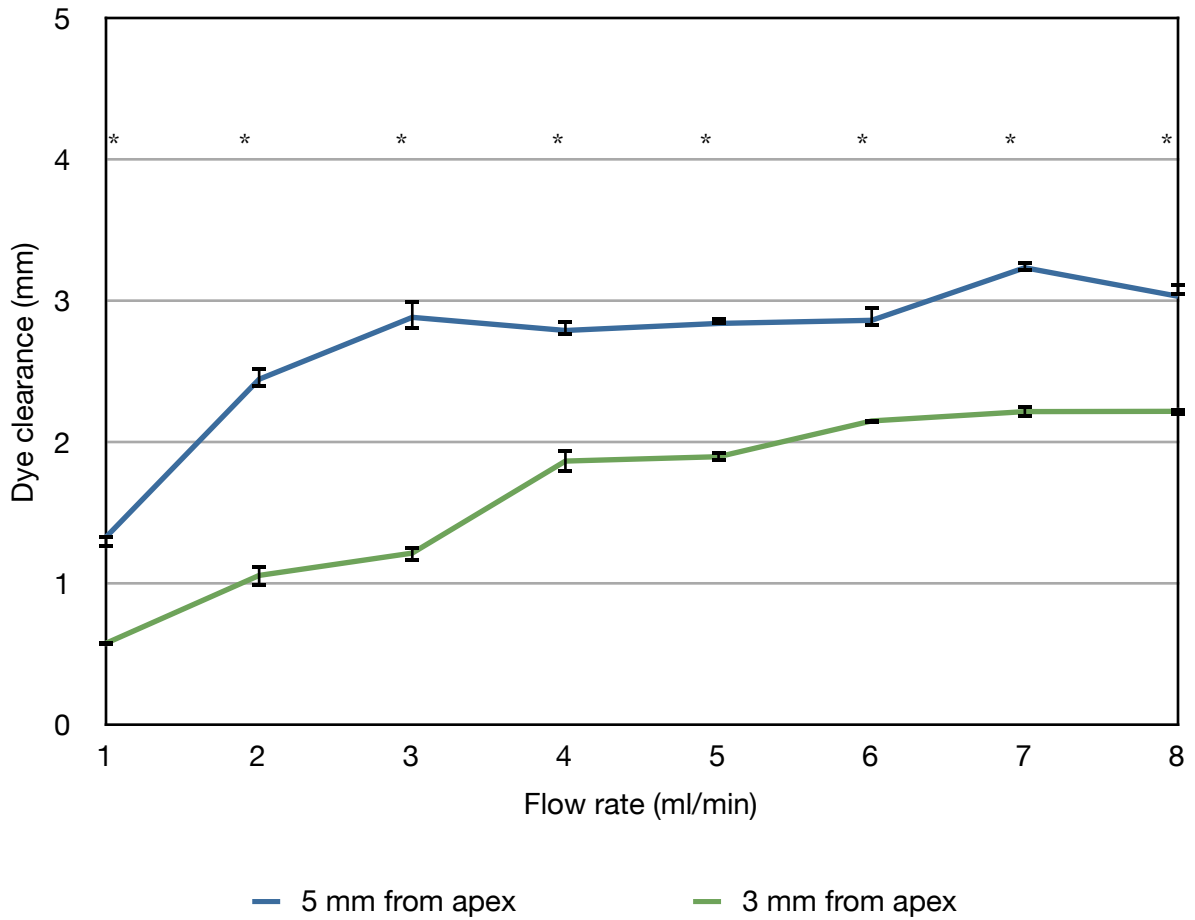
\* statistically significant (P<0.05) difference between placement at 5 mm and 3 mm

**Figure 4.5 Dye clearance during positive pressure irrigation with a 27 ga slotted open-ended (Monoject) needle at 5 mm and 3 mm from the apex**

Source	df	Sum of Squares	Mean Square	F	Sig.	% of total variation
interaction	14	5.891	0.4208	38.10	<0.0001	5.34
depth	1	17.14	17.14	1552	<0.0001	15.53
flow rate	14	86.67	6.191	560.5	<0.0001	78.53
error	60	0.6627	0.01104			

**Table 4.9 Two-way ANOVA for dye clearance during PPI 5 mm and 3 mm from the apex with a 27 ga slotted open-ended (Monoject) needle**

**Dye clearance during PPI with a 30 ga side-vented closed-ended needle**



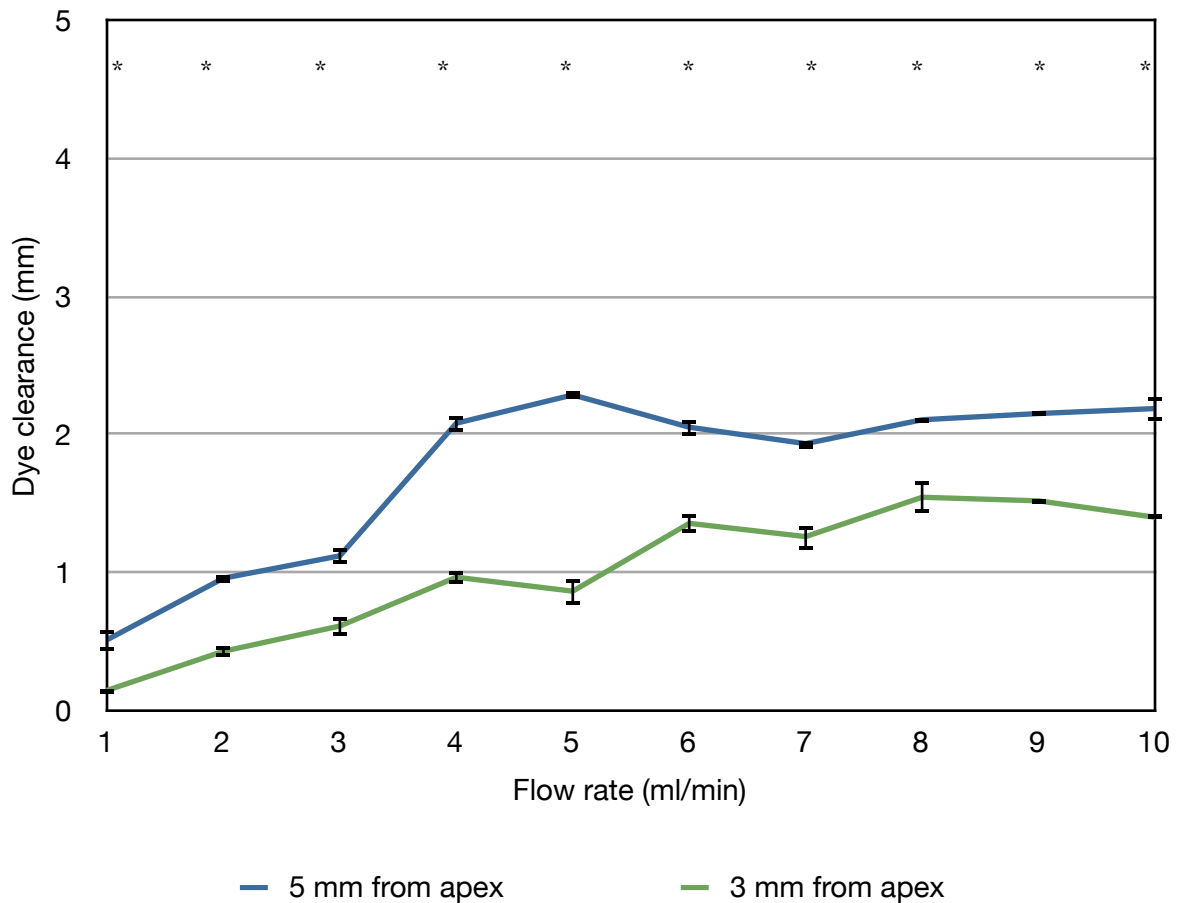
\* statistically significant ( $P < 0.05$ ) difference between placement at 5 mm and 3 mm

**Figure 4.6 Dye clearance during positive pressure irrigation with a 30 ga side-vented closed-ended (ProRinse) needle at 5 mm and 3 mm from the apex**

Source	df	Sum of Squares	Mean Square	F	Sig.	% of total variation
interaction	7	1.170	0.1671	30.90	<0.0001	4.15
depth	1	12.66	12.66	2342	<0.0001	44.92
flow rate	7	14.19	2.027	374.8	<0.0001	50.52
error	32	0.1730	0.005407			

**Table 4.10 Two-way ANOVA for dye clearance during PPI 5 mm and 3 mm from the apex with a 30 ga side-vented closed-ended (ProRinse) needle**

### Dye clearance during PPI with an ISO 32 EndoVac needle



\* statistically significant ( $P < 0.05$ ) difference between placement at 5 mm and 3 mm

**Figure 4.7** Dye clearance during positive pressure irrigation with an ISO 32 closed-ended needle with multiple perforations (EndoVac) at 5 mm and 3 mm from the apex

Source	df	Sum of Squares	Mean Square	F	Sig.	% of total variation
interaction	9	1.356	0.1506	37.41	<0.0001	5.38
depth	1	8.099	8.099	2011	<0.0001	32.14
flow rate	9	15.59	1.732	430.1	<0.0001	61.84
error	40	0.1611	0.004027			

**Table 4.11** Two-way ANOVA for dye clearance during PPI 5 mm and 3 mm from the apex with an ISO 32 closed-ended needle with multiple perforations (EndoVac).

## 4.2 Dye clearance measurement using negative pressure irrigation

When measuring the clearance of dye during negative pressure irrigation beyond the end of the needle tip at 5 mm and 3 mm from the working length, some needle tips showed an overall flow rate dependent increase in dye clearance, with certain needles showing stabilization at flow rates beyond 4 ml/min (Figure 4.8, 4.9). This was in contrast to the increase in dye clearance during positive pressure irrigation with all needle tips until stabilization at flow rates beyond 4 ml/min.

During negative pressure irrigation at 5 mm from the apex with all five needles (Figure 4.8), two-way ANOVA revealed significant interaction ( $P < 0.05$ ) (Table 4.12). The 30 ga side-vented closed-ended needle was excluded from this analysis due to the limited range of flow rates achievable during negative pressure irrigation with this particular needle. The post hoc Bonferroni test demonstrated that the 25 ga and 30 ga blunt open-ended needle cleared significantly more dye at all flow rates than the remaining needles ( $P < 0.05$ ) (Figure 4.8). The 25 ga blunt open-ended needle also cleared significantly more dye at all flow rates than the 30 ga blunt open-ended needle ( $P < 0.05$ ) (Figure 4.8). Visual inspection of figure 4.8 showed interaction in the flow rate range of 1 - 4 ml/min, and a plateau in the length of dye cleared during irrigation beyond 4 ml/min. Thus, two-way ANOVA was repeated for two separate subsets of data: for the 25 ga and 30 ga blunt open-ended needles in the flow rate range of 1 - 4 ml/min (Table 4.13), and in the flow rate range of 5 - 8 ml/min (Table 4.14). Two-way ANOVA for data in the flow rate range of 1 - 4 ml/min showed significant interaction ( $P < 0.05$ ) as expected, with needle design comprising 62.10% of the total variance, and flow rate comprising 25.61% of the total variance. The effect of the needle design and

flow rate were also statistically significant ( $P < 0.05$ ). Two-way ANOVA for data in the flow rate range of 5 - 8 ml/min did not show significant interaction ( $P = 0.0577$ ), with needle design comprising 90.28% of the total variance, and flow rate comprising 0.81% of the total variance. Flow rate was not a significant source of variation in the flow rate range from 5 - 8 ml/min ( $P = 0.5300$ ).

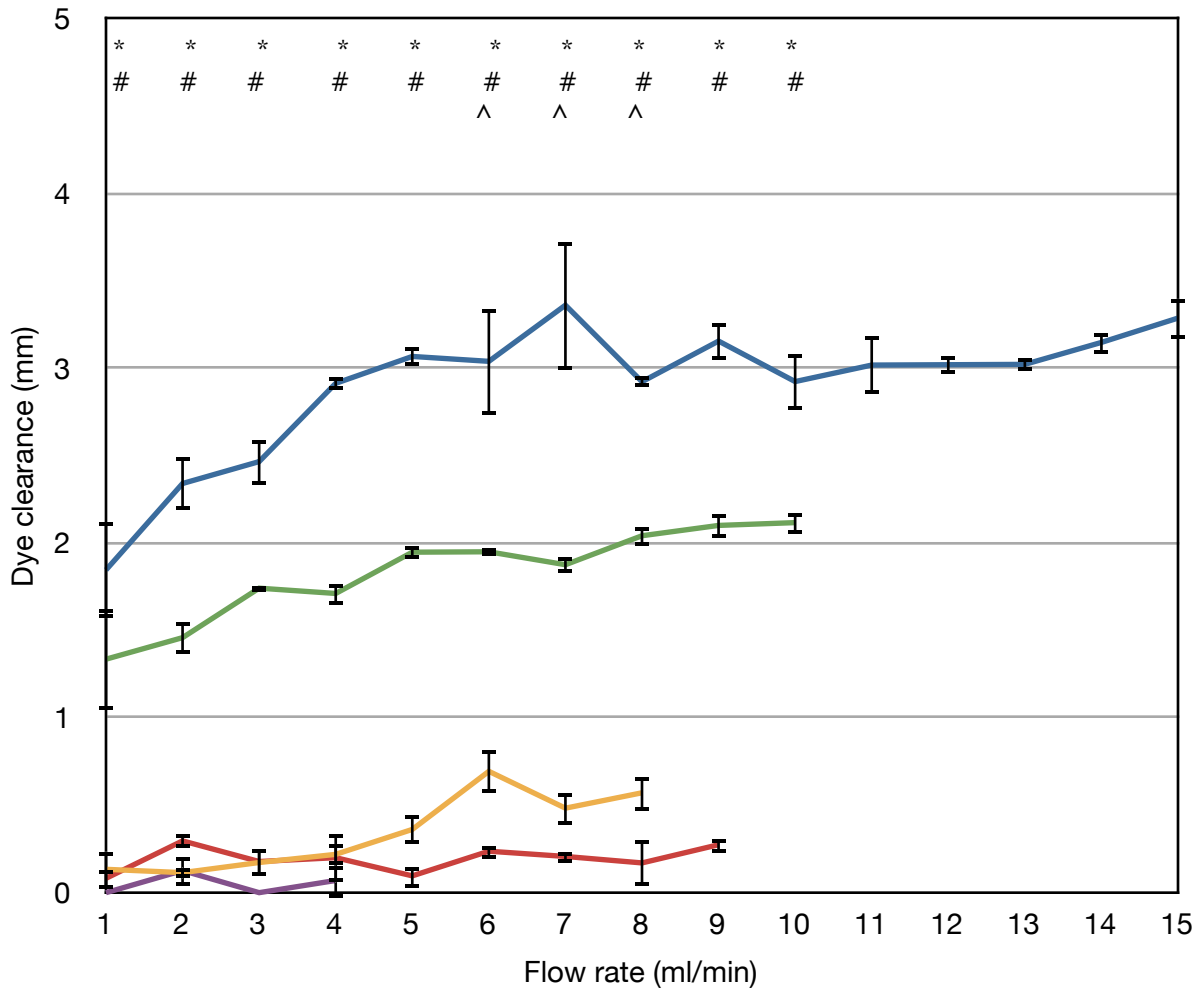
When looking at negative pressure irrigation at 3 mm from the apex with all five needles (Figure 4.9), two-way ANOVA revealed significant interaction ( $P < 0.05$ ) (Table 4.15). The 30 ga side-vented closed-ended needle was excluded from this analysis due to the limited range of flow rates achievable during negative pressure irrigation with this particular needle. The Bonferroni post hoc test demonstrated that the 25 ga and 30 ga blunt open-ended needle cleared significantly more dye at all flow rates than the remaining needles ( $P < 0.05$ ) (Figure 4.9). The 25 ga blunt open-ended needle also cleared significantly more dye at all flow rates than the 30 ga blunt open-ended needle ( $P < 0.05$ ) (Figure 4.9). In previous figures (Figure 4.6, 4.7, 4.8) interaction at the lower range of flow rates could be detected visually, thus prompting the use of two-way ANOVA on subsets of the data. This particular trend was not visually detected in figure 4.9, but two-way ANOVA on the same subsets of data was performed for completeness. Thus, two-way ANOVA was repeated for two separate subsets of data: for the 25 ga and 30 ga blunt open-ended needles in the flow rate range of 1 - 4 ml/min (Table 4.16), and in the flow rate range of 5 - 8 ml/min (Table 4.17).

Two-way ANOVA for data in the flow rate range of 1 - 4 ml/min did not show significant interaction ( $P = 0.4814$ ), with needle design comprising 92.66% of the total variance, and flow rate comprising 5.42% of the total variance. The effect of the needle design and

flow rate were also statistically significant ( $P < 0.05$ ). Two-way ANOVA for data in the flow rate range of 5 - 8 ml/min showed significant interaction, with needle design comprising 87.44% of the total variance, and flow rate comprising 1.35% of the total variance. Flow rate was not a significant source of variation in the flow rate range from 5 - 8 ml/min ( $P = 0.1488$ ). For the 25 ga and 30 ga blunt open-ended needle and the 27 ga slotted open-ended needle, two-way ANOVA revealed significant ( $P < 0.05$ ) interaction for the independent variables depth of placement of needle in the canal, and flow rate. For the 30 ga side-vented open-ended needle and ISO 32 EndoVac needle, there was no significant interaction ( $P > 0.05$ ) between the two independent variables, depth of needle placement, and flow rate. Regardless of whether interaction was significant or not, there was no overall statistically significant difference in the length of dye clearance when comparing needle placement at 5 mm and 3 mm from working length during negative pressure irrigation. The isolated incidents where statistical significances were detected are noted in figures 4.9 - 4.13 by asterisks.

When strictly comparing the numerical length of dye clearance between different needle designs, the EndoVac microcannula, 30 gauge side-vented closed-ended (ProRinse) needle, and the 27 gauge slotted open-ended (Monoject) needle cleared less than 1 mm of dye from the end of the needle tip - less dye than the 25 gauge and 30 gauge blunt open-ended needle tips at both depths of placement in the canal and for all flow rates. The ranking of needles from most to least effective in dye clearance during negative pressure irrigation at all flow rates at 5 mm and 3 mm from working length is: 25 ga blunt open-ended needle (FlexiGlide) > 30 ga blunt open-ended needle (FlexiGlide) > EndoVac, 30 ga side-vented closed-ended needle (ProRinse), 27 ga slotted open-ended needle (Monoject).

### Dye Clearance during NPI 5 mm from the apex



- 25 ga blunt open-ended needle (FlexiGlide)
- 30 ga blunt open-ended needle (FlexiGlide)
- ISO size 32 closed-ended needle with 12 laterally positioned holes (EndoVac)
- 27 ga slotted open-ended needle (Monoject)
- 30 ga side-vented closed-ended needle (ProRinse)

\* statistically significant (P<0.05) difference between 25 ga FlexiGlide and 30 ga FlexiGlide  
 # statistically significant (P<0.05) difference between 25 ga, 30 ga FlexiGlide and all other needles

^ statistically significant (P<0.05) difference between ISO 32 EndoVac and 27 ga Monoject

**Figure 4.8 Dye clearance measurement during negative pressure irrigation at 5 mm from the apex using 5 different irrigation needle tips**

Source	df	Sum of Squares	Mean Square	F	Sig.	% of total variation
interaction	21	3.099	0.1476	8.056	<0.0001	2.69
needle	3	106.7	35.55	1941	<0.0001	95.52
flow rate	7	4.353	0.6218	33.95	<0.0001	3.78
error	63	1.172	1.172			

**Table 4.12 Two-way ANOVA for dye clearance during NPI 5 mm from the apex using 4 different irrigation needle tips (excludes 30 ga ProRinse) at 1 - 8 ml/min.**

Source	df	Sum of squares	Mean Square	F	Sig.	% of total variation
interaction	3	0.3810	0.1270	4.671	0.0158	5.74
needle	1	4.123	4.123	151.6	<0.0001	62.10
flow rate	3	1.700	0.5667	20.84	<0.0001	25.61
error	16	0.4351	0.02719			

**Table 4.13 Two-way ANOVA for dye clearance during NPI 5 mm from the apex using 2 different irrigation needle tips (25 ga, 30 ga FlexiGlide) at 1 - 4 ml/min.**

Source	df	Sum of squares	Mean Square	F	Sig.	% of total variation
interaction	3	0.2827	0.09424	3.073	0.0577	3.25
needle	1	7.838	7.838	255.6	<0.0001	90.28
flow rate	3	0.07039	0.02346	0.7652	0.5300	0.81
error	16	0.4906	0.03066			

**Table 4.14 Two-way ANOVA for dye clearance during NPI 5 mm from the apex using 2 different irrigation needle tips (25 ga, 30 ga FlexiGlide) at 5 - 8 ml/min**

### Dye Clearance during NPI 3 mm from the apex

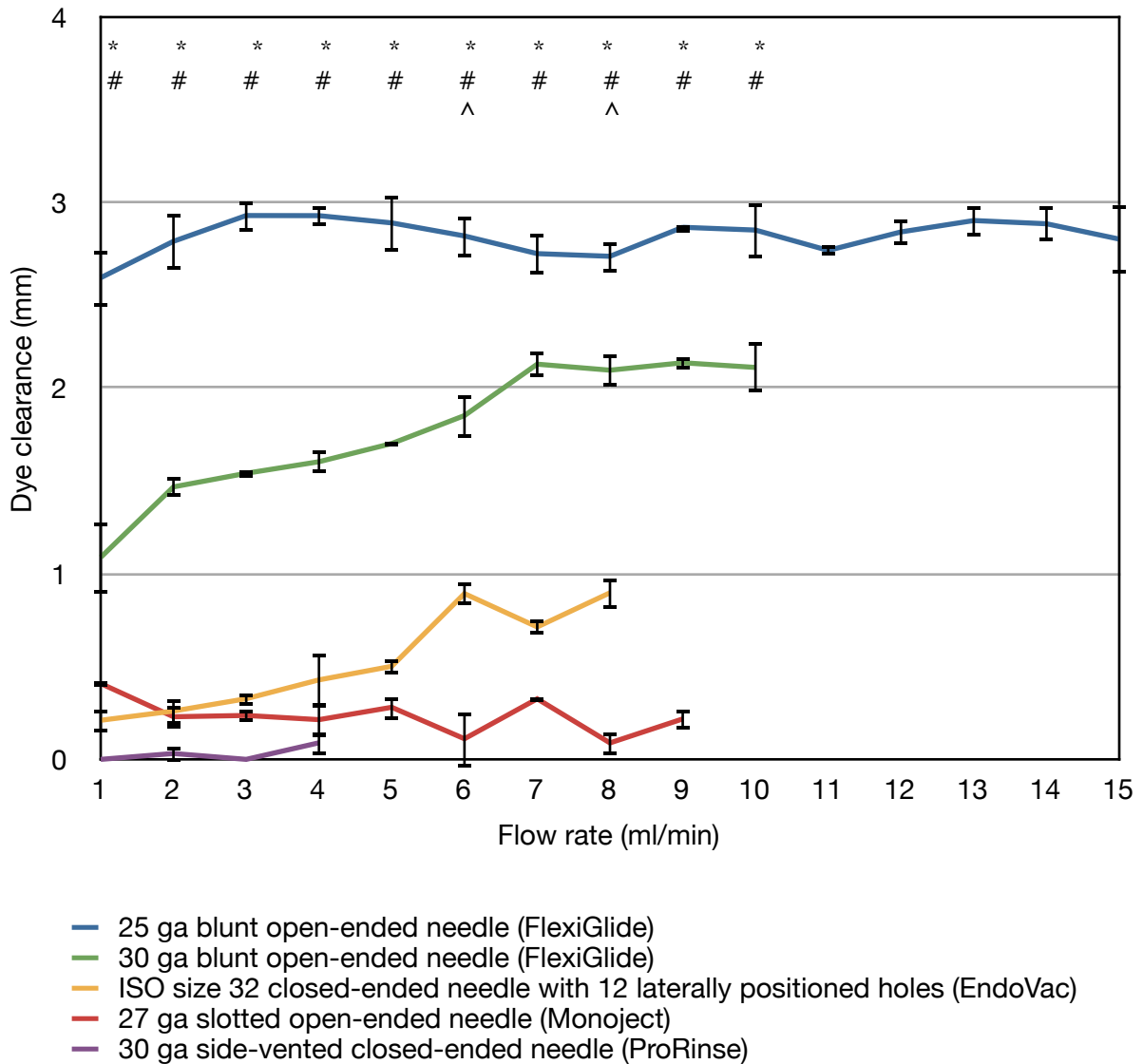


**Figure 4.9** Dye clearance measurement during negative pressure irrigation at 3 mm from the apex using 5 different irrigation needle tips

Source	df	Sum of Squares	Mean Square	F	Sig.	% of total variation
interaction	21	3.008	0.1432	16.15	<0.0001	2.89
needle	3	98.90	32.97	3718	<0.0001	95.04
flow rate	7	1.581	0.2259	0.2249	<0.0001	1.52
error	64	0.5675	0.5675			

**Table 4.15 Two-way ANOVA for dye clearance during NPI 3 mm from the apex using 4 different irrigation needle tips (excludes 30 ga ProRinse) at all flow rates.**

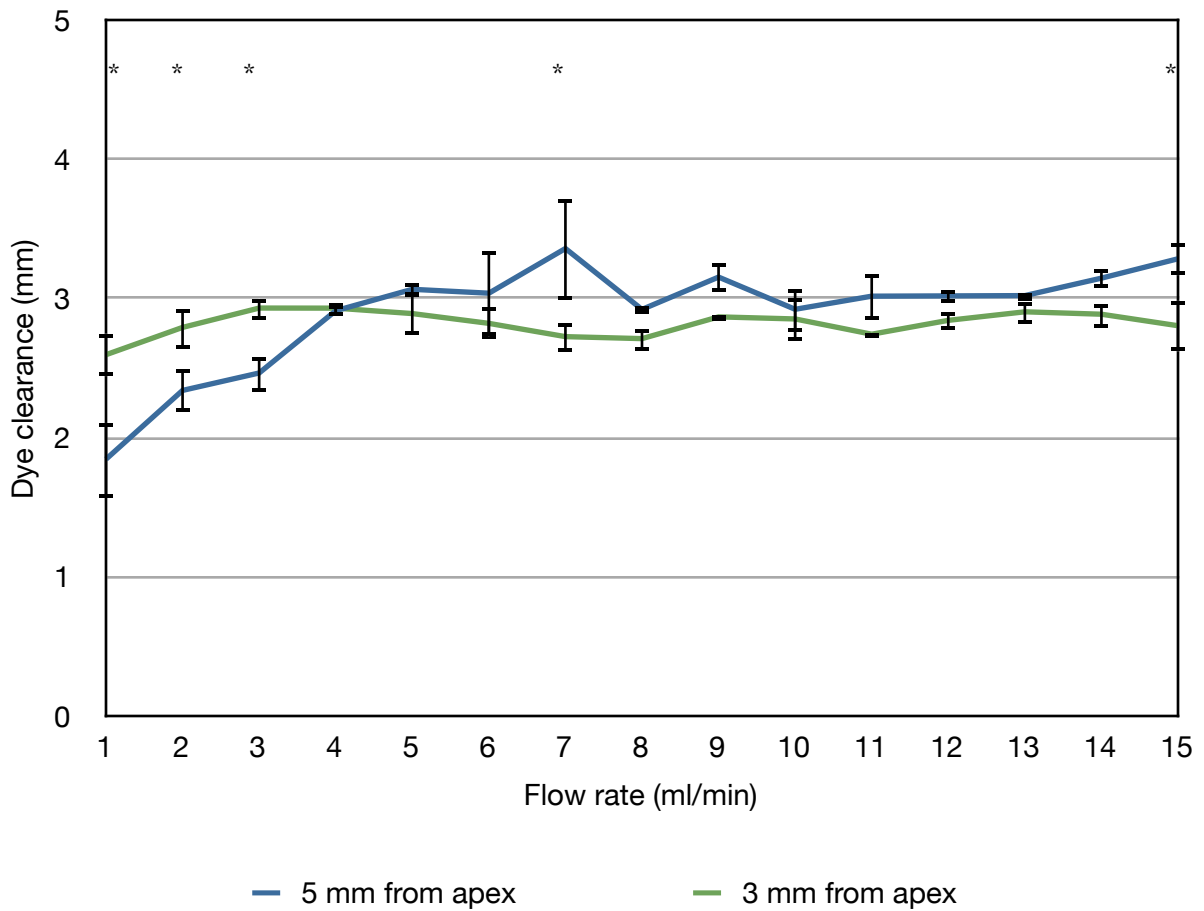
Source	df	Sum of Squares	Mean Square	F	Sig.	% of total variation
interaction	3	0.03220	0.01107	0.8609	0.4814	0.27
needle	1	11.53	11.53	896.9	<0.0001	92.66
flow rate	3	0.6746	0.2249	17.49	<0.0001	5.42
error	16	0.2057	0.01286			

**Table 4.16 Two-way ANOVA for dye clearance during NPI 3 mm from the apex using 2 different irrigation needle tips (25 ga, 30 ga FlexiGlide) at 1 - 4 ml/min.**

Source	df	Sum of Squares	Mean Square	F	Sig.	% of total variation
interaction	3	0.3737	0.1246	11.62	0.0003	7.69
needle	1	4.250	4.250	396.6	<0.0001	87.44
flow rate	3	0.06558	0.02186	2.040	0.1488	1.35
error	16	0.1715	0.01072			

**Table 4.17 Two-way ANOVA for dye clearance during NPI 3 mm from the apex using 2 different irrigation needle tips (25 ga, 30 ga FlexiGlide) at 5 - 8 ml/min.**

### Dye clearance during NPI with a 25 ga blunt open-ended needle



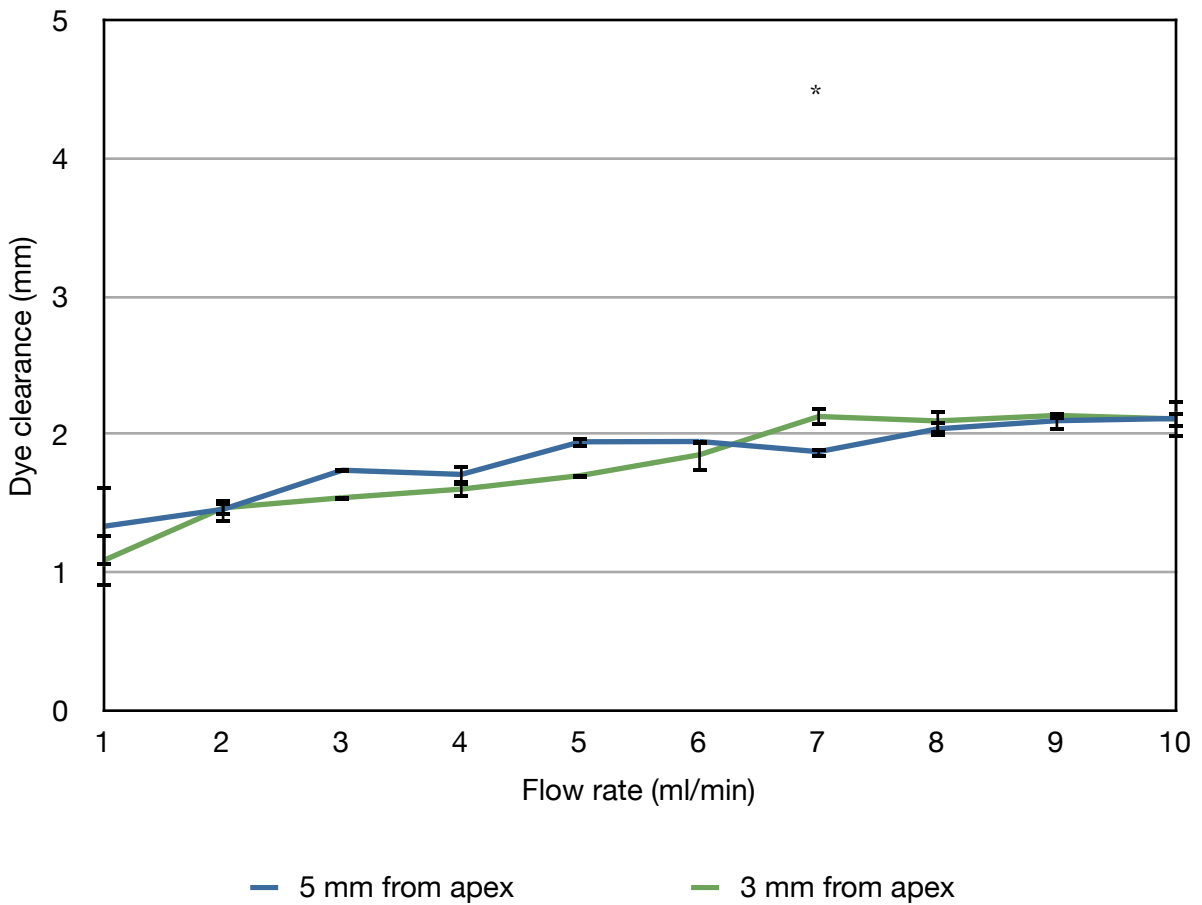
\* statistically significant (P<0.05) difference between placement at 5 mm and 3 mm

**Figure 4.10** Dye clearance measurement during negative pressure irrigation at 5 mm and 3 mm from the apex using a 25 ga blunt open-ended (FlexiGlide) needle

Source	df	Sum of Squares	Mean Square	F	Sig.	% of total variation
interaction	14	2.873	0.2052	9.596	<0.0001	34.35
depth	1	0.1455	0.1455	6.803	0.0115	1.74
flow rate	14	4.064	0.2903	13.57	<0.0001	48.57
error	60	1.283	0.02139			

**Table 4.18** Two-way ANOVA for dye clearance during NPI 5 mm and 3 mm from the apex with a 25 ga blunt open-ended (FlexiGlide) needle

**Dye clearance during NPI with a 30 ga blunt open-ended needle**



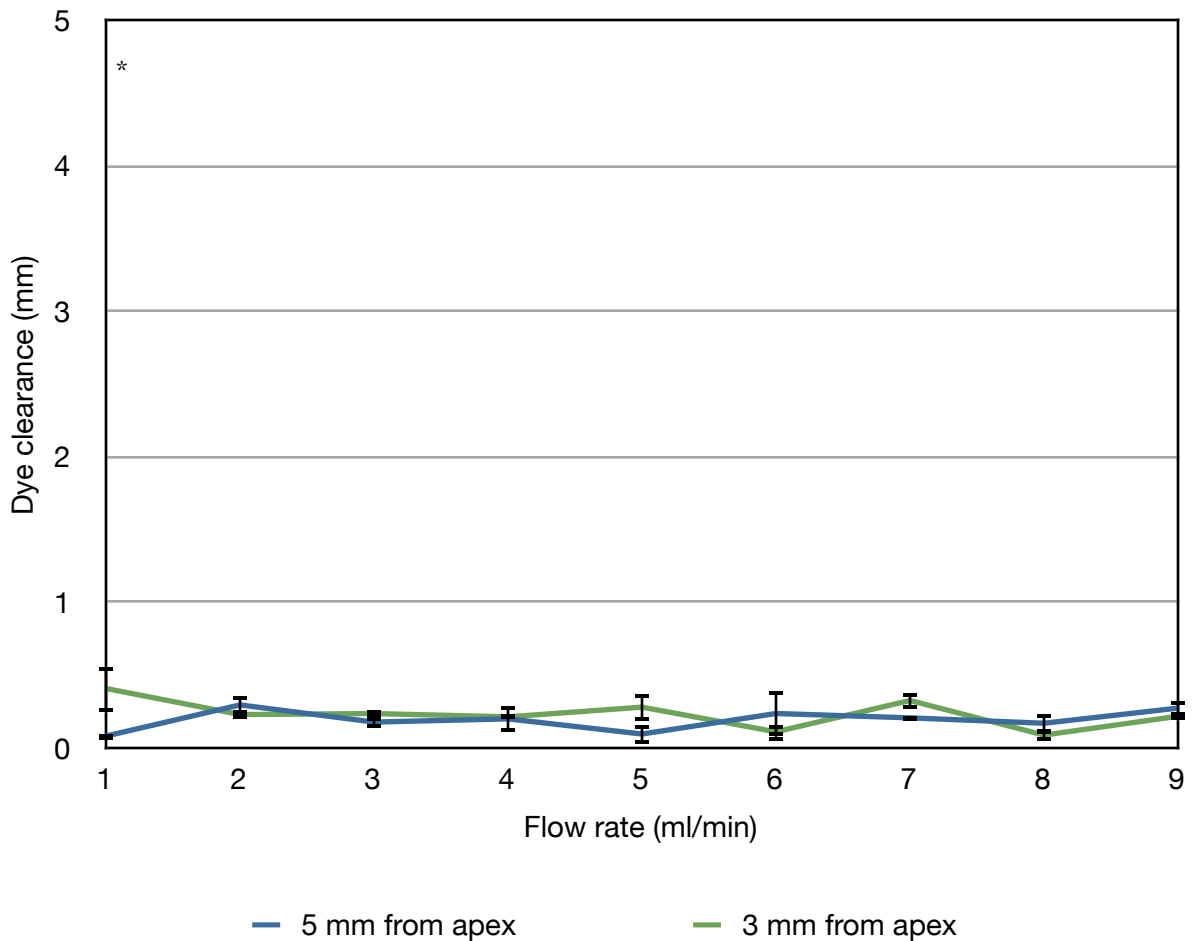
\* statistically significant (P<0.05) difference between placement at 5 mm and 3 mm

**Figure 4.11 Dye clearance measurement during negative pressure irrigation at 5 mm and 3 mm from the apex using a 30 ga blunt open-ended (FlexiGlide) needle**

Source	df	Sum of Squares	Mean Square	F	Sig.	% of total variation
interaction	9	0.3324	0.03693	3.512	0.0028	5.76
depth	1	0.04285	0.04285	4.075	0.0503	0.74
flow rate	9	4.973	0.5526	52.55	<0.0001	86.20
error	40	0.4206	0.01052			

**Table 4.19 Two-way ANOVA for dye clearance during NPI 5 mm and 3 mm from the apex with a 30 ga blunt open-ended (FlexiGlide) needle**

### Dye clearance during NPI with a 27 ga slotted open-ended needle



\* statistically significant ( $P < 0.05$ ) difference between placement at 5 mm and 3 mm

**Figure 4.12** Dye clearance measurement during negative pressure irrigation at 5 mm and 3 mm from the apex using a 27 ga slotted open-ended (Monoject) needle

Source	df	Sum of Squares	Mean Square	F	Sig.	% of total variation
interaction	8	0.2598	0.03248	5.261	0.0002	42.92
depth	1	0.02327	0.02327	3.700	0.0600	3.84
flow rate	8	0.1001	0.01251	2.027	0.0708	16.54
error	36	0.2222	0.006172			

**Table 4.20** Two-way ANOVA for dye clearance during NPI 5 mm and 3 mm from the apex with a 27 ga slotted open-ended (Monoject) needle

**Dye clearance during NPI with a 30 ga side-vented closed-ended needle**

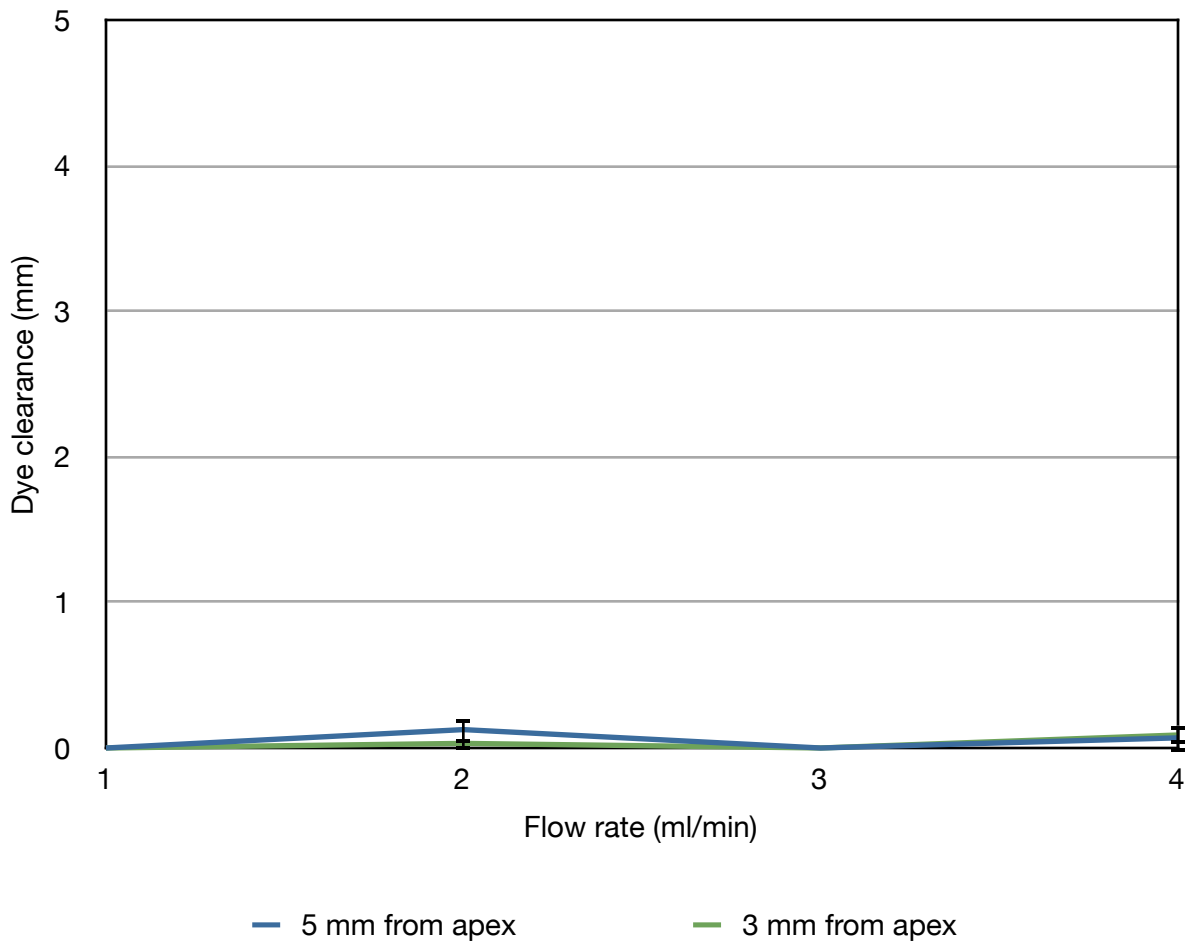
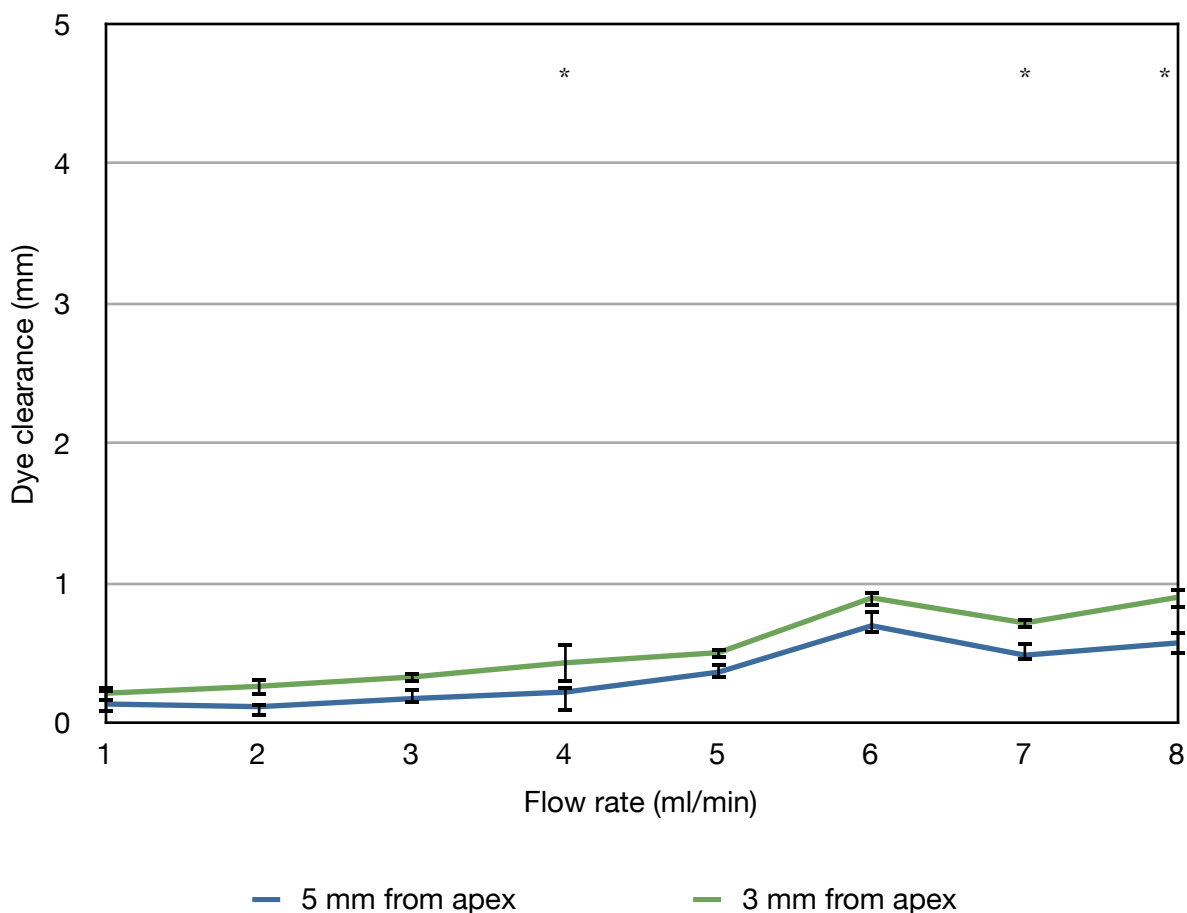


**Figure 4.13 Dye clearance measurement during negative pressure irrigation at 5 mm and 3 mm from the apex using a 30 ga side-vented closed-ended (ProRinse) needle**

Source	df	Sum of Squares	Mean Square	F	Sig.	% of total variation
interaction	3	0.01991	0.003971	1.314	0.3044	11.91
depth	1	0.002109	0.002109	0.6980	0.4158	2.11
flow rate	3	0.03768	0.01256	4.156	0.0235	37.66
error	16	0.04835	0.003022			

**Table 4.21 Two-way ANOVA for dye clearance during NPI 5 mm and 3 mm from the apex with a 30 ga side-vented closed-ended (ProRinse) needle**

### Dye clearance during NPI with an ISO 32 EndoVac needle



\* statistically significant (P<0.05) difference between placement at 5 mm and 3 mm

**Figure 4.14 Dye clearance measurement during negative pressure irrigation at 5 mm and 3 mm from the apex using an ISO 32 closed-ended needle with multiple perforations (EndoVac)**

Source	df	Sum of Squares	Mean Square	F	Sig.	% of total variation
interaction	7	0.05864	0.008378	1.186	0.3387	1.82
depth	1	0.4129	0.4129	58.42	<0.0001	12.78
flow rate	7	0.2532	0.3617	51.18	<0.0001	78.40
error	32	0.2261	0.007067			

**Table 4.22 Two-way ANOVA for dye clearance during NPI 5 mm and 3 mm from the apex with an ISO 32 closed-ended needle with multiple perforations (EndoVac)**

### **4.3 Apical pressure measurement using positive pressure irrigation**

All needles showed an increase in apical pressure as the flow rate increased during positive pressure irrigation (Figure 4.14 - 4.16). Two-way ANOVA was performed for the 30 ga blunt open-ended (FlexiGlide) needle, the 25 ga blunt open-ended (FlexiGlide) needle, the 27 ga slotted open-ended (Monoject) needle, and the 25 ga side-vented closed-ended (Max-I-Probe) needle at 5 mm from the apex, as visual inspection of figure 4.14 showed interaction in the flow rate range of 1 - 12 ml/min, as well as a wide and high range of apical pressures in comparison to the other needle tips. When the needles were placed at 5 mm from the apex, significant interaction ( $P<0.05$ ) was shown, with needle design comprising 34.79% of the total variance, and flow rate comprising 47.31% of the total variance (Table 4.23). Post hoc Bonferroni analysis showed statistically significant differences ( $P<0.05$ ) between the apical pressures generated by these four needles (Figure 4.14). The apical pressures generated by the use of the 30 gauge blunt open-ended (FlexiGlide) needle at 5 mm from working length were significantly higher than the mean apical pressures generated by the other needle tips ( $P<0.05$ ) in the flow rate range of 1 - 12 ml/min.

When the needles were placed at 3 mm from the apex (Figure 4.15), significant interaction ( $P<0.05$ ) was shown, with needle design comprising 37.10% of the total variance, and flow rate comprising 45.78% of the total variance (Table 4.24). Post hoc Bonferroni analysis showed statistically significant differences ( $P<0.05$ ) between the apical pressures generated by these four needles (Figure 4.15). The mean apical pressures generated by the use of the 25 gauge and 30 gauge blunt open-ended (FlexiGlide) needle at 3 mm from working length were significantly higher ( $P<0.05$ ) than those produced by all other needles.

For completeness of analysis, two-way ANOVA was performed for the remaining needles at 5 mm and 3 mm from the apex for the flow rate range 1 - 8 ml/min, where the apical pressures generated are under 10mmHg (Figure 4.14, 4.15). Significant interaction was shown ( $P<0.05$ ), but the ANOVA table and post-hoc Bonferroni tests are not shown.

When the needles were placed at 1 mm from the apex (Figure 4.16), only three needles could be placed at this level in the root canal without binding of the needle tip. These needles included the 30 ga blunt open-ended (FlexiGlide) needle, the 30 ga side-vented closed-ended (ProRinse) needle, and the ISO 32 EndoVac needle. Significant interaction ( $P<0.05$ ) was shown, with needle design comprising 30.45% of the total variance, and flow rate comprising 50.22% of the total variance (Table 4.25). Post hoc Bonferroni analysis showed statistically significant differences ( $P<0.05$ ) between the apical pressures generated by these needles (Figure 4.16), notably between the 30 ga blunt open-ended (FlexiGlide) needle and the 30 ga side-vented closed-ended (ProRinse) needle or ISO 32 EndoVac needle. The needle that generated the highest apical pressures was the 30 gauge blunt open-ended needle. When the 30-gauge side-vented closed-ended needle was placed at 1 mm from working length, the apical pressure was unpredictable, and oscillated between high and low apical pressures (Figure 4.16).

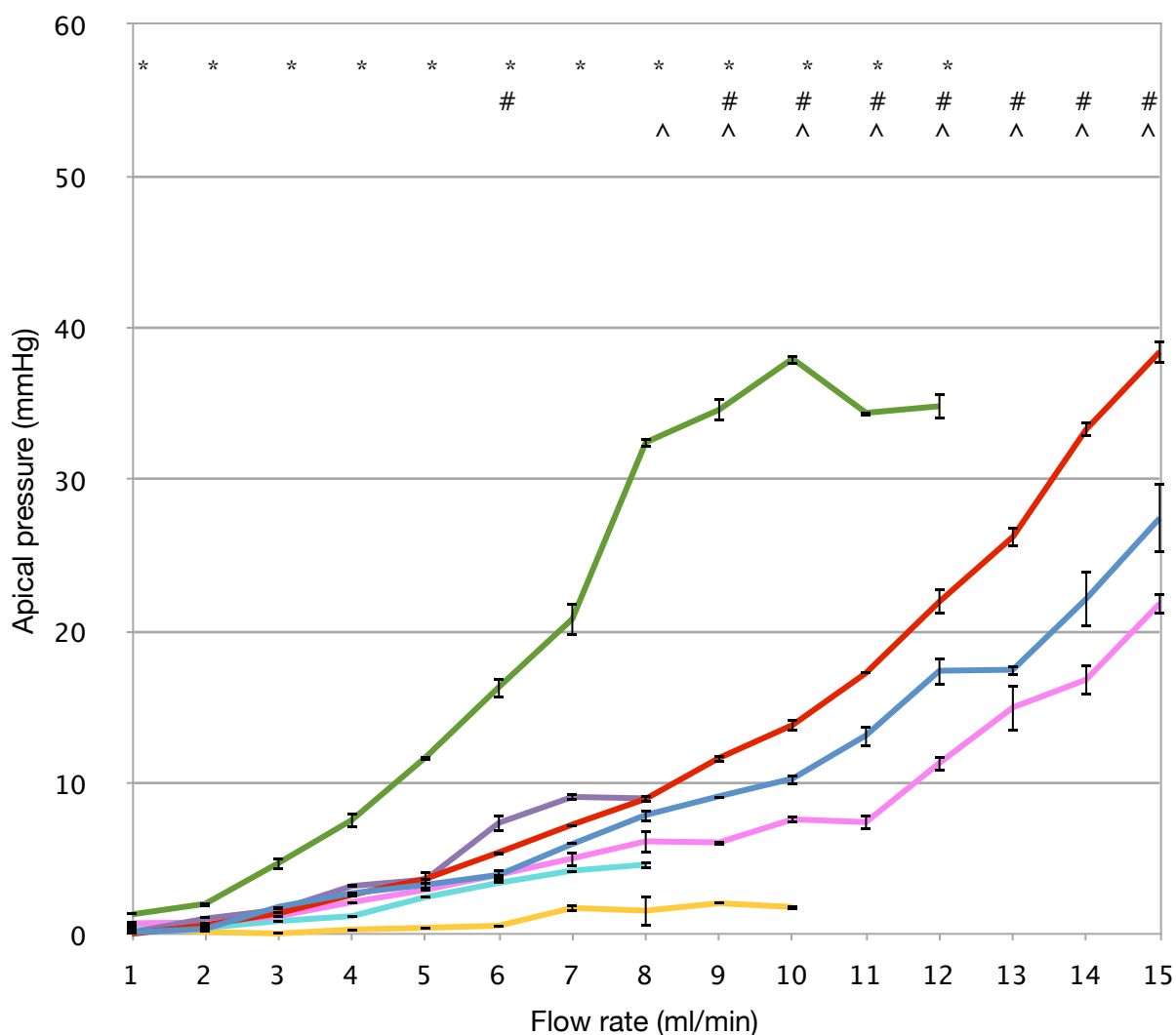
When considering each irrigation needle individually, two-way ANOVA revealed that interaction was significant ( $P<0.05$ ) between depth of needle placement and flow rate for each of the seven needle tips used (Table 4.26 - 4.32). The results of the post hoc Bonferroni analyses are shown in figures 4.17 - 4.23, showing that overall, the apical pressures caused by the irrigant at different depths in the canal were significantly different, with many needles

showing a significant effect at higher irrigation flow rates, such as the 25 ga and 30 ga blunt open-ended (FlexiGlide) needle, the 25 ga side-vented closed-ended needle (Max-I-Probe), the 27 ga slotted open-ended (Monoject) needle, and the ISO 32 EndoVac needle.

Statistically there was one exception: when the 30 gauge side-vented closed-ended needle was placed at 5 mm and 3 mm from working length, there was no difference in the mean apical pressure generated by the irrigant (Figure 4.21). When the 30-gauge side-vented closed-ended needle was placed at 1 mm from working length, the apical pressure was unpredictable, and oscillated between high and low apical pressures, as previously mentioned (Figure 4.21).

The highest and widest range of apical pressures were produced by the blunt open-ended needles, the slotted open-ended needle, and the largest diameter side-vented closed-ended needles. The remaining smaller diameter closed-ended needle designs produced a lower and smaller range of apical pressures, and operated within a lower range of flow rates in this study.

### Apical pressure during PPI at 5 mm from the apex



- 25 ga blunt open-ended needle (FlexiGlide)
- 30 ga blunt open-ended needle (FlexiGlide)
- 27 ga slotted open-ended needle (Monoject)
- 30 ga side-vented closed-ended needle (ProRinse)
- 25 ga side-vented closed-ended needle (Max-I-Probe)
- 27 ga side-vented closed-ended needle (VistaProbe)
- ISO 32 closed-ended needle with 12 laterally positioned holes (EndoVac)

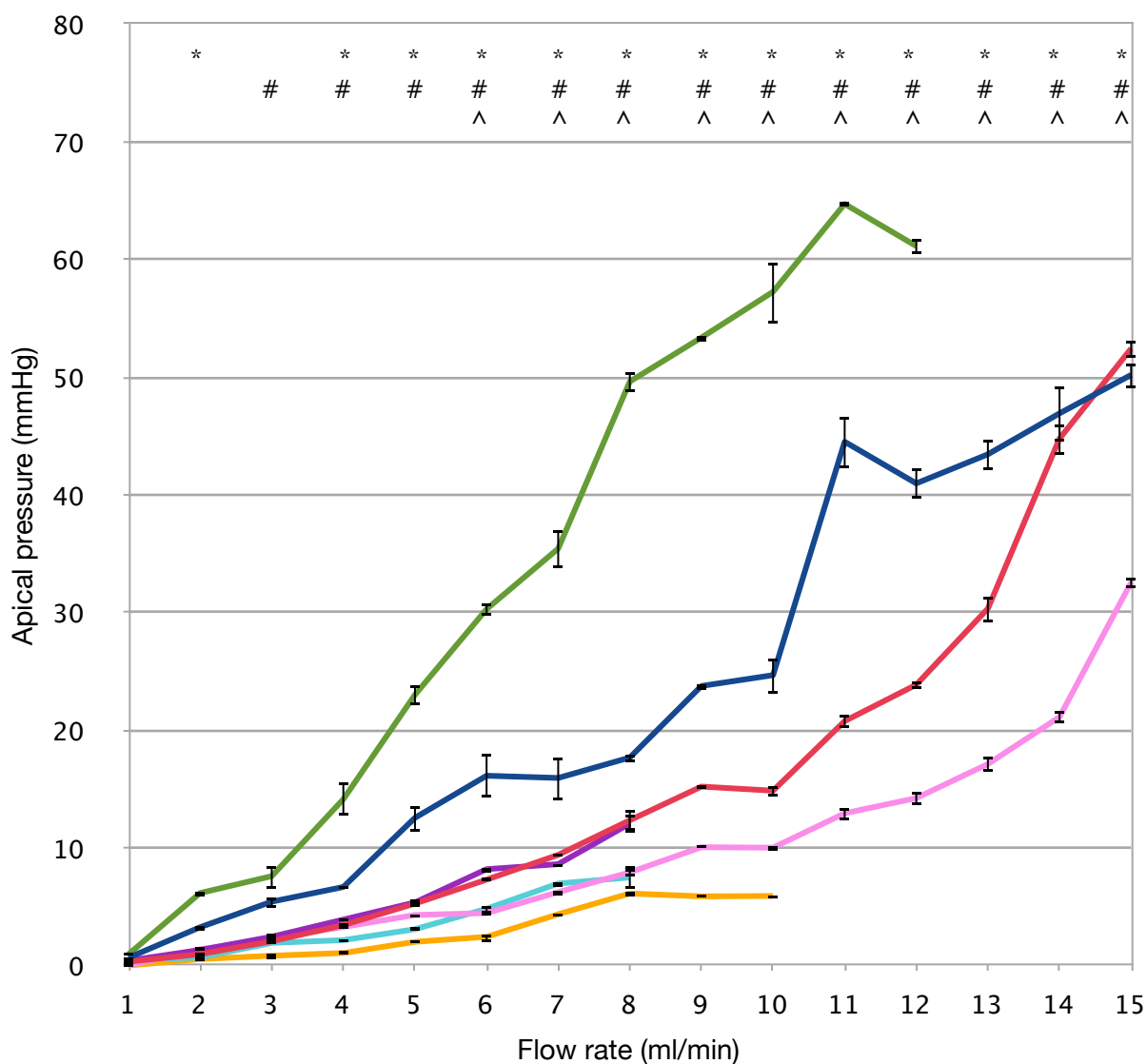
\* statistically significant ( $P < 0.05$ ) difference between 30 ga FlexiGlide and 27 ga Monoject  
 # statistically significant ( $P < 0.05$ ) difference between 27 ga Monoject and 25 ga FlexiGlide  
 ^ statistically significant ( $P < 0.05$ ) difference between 25 ga FlexiGlide and 25 ga Max-I-Probe

**Figure 4.15** Apical pressure measurement during positive pressure irrigation at 5 mm from the apex using 7 different irrigation needle tips

Source	df	Sum of Squares	Mean Square	F	Sig.	% of total variation
interaction	33	2651	80.34	398.0	<0.0001	17.77
needle	3	5191	1370	8570	<0.0001	34.79
flow rate	11	7058	641.6	3178	<0.0001	47.31
error	96	19.38	0.2019			

**Table 4.23 Two-way ANOVA for apical pressure during positive pressure irrigation 5 mm from the apex with 25 ga FlexiGlide, 30 ga FlexiGlide, 27 ga Monoject, and 25 ga Max-I-Probe for the flow rate range 1 - 12 ml/min**

### Apical pressure during PPI at 3 mm from the apex



- 25 ga blunt open-ended needle (FlexiGlide)
- 30 ga blunt open-ended needle (FlexiGlide)
- 27 ga slotted open-ended needle (Monoject)
- 30 ga side-vented closed-ended needle (ProRinse)
- 25 ga side-vented closed-ended needle (Max-I-Probe)
- 27 ga side-vented closed-ended needle (VistaProbe)
- ISO 32 closed-ended needle with 12 laterally positioned perforations (EndoVac)

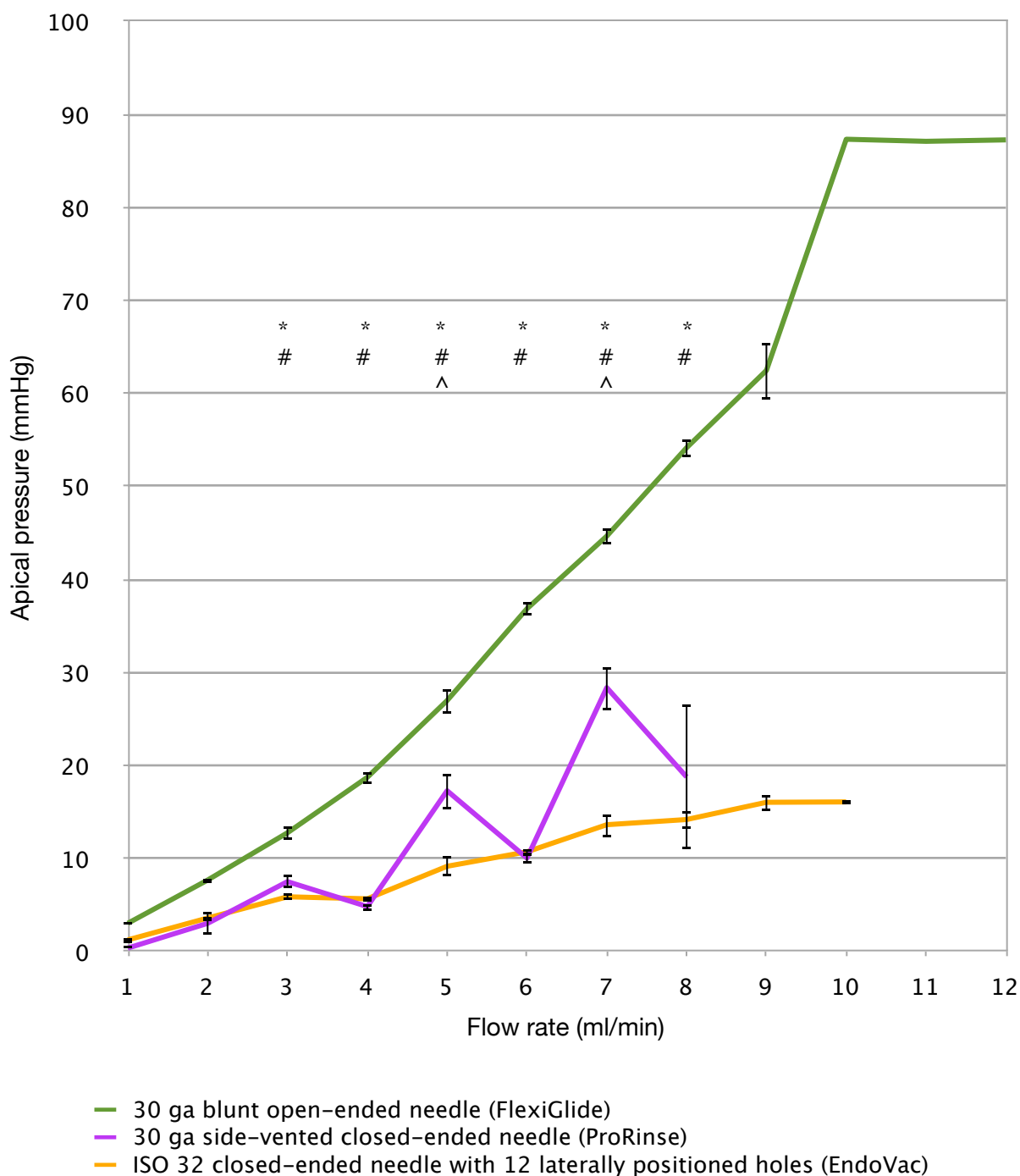
\* statistically significant ( $P < 0.05$ ) difference between 30 ga FlexiGlide and 27 ga Monoject  
 # statistically significant ( $P < 0.05$ ) difference between 27 ga Monoject and 25 ga FlexiGlide  
 ^ statistically significant ( $P < 0.05$ ) difference between 25 ga FlexiGlide and 25 ga Max-I-Probe

**Figure 4.16 Apical pressure measurement during positive pressure irrigation at 3 mm from the apex using 7 different irrigation needle tips**

Source	df	Sum of Squares	Mean Square	F	Sig.	% of total variation
interaction	33	7287	220.8	287.5	<0.0001	16.95
needle	3	15947	5316	6920	<0.0001	37.10
flow rate	11	19678	1789	1789	<0.0001	45.78
error	96	73.74	0.7681			

**Table 4.24 Two-way ANOVA for apical pressure during positive pressure irrigation 3 mm from the apex with 25 ga FlexiGlide, 30 ga FlexiGlide, 27 ga Monoject, and 25 ga Max-I-Probe for the flow rate range 1 - 12 ml/min**

### Apical pressure during PPI at 1 mm from the apex



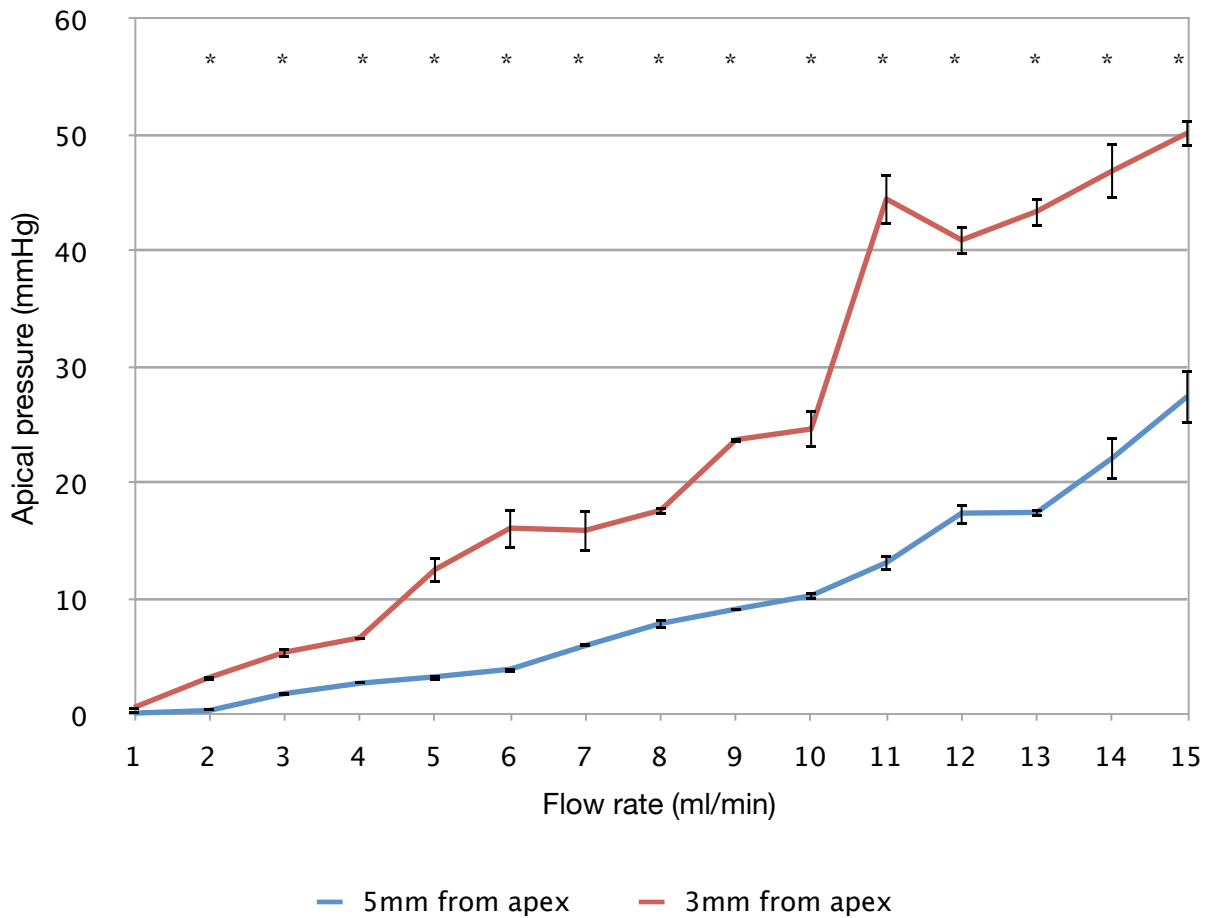
\* statistically significant ( $P < 0.05$ ) difference between 30 ga FlexiGlide and 30 ga ProRinse  
 # statistically significant ( $P < 0.05$ ) difference between 30 ga FlexiGlide and ISO 32 EndoVac  
 ^ statistically significant ( $P < 0.05$ ) difference between 30 ga ProRinse and ISO 32 EndoVac

**Figure 4.17 Apical pressure measurement during positive pressure irrigation at 1 mm from the apex using 3 different irrigation needle tips**

Source	df	Sum of Squares	Mean Square	F	Sig.	% of total variation
interaction	14	2482	177.3	51.16	<0.0001	18.03
needle	2	4204	2102	606.6	<0.0001	30.45
flow rate	7	6912	987.5	284.9	<0.0001	50.22
error	48	166.4	3.466			

**Table 4.25 Two-way ANOVA for apical pressure during positive pressure irrigation 1 mm from the apex for the flow rate range 1 - 8 ml/min**

**Apical pressure during PPI with a 25 ga blunt open-ended needle**



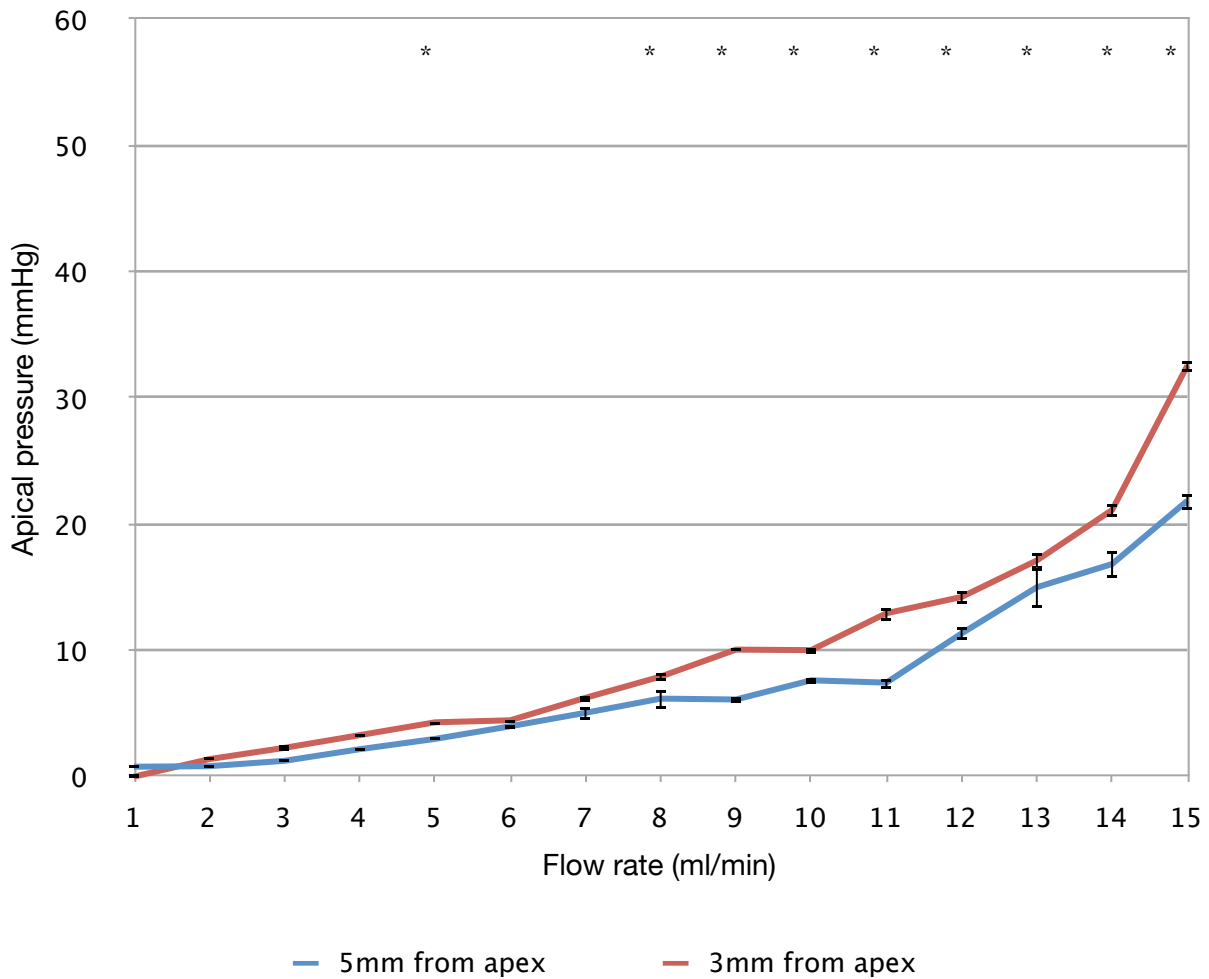
\* statistically significant (P<0.05) difference between placement at 5 mm and 3 mm

**Figure 4.18 Apical pressure measurement during positive pressure irrigation with a 25 gauge blunt open-ended (FlexiGlide) needle**

Source	df	Sum of Squares	Mean Square	F	Sig.	% of total variation
interaction	14	1957	139.8	107.9	<0.0001	9.77
depth	1	4377	4377	3377	<0.0001	21.85
flow rate	14	13621	972.9	750.7	<0.0001	67.99
error	60	77.76	77.76			

**Table 4.26 Two-way ANOVA for apical pressure during positive pressure irrigation 5 mm and 3 mm from the apex with a 25 ga blunt open-ended (FlexiGlide) needle**

**Apical pressure during PPI with a 25 ga side-vented closed-ended needle**



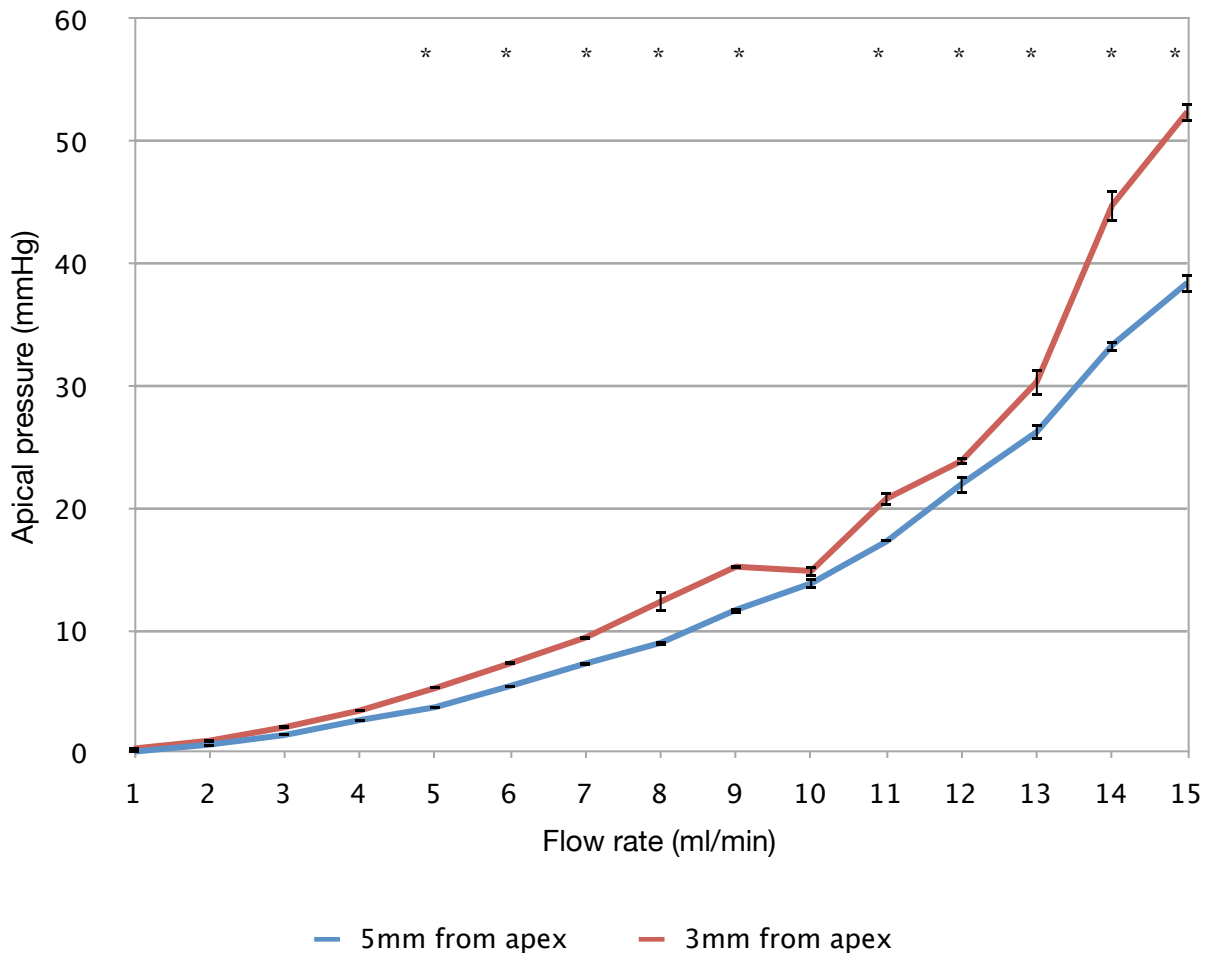
\* statistically significant (P<0.05) difference between placement at 5 mm and 3 mm

**Figure 4.19 Apical pressure measurement during positive pressure irrigation with a 25 gauge side-vented closed-ended (Max-I-Probe) needle.**

Source	df	Sum of Squares	Mean Square	F	Sig.	% of total variation
interaction	14	162.3	11.59	42.51	<0.0001	3.20
depth	1	148.0	148.0	542.7	<0.0001	2.92
flow rate	14	4738	338.4	1241	<0.0001	93.55
error	60	16.37	0.2728			

**Table 4.27 Two-way ANOVA for apical pressure during positive pressure irrigation 5 mm & 3 mm from the apex with a 25 ga side-vented closed-ended (Max-I-Probe) needle**

### Apical pressure during PPI with a 27 ga slotted open-ended needle



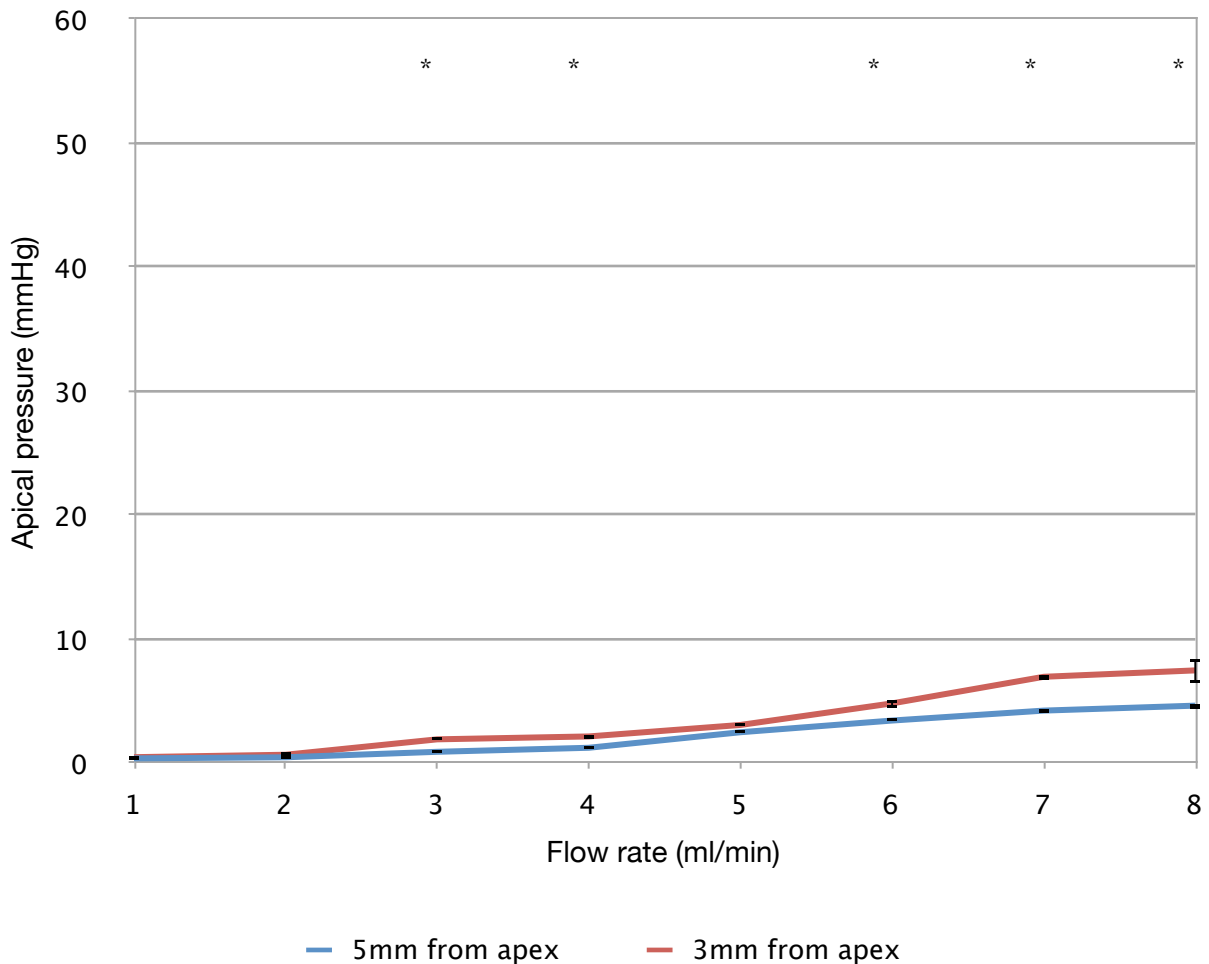
\* statistically significant (P<0.05) difference in placement at 5 mm and 3 mm

**Figure 4.20** Apical pressure measurement during positive pressure irrigation with a 27 gauge slotted open-ended (Monoject) needle.

Source	df	Sum of Squares	Mean Square	F	Sig.	% of total variation
interaction	14	339.9	24.28	89.18	<0.0001	1.99
depth	1	253.7	253.7	932.0	<0.0001	1.48
flow rate	14	16478	1177	4324	<0.0001	96.43
error	60	16.33	0.2722			

**Table 4.28** Two-way ANOVA for apical pressure during positive pressure irrigation 5 mm and 3 mm from the apex with a 27 ga slotted open-ended (Monoject) needle

**Apical pressure during PPI with a 27 ga side-vented closed-ended needle**



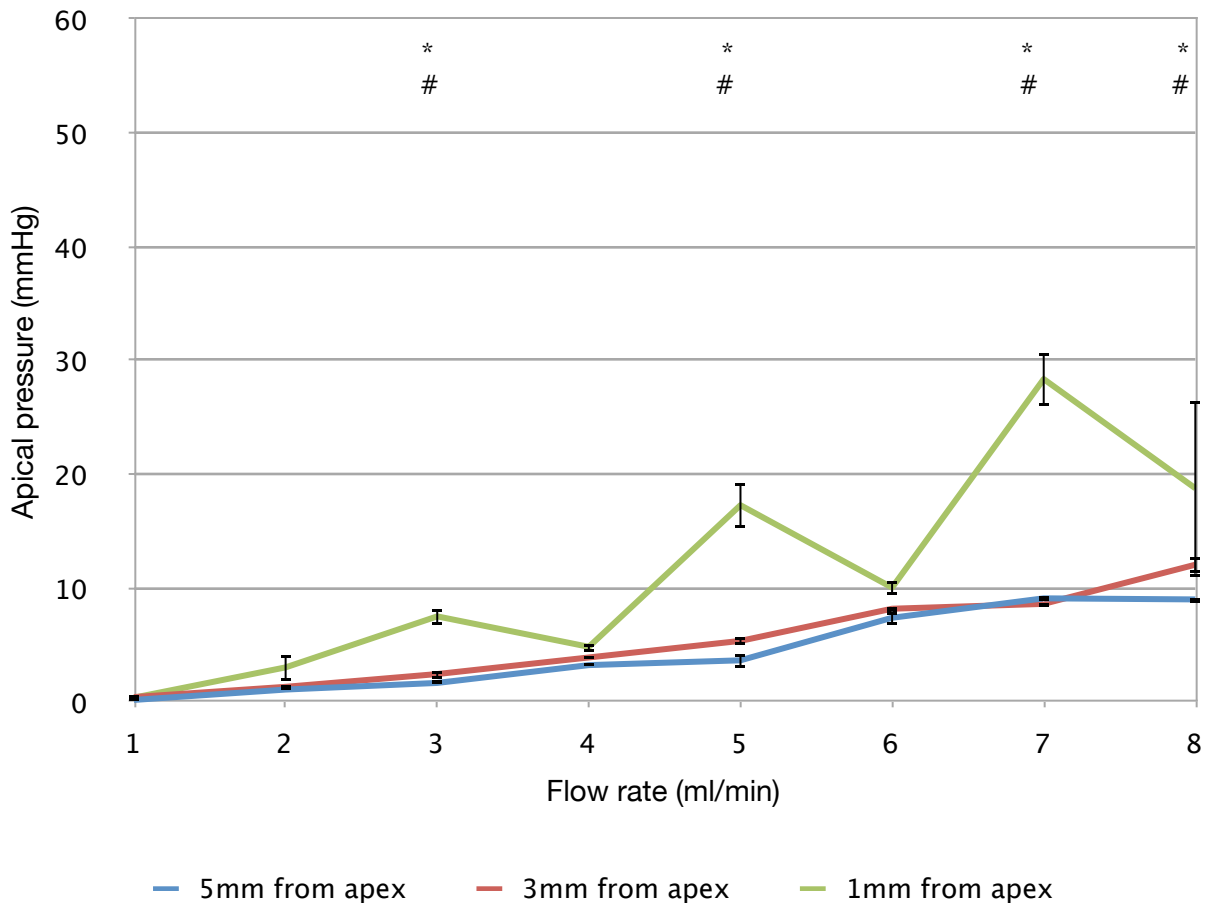
\* statistically significant (P<0.05) difference in placement at 5 mm and 3 mm

**Figure 4.21 Apical pressure measurement during positive pressure irrigation with a 27 gauge side-vented closed-ended (Vista-Probe) needle**

Source	df	Sum of Squares	Mean Square	F	Sig.	% of total variation
interaction	7	11.64	1.663	18.70	<0.0001	4.94
depth	1	17.88	17.88	201.0	<0.0001	7.58
flow rate	7	29.05	29.05	326.7	<0.0001	86.27
error	32	2.846	0.08892			

**Table 4.29 Two-way ANOVA for apical pressure during positive pressure irrigation 5 mm and 3 mm from the apex with a 27 ga side-vented closed-ended (VistaProbe) needle**

**Apical pressure during PPI with a 30 ga side-vented closed-ended needle**



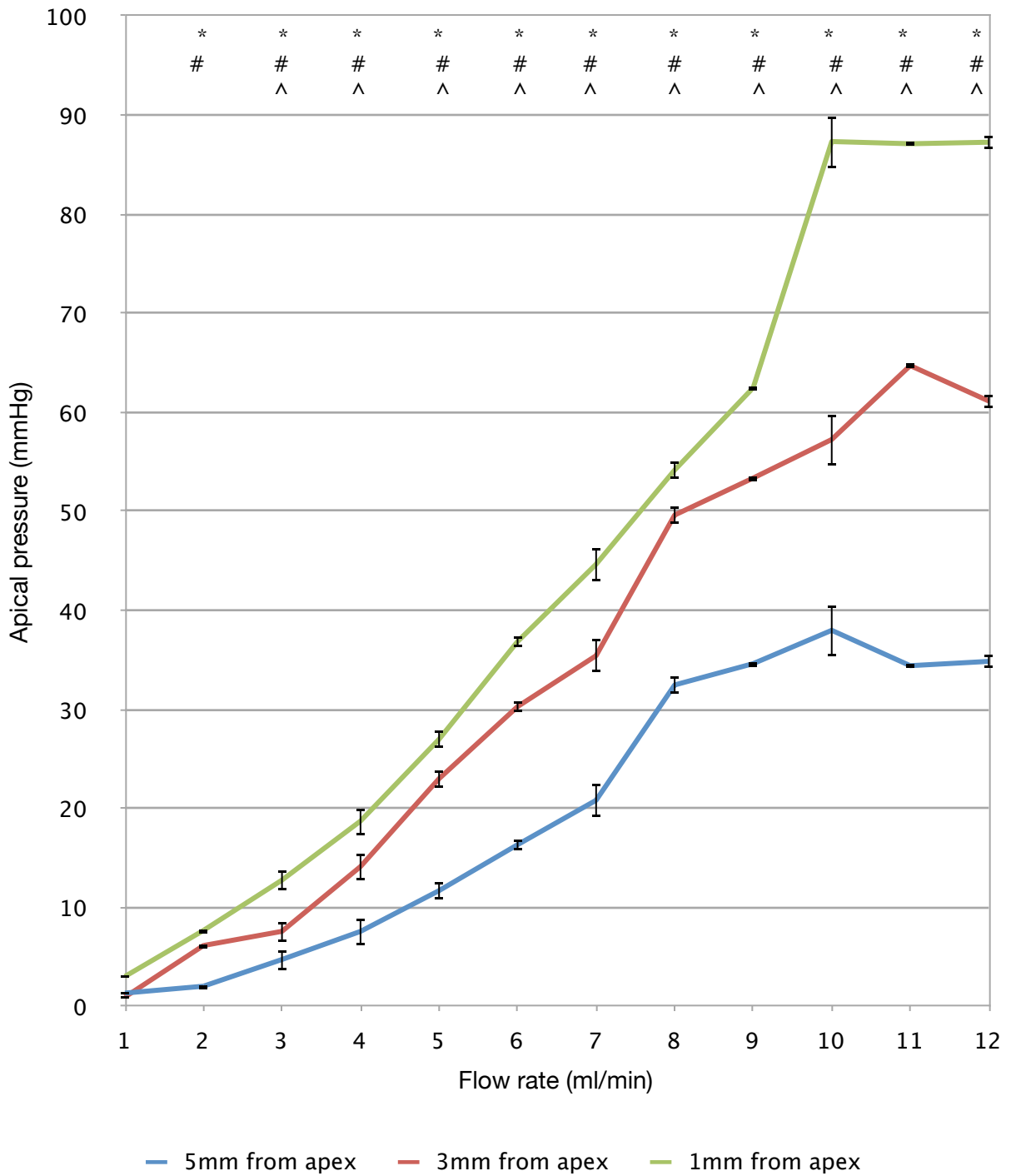
\* statistically significant difference (P<0.05) between placement at 5 mm and 1 mm  
 # statistically significant difference (P<0.05) between placement at 3 mm and 1 mm

**Figure 4.22 Apical pressure measurement during positive pressure irrigation with a 30 gauge side-vented closed-ended (ProRinse) needle**

Source	df	Sum of Squares	Mean Square	F	Sig.	% of total variation
interaction	14	654.9	46.78	14.99	<0.0001	19.72
depth	2	670.4	355.2	107.4	<0.0001	20.18
flow rate	7	1847	263.8	263.8	<0.0001	55.59
error	48	149.8	3.120			

**Table 4.30 Two-way ANOVA for apical pressure during positive pressure irrigation 5 , 3, and 1 mm from the apex with a 30 ga side-vented closed-ended (ProRinse) needle**

**Apical pressure during PPI with a 30 ga blunt open-ended needle**



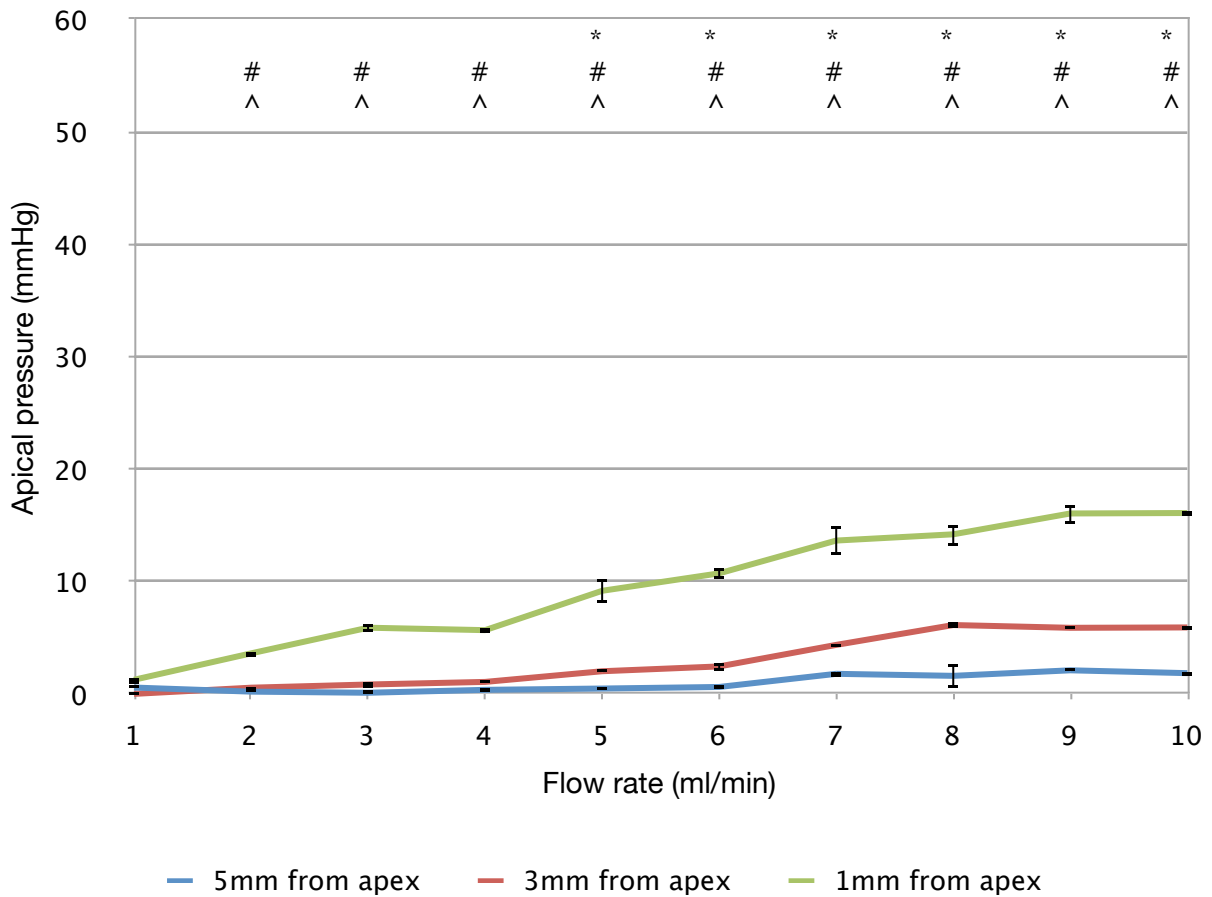
\* statistically significant difference (P<0.05) between placement at 5 mm and 3 mm  
 # statistically significant difference (P<0.05) between placement at 5 mm and 1 mm  
 ^ statistically significant difference (P<0.05) between placement at 3 mm and 1 mm

**Figure 4.23 Apical pressure measurement during positive pressure irrigation with a 30 gauge blunt open-ended (FlexiGlide) needle**

Source	df	Sum of Squares	Mean Square	F	Sig.	% of total variation
interaction	22	5686	258.5	262.5	<0.0001	8.33
depth	2	10583	5291	5373	<0.0001	15.51
flow rate	11	51896	4718	4790	<0.0001	76.05
error	72	70.91	0.9848			

**Table 4.31 Two-way ANOVA for apical pressure during positive pressure irrigation 5 , 3, and 1 mm from the apex with a 30 ga blunt open-ended (FlexiGlide) needle**

### Apical pressure during PPI with an ISO size 32 EndoVac needle



\* statistically significant difference (P<0.05) between placement at 5 mm and 3 mm  
 # statistically significant difference (P<0.05) between placement at 5 mm and 1 mm  
 ^ statistically significant difference (P<0.05) between placement at 3 mm and 1 mm

**Figure 4.24 Apical pressure measurement during positive pressure irrigation with an ISO size 32 closed-ended needle with 12 laterally positioned offset holes (EndoVac)**

Source	df	Sum of Squares	Mean Square	F	Sig.	% of total variation
interaction	18	309.8	17.21	69.92	<0.0001	14.08
depth	2	1238	619.2	2516	<0.0001	56.29
flow rate	9	637.1	70.79	287.6	<0.0001	28.96
error	60	14.77	0.2461			

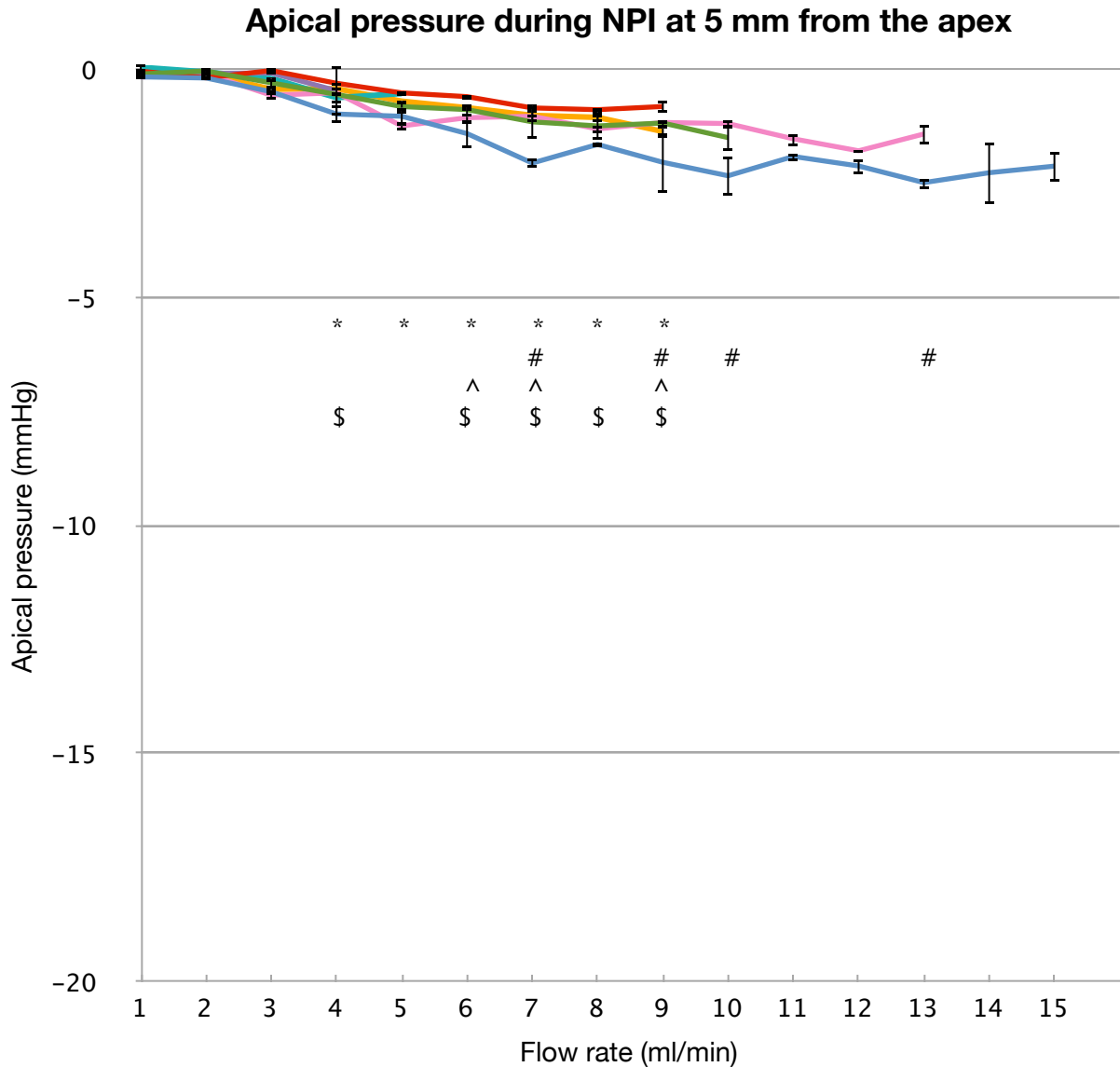
**Table 4.32 Two-way ANOVA for apical pressure during positive pressure irrigation 5, 3, and 1 mm from the apex with an ISO 32 EndoVac needle**

#### **4.4 Apical pressure measurement using negative pressure irrigation**

The apical pressures caused by the irrigant during negative pressure irrigation with all needle tips were negative values. No positive pressures were generated when using negative pressure irrigation, even when the needle tip was placed at 1 mm from the working length. When all of the needles were placed at 5 mm from working length (Figure 4.24), two-way ANOVA revealed significant ( $P < 0.05$ ) interaction (Table 4.33). The results of the post hoc Bonferroni analysis (which excluded the 30 ga ProRinse needle and the 27 ga VistaProbe needle due to the limited range of flow rates achievable with these particular needle designs) revealed intermittent significant differences in apical pressures between the 25 ga blunt open-ended (FlexiGlide) needle and the remaining four needles in the post hoc analysis (Figure 4.24). Overall, the 25 ga blunt open-ended (FlexiGlide) needle was able to achieve the most negative apical pressures compared to the other needle tips. However, all of the needle tips used generated negative (as opposed to positive) apical pressures, not greater than -3 mmHg. When the needles were placed at 3 mm from working length, two-way ANOVA revealed significant interaction ( $P < 0.05$ ) (Table 4.34). The results of the post hoc Bonferroni analysis (which excluded the 30 ga ProRinse needle and the 27 ga VistaProbe needle due to the limited range of flow rates achievable with these particular needle designs) revealed significant differences in apical pressures between the 25 ga blunt open-ended (FlexiGlide) needle and the remaining four needles in the post hoc analysis (Figure 4.25). Overall, the 25 ga blunt open-ended (FlexiGlide) needle was able to achieve the most negative apical pressures compared to the other needle tips, reaching approximately -17 mmHg in the higher range of flow rates.

When the needles were placed at 1 mm from working length, only three needles could be placed at this level in the canal without binding: the 30 gauge blunt open-ended needle (FlexiGlide), the 30 gauge side-vented closed-ended needle (ProRinse), and the EndoVac needle tip (Figure 4.26). Two-way ANOVA revealed significant interaction ( $P < 0.05$ ) (Table 4.35). The results of the post hoc Bonferroni analysis, which excluded the 30 ga ProRinse needle due to the limited range of flow rates achievable with this needle) revealed statistically significant ( $P > 0.05$ ) differences in apical pressure between the 30 ga blunt open-ended (FlexiGlide) needle and the ISO 32 EndoVac needle (Figure 4.26). The 30 ga blunt open-ended needle was able to achieve the most negative apical pressures, not exceeding -17 mmHg at the higher range of irrigation flow rates.

When considering each individual needle separately, all needles showed statistically significant interaction ( $P > 0.05$ ) (Tables 4.36 - 4.42). Post hoc Bonferroni tests were done for all needles, and significant differences illustrated in the figures (Figures 4.27 - 4.33). The most negative apical pressure values were achieved by the 25 ga blunt open-ended (FlexiGlide) needle when placed at 3 mm from the apex, the 30 ga blunt open-ended needle when placed at 1 mm from the apex, and the ISO 32 EndoVac needle when placed at 1 mm from the apex. All needles, however, at all flow rates and depth of placement in the canal generated negative apical pressures during negative pressure irrigation.



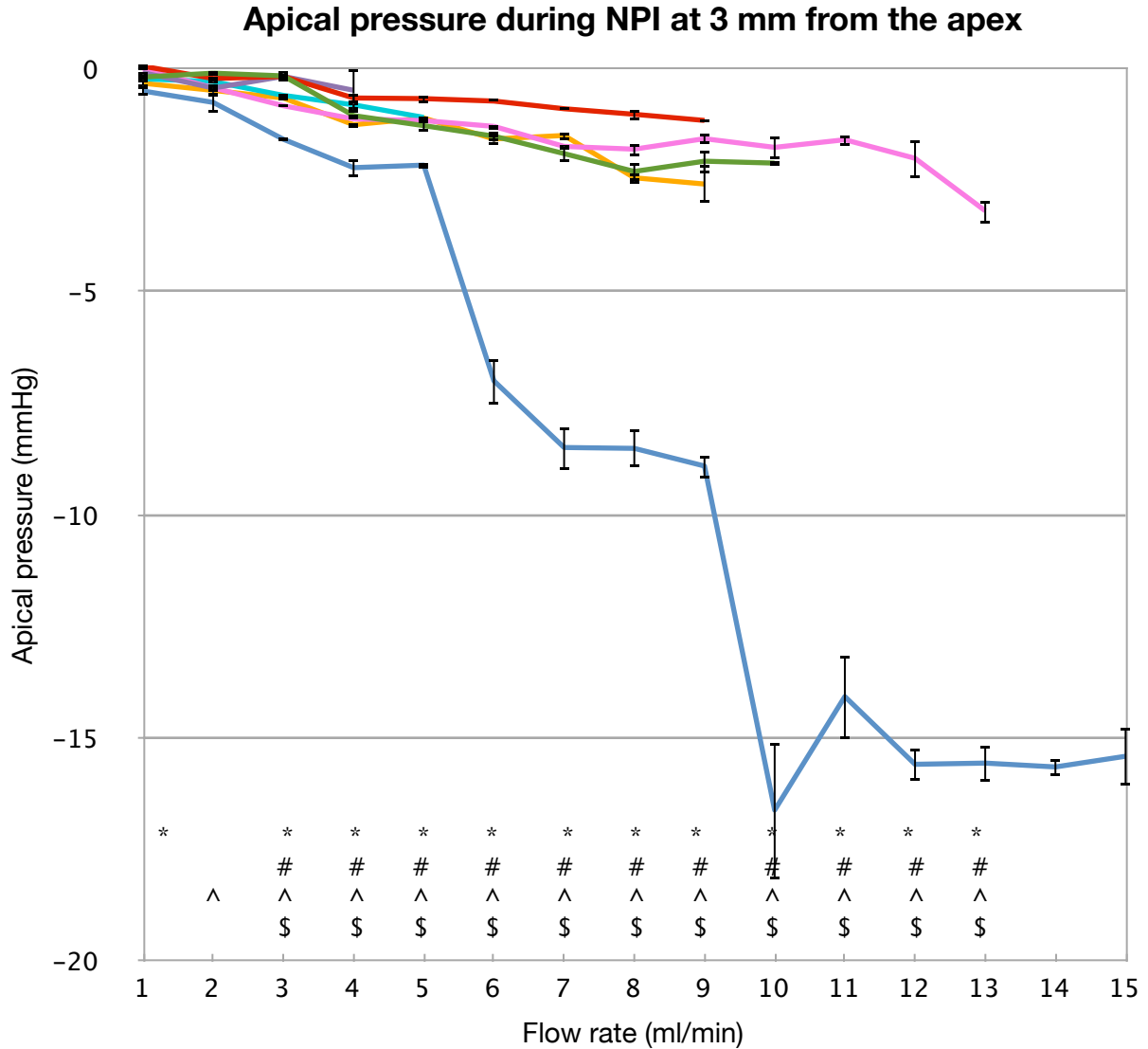
- 25 ga blunt open-ended needle (FlexiGlide)
- 30 ga blunt open-ended needle (FlexiGlide)
- 27 ga slotted open-ended needle (Monoject)
- 30 ga side-vented closed-ended needle (ProRinse)
- 25 ga side-vented closed-ended needle (Max-I-Probe)
- 27 ga side-vented closed-ended needle (VistaProbe)
- ISO 32 closed-ended needle with 12 laterally positioned holes (EndoVac)

\* statistically significant (P<0.05) difference between 25 ga FlexiGlide and 27 ga Monoject  
 # statistically significant (P<0.05) difference between 25 ga Monoject and 25 ga Max-I-Probe  
 ^ statistically significant (P<0.05) difference between 25 ga FlexiGlide and 30 ga FlexiGlide  
 \$ statistically significant (P<0.05) difference between 25 ga FlexiGlide and ISO 32 EndoVac

**Figure 4.25 Apical pressure measurement during negative pressure irrigation at 5 mm from the apex using 7 different irrigation needle tips**

Source	df	Sum of Squares	Mean Square	F	Sig.	% of total variation
interaction	32	3.706	0.1158	4.479	<0.0001	9.51
needle	4	5.960	1.490	57.63	<0.0001	15.30
flow rate	8	26.96	3.370	130.4	<0.0001	69.21
error	90	2.327	0.02586			

**Table 4.33 Two-way ANOVA for apical pressure during negative pressure irrigation 5 mm from the apex with 5 irrigation needles (excludes 30 ga ProRinse, 27 ga VistaProbe) for the flow rate range 1 - 9 ml/min**



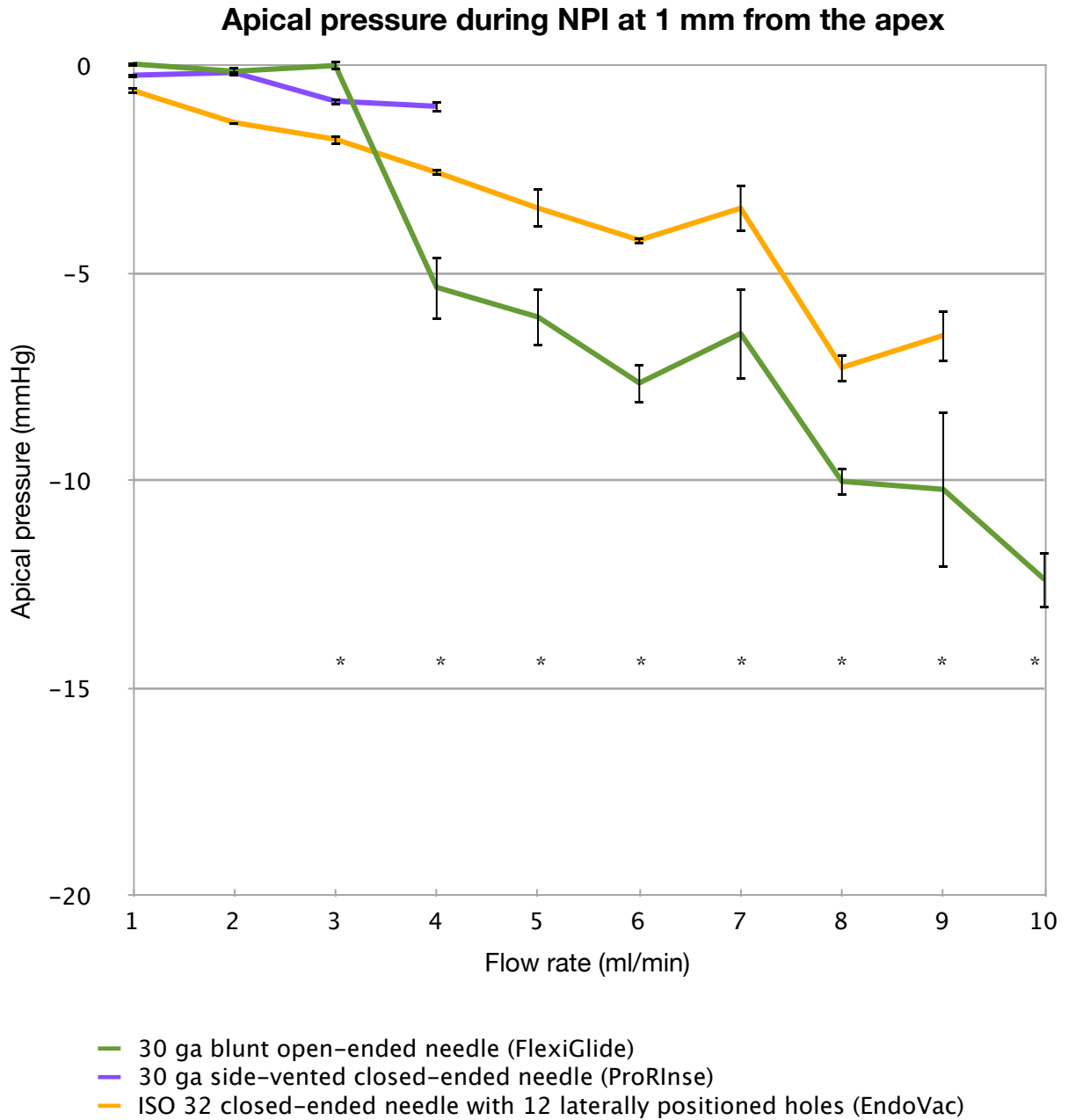
- 25 ga blunt open-ended needle (FlexiGlide)
- 30 ga blunt open-ended needle (FlexiGlide)
- 27 ga slotted open-ended needle (Monoject)
- 30 ga side-vented closed-ended (ProRInse)
- 25 ga side-vented closed-ended (Max-I-Probe)
- 27 ga side-vented closed-ended (VistaProbe)
- ISO 32 closed-ended needle with 12 laterally positioned holes (EndoVac)

\* statistically significant (P<0.05) difference between 25 ga FlexiGlide and 27 ga Monoject  
 # statistically significant (P<0.05) difference between 25 ga FlexiGlide and 25 ga Max-I-Probe  
 ^ statistically significant (P<0.05) difference between 25 ga FlexiGlide and 30 ga FlexiGlide  
 \$ statistically significant (P<0.05) difference between 25 ga FlexiGlide and ISO 32 EndoVac

**Figure 4.26 Apical pressure measurement during negative pressure irrigation at 3 mm from the apex using 7 different irrigation needle tips**

Source	df	Sum of Squares	Mean Square	F	Sig.	% of total variation
interaction	32	185.5	5.796	169.8	<0.0001	29.54
needle	4	258.3	64.57	1892	<0.0001	41.13
flow rate	8	181.1	22.64	663.2	<0.0001	28.84
error	90	3.072	0.03414			

**Table 4.34 Two-way ANOVA for apical pressure during negative pressure irrigation 3 mm from the apex with 5 irrigation needles (excludes 30 ga ProRinse, 27 ga VistaProbe) for the flow rate range 1 - 9 ml/min**



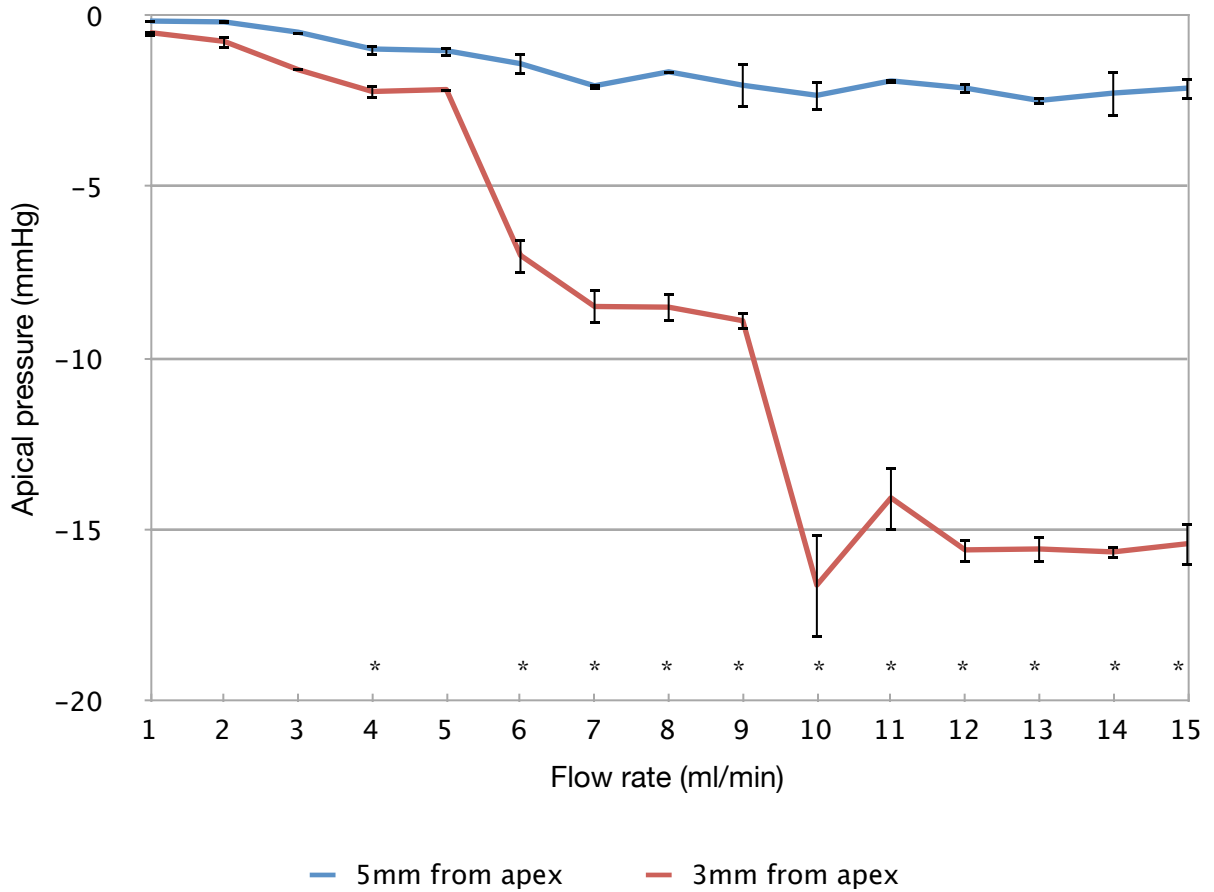
\* statistically significant ( $P < 0.05$ ) difference between 30 ga FlexiGlide and ISO 32 EndoVac

**Figure 4.27** Apical pressure measurement during negative pressure irrigation at 1 mm from the apex using 3 different irrigation needle tips

Source	df	Sum of Squares	Mean Square	F	Sig.	% of total variation
interaction	8	57.04	7.130	17.14	<0.0001	9.79
needle	1	35.83	35.83	86.13	<0.0001	6.15
flow rate	8	474.8	59.35	142.7	<0.0001	81.49
error	36	14.98	0.4160			

**Table 4.35 Two-way ANOVA for apical pressure during negative pressure irrigation 1 mm from the apex with 2 irrigation needles (excludes 30 ga ProRinse) for the flow rate range 1 - 9 ml/min**

**Apical pressure during NPI with a 25 ga blunt open-ended needle**



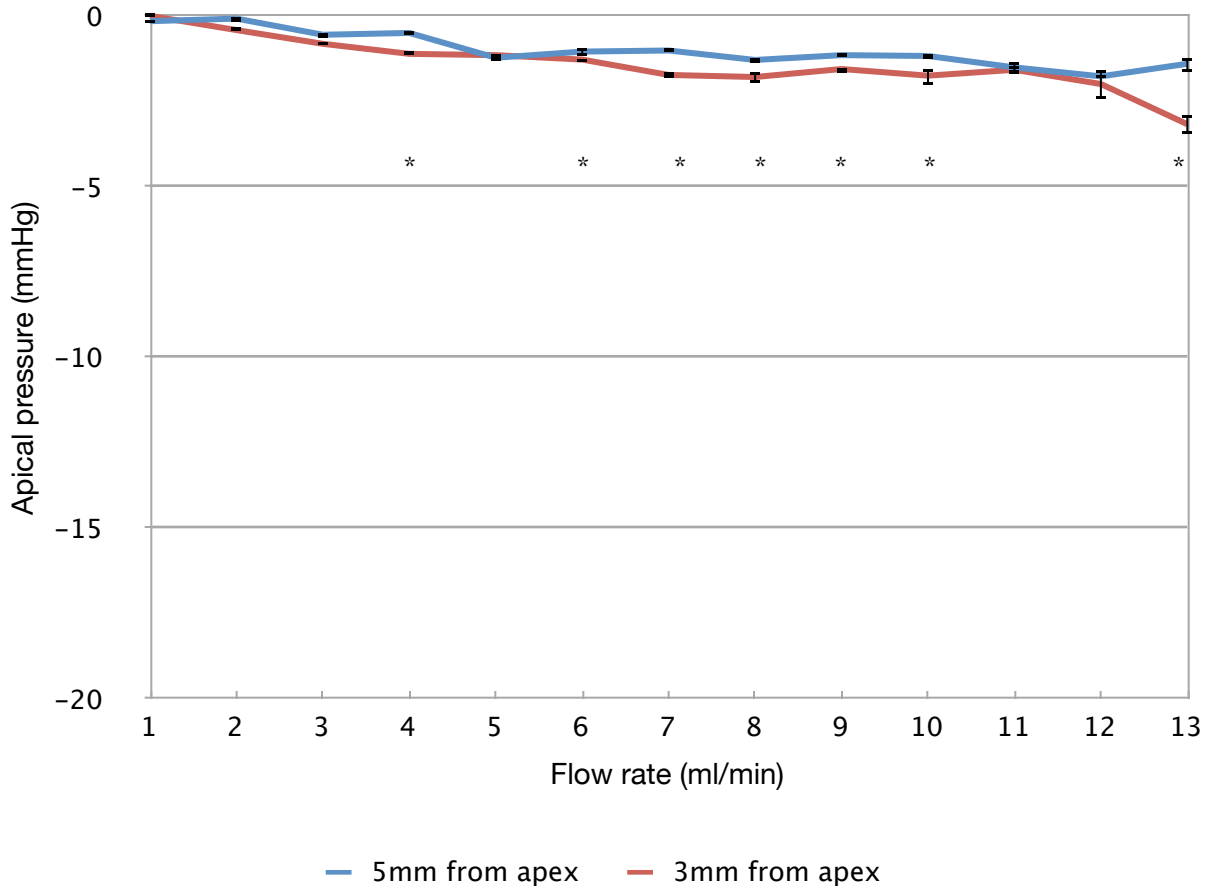
\* statistically significant ( $P < 0.05$ ) difference between placement at 5 mm and 3 mm

**Figure 4.28 Apical pressure during negative pressure irrigation with a 25 ga blunt open-ended (FlexiGlide) needle**

Source	df	Sum of Squares	Mean Square	F	Sig.	% of total variation
interaction	14	642.5	45.90	210.4	<0.0001	22.22
depth	1	1207	1207	5534	<0.0001	41.74
flow rate	14	1209	73.47	336.9	<0.0001	35.58
error	60	13.09	0.2181			

**Table 4.36 Two-way ANOVA for apical pressure during negative pressure irrigation at 5 mm and 3 mm from the apex with a 25 ga blunt open-ended (FlexiGlide) needle**

**Apical pressure during NPI with a 25 ga side-vented closed-ended needle**



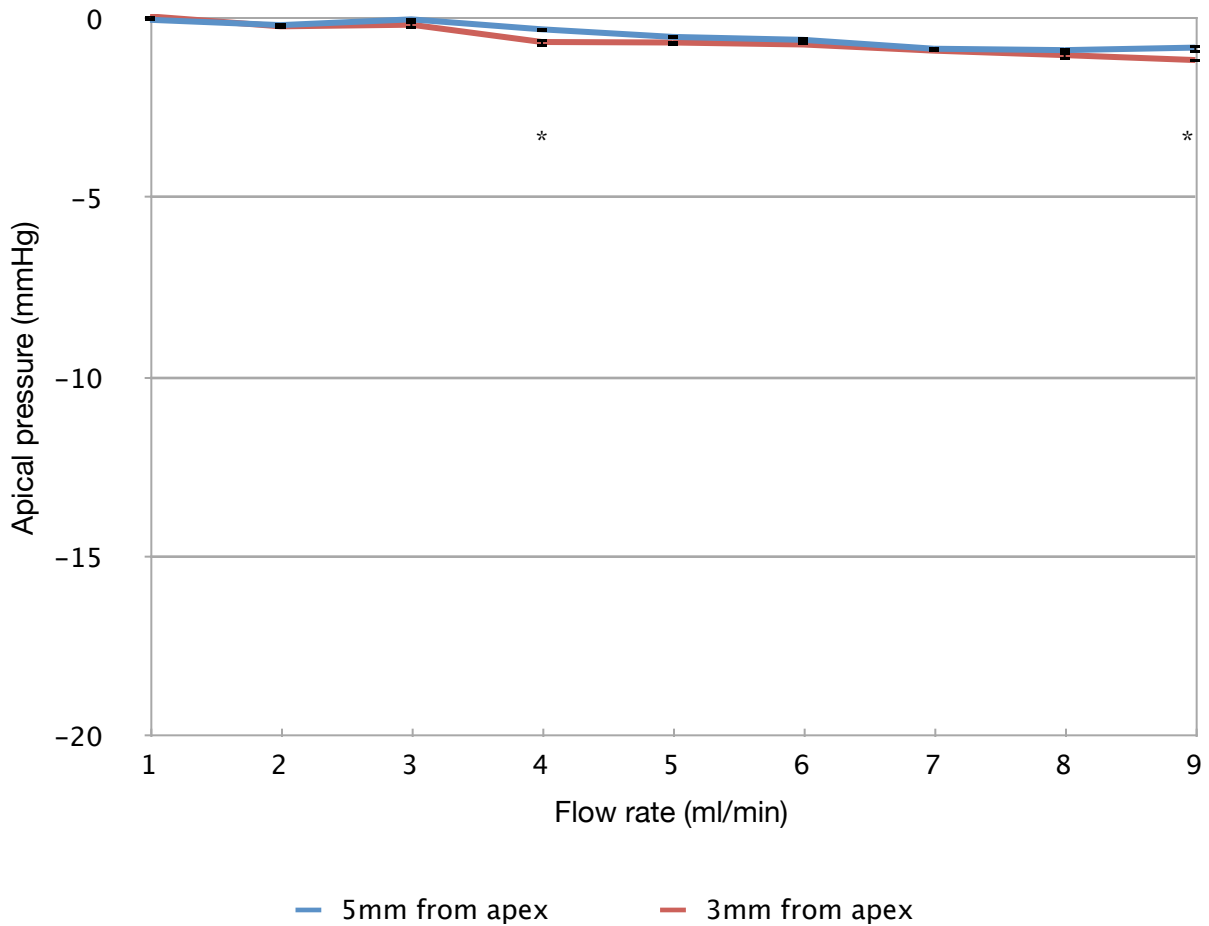
\* statistically significant (P<0.05) difference between placement at 5 mm and 3 mm

**Figure 4.29 Apical pressure during negative pressure irrigation with a 25 ga side-vented closed-ended (Max-I-Probe) needle**

Source	df	Sum of Squares	Mean Square	F	Sig.	% of total variation
interaction	12	4.176	0.3480	15.70	<0.0001	11.48
depth	1	3.466	3.466	156.4	<0.0001	9.53
flow rate	12	27.59	2.299	103.7	<0.0001	75.83
error	52	1.152	0.2216			

**Table 4.37 Two-way ANOVA for apical pressure during negative pressure irrigation at 5 mm & 3 mm from the apex with a 25 ga side-vented closed-ended (Max-I-Probe) needle**

**Apical pressure during NPI with a 27 ga slotted open-ended needle**



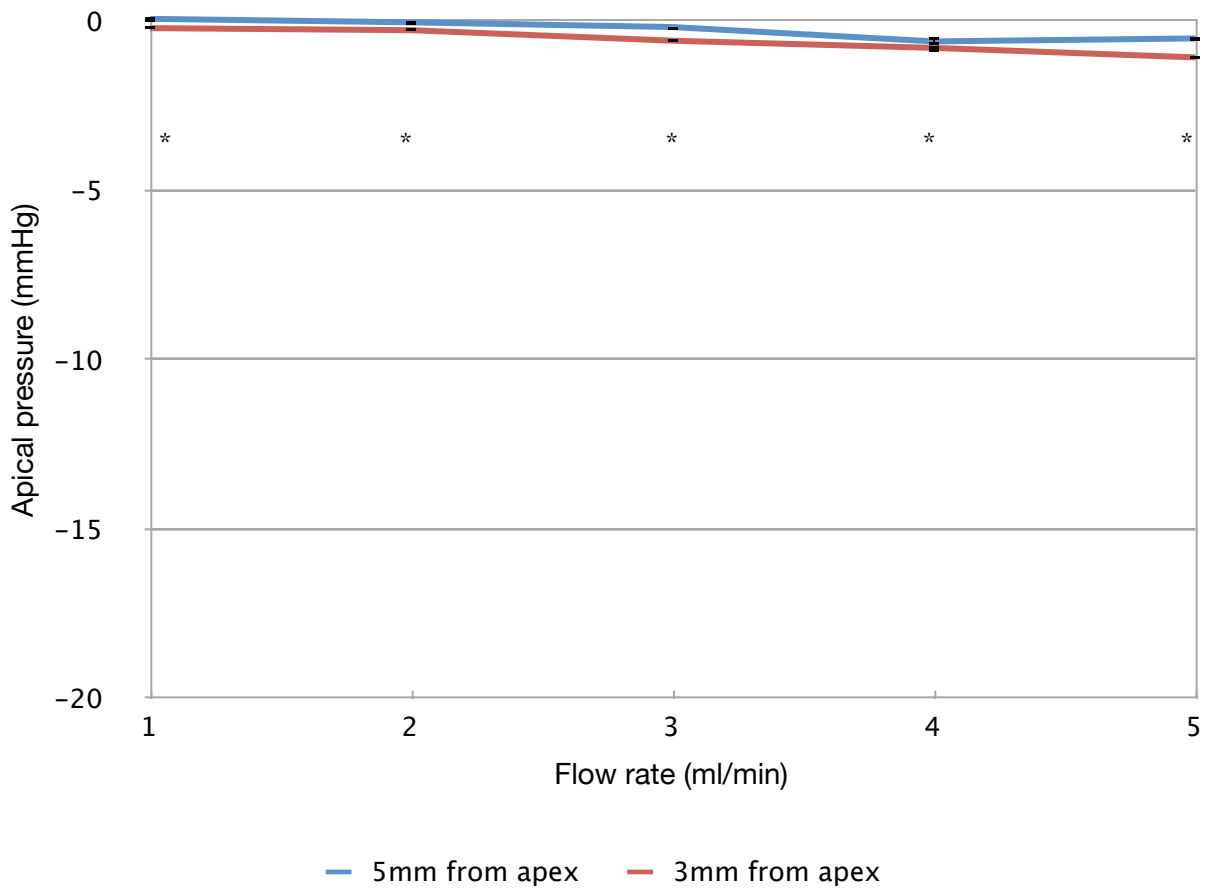
\* statistically significant (P<0.05) difference between placement at 5 mm and 3 mm

**Figure 4.30 Apical pressure during negative pressure irrigation with a 27 ga slotted open-ended (Monoject) needle**

Source	df	Sum of Squares	Mean Square	F	Sig.	% of total variation
interaction	8	0.2442	0.03052	4.570	0.0007	3.29
depth	1	0.2678	0.2678	40.10	<0.0001	3.61
flow rate	8	6.660	0.8324	124.6	<0.0001	89.85
error	36	0.2404	0.006678			

**Table 4.38 Two-way ANOVA for apical pressure during negative pressure irrigation at 5 mm & 3 mm from the apex with a 27 ga slotted open-ended (Monoject) needle**

**Apical pressure during NPI with a 27 ga side-vented closed-ended needle**



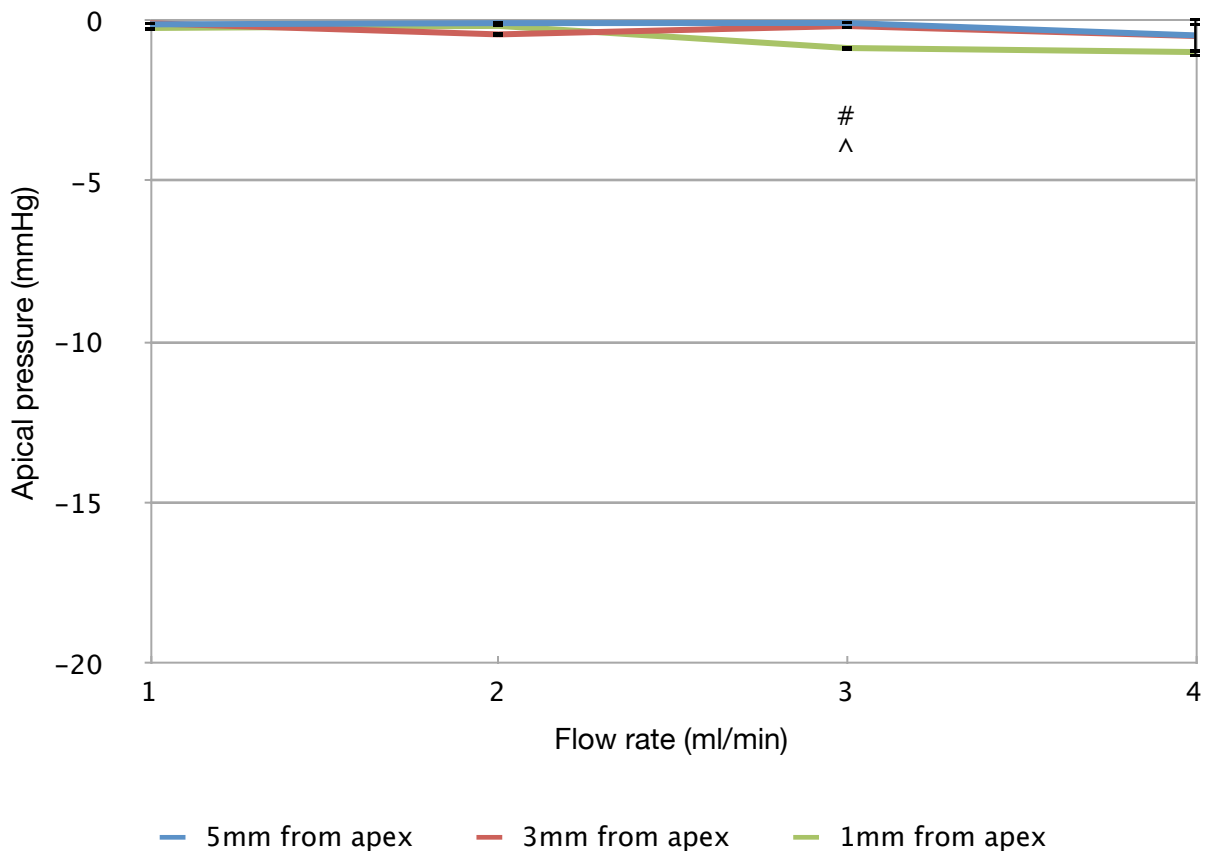
\* statistically significant (P<0.05) difference between placement at 5 mm and 3 mm

**Figure 4.31 Apical pressure during negative pressure irrigation with a 27 ga side-vented closed-ended (VistaProbe) needle**

Source	df	Sum of Squares	Mean Square	F	Sig.	% of total variation
interaction	4	0.1362	0.03405	6.574	0.0015	3.86
depth	1	0.8292	0.8292	160.1	<0.0001	23.52
flow rate	4	2.457	0.6142	118.6	<0.0001	69.68
error	20	0.1036	0.005179			

**Table 4.39 Two-way ANOVA for apical pressure during negative pressure irrigation at 5 mm & 3 mm from the apex with a 27 ga side-vented closed-ended (VistaProbe) needle**

**Apical pressure during NPI with a 30 ga side-vented closed-ended needle**

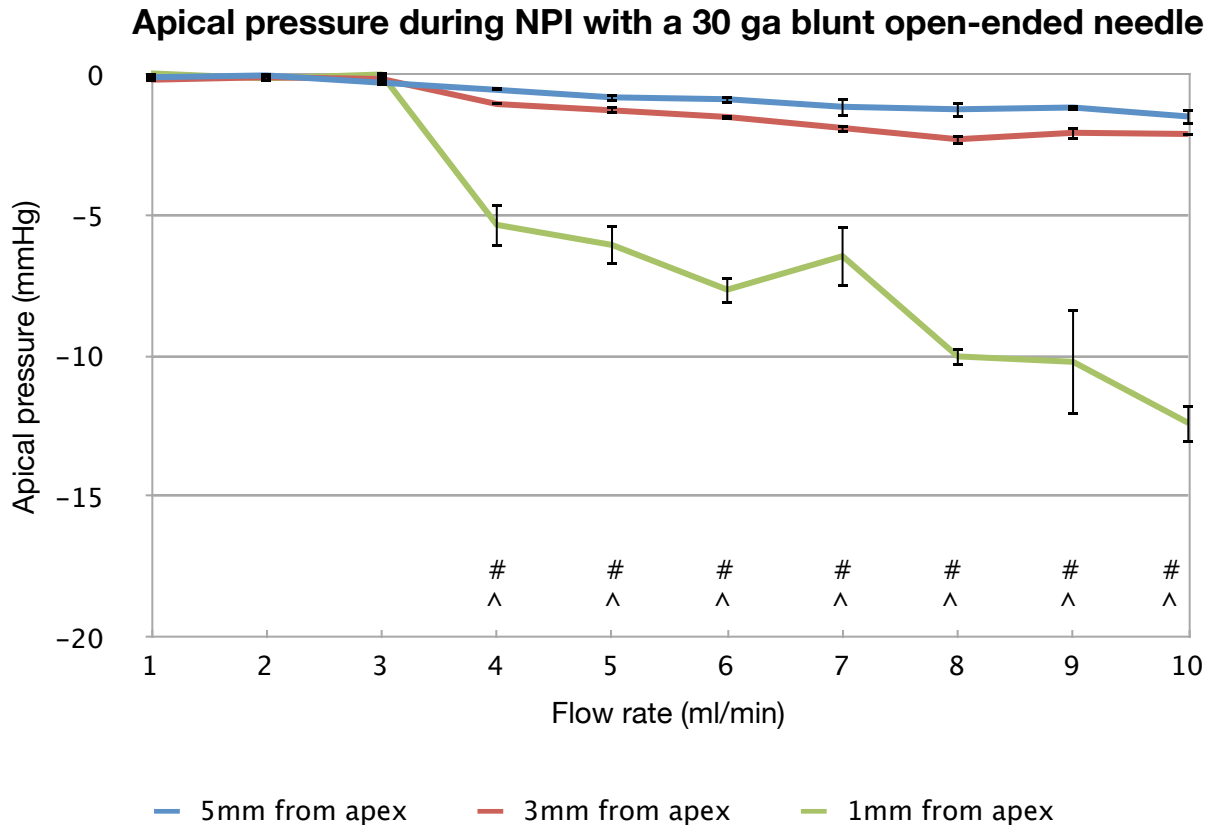


\* statistically significant (P<0.05) difference between placement at 5 mm and 3 mm  
 # statistically significant (P<0.05) difference between placement at 5 mm and 1 mm  
 ^ statistically significant (P<0.05) difference between placement at 3 mm and 1 mm

**Figure 4.32 Apical pressure during negative pressure irrigation with a 30 ga side-vented closed-ended (ProRinse) needle**

Source	df	Sum of Squares	Mean Square	F	Sig.	% of total variation
interaction	6	0.9506	0.1584	3.127	0.0208	21.93
depth	2	0.8897	0.4449	8.781	0.0014	20.53
flow rate	3	1.279	0.4262	8.413	0.0005	29.50
error	24	1.216	0.05066			

**Table 4.40 Two-way ANOVA for apical pressure during negative pressure irrigation at 5 mm & 3 mm from the apex with a 30 ga side-vented closed-ended (ProRinse) needle**

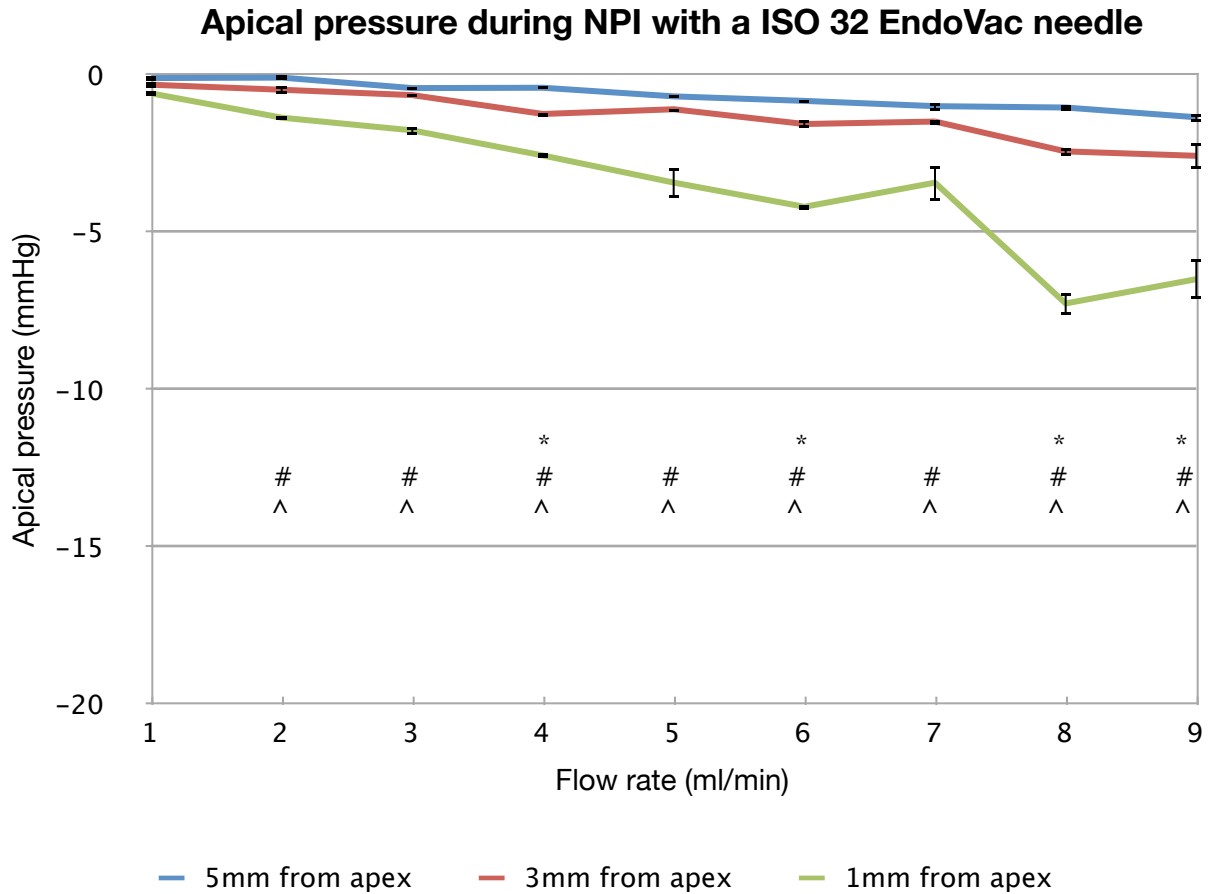


\* statistically significant ( $P < 0.05$ ) difference between placement at 5 mm and 3 mm  
 # statistically significant ( $P < 0.05$ ) difference between placement at 5 mm and 1 mm  
 ^ statistically significant ( $P < 0.05$ ) difference between placement at 3 mm and 1 mm

**Figure 4.33 Apical pressure during negative pressure irrigation with a 30 ga blunt open-ended (FlexiGlide) needle**

Source	df	Sum of Squares	Mean Square	F	Sig.	% of total variation
interaction	18	272.0	15.11	60.86	<0.0001	25.64
depth	2	465.2	232.6	936.6	<0.0001	43.84
flow rate	9	308.9	34.32	138.2	<0.0001	29.11
error	60	14.90	0.2483			

**Table 4.41 Two-way ANOVA for apical pressure during negative pressure irrigation at 5 mm, 3 mm, and 1 mm from the apex with a 30 ga blunt open-ended (FlexiGlide) needle**



\* statistically significant ( $P < 0.05$ ) difference between placement at 5 mm and 3 mm  
 # statistically significant ( $P < 0.05$ ) difference between placement at 5 mm and 1 mm  
 ^ statistically significant ( $P < 0.05$ ) difference between placement at 3 mm and 1 mm

**Figure 4.34** Apical pressure during negative pressure irrigation with an ISO 32 EndoVac needle

Source	df	Sum of Squares	Mean Square	F	Sig.	% of total variation
interaction	16	46.87	2.929	53.09	<0.0001	18.02
depth	2	115.5	57.73	1046	<0.0001	44.40
flow rate	8	94.73	11.84	214.6	<0.0001	36.43
error	54	2.979	0.05517			

**Table 4.42** Two-way ANOVA for apical pressure during negative pressure irrigation at 5 mm, 3 mm, and 1 mm from the apex with an ISO 32 EndoVac needle

## Chapter 5: Discussion

This study describes the first attempt to measure apical pressure during root canal irrigation using an *in vitro* human tooth model. This novel method is reproducible, and represents an exciting way to validate CFD estimations of apical pressure during irrigation; there is potential to use this method to assess safety of current and new irrigating conditions and techniques. The parallel set-up of the measurement of apical pressure and dye clearance using similar root canal models allows the comparison of these two variables, representing a measure of safety, and a measure of effectiveness.

The measurement of the length of dye clearance beyond the end of the irrigating needle tips used in this study revealed that in the clinically relevant range of flow rates from 1-15 ml/min, there was no further increase of clearance of dye at irrigation flow rates beyond 4 ml/min for all needle tip designs and sizes used during positive pressure irrigation. This was also demonstrated by the use of two-way ANOVA on a subsets of the data group from the flow rate range of 4 - 8 ml/min, indicating that flow rate was not a significant source of the total variation in the data. The two needle tips that were able to clear the greatest length of dye during positive pressure irrigation were a 30 gauge blunt open-ended needle tip, and a 27 gauge slot tipped needle. As both of the aforementioned needles are equally effective in irrigant replenishment in a canal, then it is logical to use the needle tip that is designed to vent irrigant laterally instead of apically for increased patient safety. It is important to consider that all of the needles (excluding the EndoVac needle) used during positive pressure irrigation cleared a length of dye within a 1 mm range of each other; should needles of varying sizes and designs have similar efficacy, then a clinician should choose a smaller

needle size, and a needle design that promotes lateral shunting of the irrigant flow, rather than directing the irrigant flow directly toward the apex of the tooth. Thus, in choosing a needle design and size for root canal irrigation, a 27 gauge or 30 gauge safe needle design can allow replenishment of irrigant as effectively as a 30 gauge blunt open-ended needle tip. A CFD study compared two 30 gauge needles of different design, and found that a blunt open-ended needle tip design was able to fully replace irrigant in a canal when placed 2 mm from the working length, while a side-vented closed-ended needle tip needed to be placed at 1 mm from the working length in order to fully clear irrigant to the apex (Boutsioukis et al., 2010a). The current *in vitro* study also found similar trends with the same needles; the 30 gauge blunt open-ended needle was able to achieve almost 1 mm more dye clearance than the 30 gauge side-vented closed-ended needle tip, but irrigation efficacy needs to be balanced with patient safety considerations and the absolute length of irrigant replenishment cannot be the sole factor in choosing an irrigation needle tip. This very concern is reinforced by the significant interaction found by two-way ANOVA between needle design, flow rate, and depth of needle placement in almost every irrigation experiment in this study.

Although the experimental set-up of using a clear plastic block filled with a dye or some other measurable fluid preparation has been used in previous studies, the irrigation flow rate used in these previous studies was either not mentioned (Ram, 1977; Kahn et al., 1995), or was not the focus of the experiment, resulting in the use of just one irrigation flow rate, such as 12 ml/min (Bronnec et al., 2010) or 16 ml/min (Chow, 1983). One study used an irrigation flow rate of 45 ml/min with a large 23 gauge needle (Salzgeber & Brilliant, 1977), which does not represent contemporary irrigation practices. In examining the dye clearance from a

range of 1 - 15 ml/min during irrigation, a range that was found to be clinically relevant with the smaller gauge needles recommended for use, a potentially important finding of no further clearance of dye, regardless of depth of placement on the canal, beyond irrigation flow rates of 4 ml/min represents one step toward understanding what contribution irrigation flow rate may have on the extent of replenishment of irrigant in a root canal. It calls into question the belief some clinicians may have that the use of higher irrigation flow rates (and higher irrigation pressures) will result in the irrigant travelling further apically into the root canal. The finding in the current study that higher irrigation flow rates may not necessarily result in greater lengths of irrigant replenishment appears to be supported by a study where the use of irrigation pressures well beyond clinical relevance did not result in considerably greater dye clearance (Ram, 1977). However, the two studies cannot be easily compared as this particular study did not mention the irrigation flow rate used, and also loosely placed the irrigation needle into the coronal third of the root. The presence of a stagnation plane or dead water zone in our study is also in agreement with the results of current CFD studies of root canal fluid flow.

Using simulated irrigation flow rates of 1.2 ml/min, 8.4 ml/min, and 15.6 ml/min in CFD modelling, one study found that irrigant replacement was limited to 1 mm beyond the end of the needle tip, while irrigation flow rates of 31.8 ml/min and 47.4 ml/min resulted in irrigant replacement of 1.5 mm beyond the end of the needle tip (Boutsioukis et al., 2009). Even though the higher flow rates used resulted in more turbulence around the needle outlet and in the immediate apical region, the irrigant replacement effect was still limited to 1-1.5 mm.

A CFD study by another research group showed that almost 3 mm of irrigant replacement was possible (Shen et al., 2010); possible reasons for the differences between these two CFD studies are the different experimental settings and a different CFD turbulence model.

Similar to positive pressure irrigation, the length of dye clearance during negative pressure irrigation is not significantly affected by flow rate. If a greater distance of dye clearance from the end of the needle tip is an indication for greater irrigation efficacy, then our results show that needle design influences negative pressure irrigation efficacy. The blunt open-ended needle design, especially the 25 gauge and 30 gauge blunt open-ended (FlexiGlide) needle used in this study, is more efficacious in this respect. There are no negative pressure irrigation CFD studies or other *in vitro* dye irrigation studies with which to compare our results of length of irrigant replacement.

As mentioned previously, this study describes the first attempt to measure apical pressure during root canal irrigation using an *in vitro* human tooth model. Our results show that the apical pressure created by the irrigant through the needle tip during positive and negative pressure irrigation is affected by flow rate, depth of placement inside the root canal, and needle design.

During positive pressure irrigation, the 25 gauge and 30 gauge blunt open-ended needles, as well as larger sized needles with design elements allowing lateral shunting of irrigant, created significantly higher apical pressures than other needle safe needle designs in smaller sizes.

This seems to support the overall effectiveness of the needle tips designed to enhance patient safety. However, clinicians must still be cautious; when the smaller needles were placed at

1 mm from the working length, both the blunt open-ended needle tip and the side-vented closed-ended needle tip created high and unpredictable apical pressures. It is not known whether this unpredictability in apical pressure when this particular needle is placed at 1 mm from the working length is a realistic representation of what might happen in a clinical scenario. It is possible that the unpredictable apical pressures could have been created by differences in positional placement of the needle; for instance, should the side-venting portion of the needle have been partially blocked by curvature in the root canal, this may have resulted in more apical shunting of the irrigant. It is also possible that slight differences in the depth of placement, such as a difference of 0.5 mm in the apical placement of the needle caused by the investigator, may have caused the unpredictable apical pressures.

The range of apical pressures generated during positive pressure irrigation in the current study shows good agreement with the range of pressures calculated using CFD analysis in a previous study (Shen et al., 2010). The irrigation flow rate used in this CFD study was 6 ml/min. If the minimum and maximum apical pressure measurement calculated in this CFD study is converted into the pressure units used in our study for a similar needle design and size, the apical pressure range is similar. The CFD study range would be 8 - 12 mmHg, in comparison to our range of 5 - 15 mmHg. Another estimation of apical pressure through CFD analysis exists through a study done by another research group (Boutsioukis et al., 2010c). In trying to compare apical pressures for the most similar flow rate conditions and needle design and size, their pressure range appears to be much higher than our closest in vitro result. However, these differences can be attributed to different experimental settings and different turbulence models.

Capillary pressure in the human body is approximately 25 mmHg in the capillary bed, 30 - 40 mmHg in the arterial end of the capillaries, and 10 - 15 mmHg on the venous end (Guyton and Hall, 2006). Lymphatic capillary pressure, although often presenting with a range of values, is generally lower than 10 mmHg (Zaugg-Vesti et al., 1993). It is not known exactly what conditions lead to a sodium hypochlorite extrusion accident, but it is logical to assume that the periapical and pulp capillaries at the venous end are a possible entry site of irrigant into the tissues. It thus seems logical that the apical pressure delivered by the irrigant should not exceed that of the capillaries. Our data demonstrates that it is quite easy to exceed capillary pressure when the needle is close to the working length, even at low flow rates. The “safe” needle design seems to confer an effective safety benefit.

During negative pressure irrigation, no positive apical pressures were generated by any of the needles. This result supports existing studies pointing to negative pressure irrigation as a safe method of irrigation with little risk of irrigant extrusion (Desai & Himel, 2009; Mitchell et al., 2010). There is likely no risk in having increasing negative apical pressures as seen with the blunt open-ended needle tips, especially at the low irrigation flow rates used in this study. Considering the results of the two parts of the current study together seems to be a step toward being able to provide a safe and effective guideline for irrigation of root canals.

During positive pressure irrigation, small gauge safety irrigation needles have been shown to be comparably effective to large and small gauge blunt open-ended irrigation needles in irrigant replenishment. When evaluating dye clearance beyond the end of the needle tip during positive pressure irrigation, it was demonstrated that above a flow rate of 4 ml/min, the dye clearance remained unchanged. A strong increase in apical pressure above

irrigation flow rates of 4 ml/min was also demonstrated with these needle tips. Therefore, in order to avoid high apical pressures and yet, gain maximum clearance of dye, one can use lower irrigation flow rates with small gauge needles using a safety design, without the concern of sacrificing irrigation effectiveness and poor replenishment of irrigant.

During negative pressure irrigation, large and small gauge blunt open-ended irrigation needles were able to replenish irrigant beyond the needle tip more effectively than other needle designs at flow rates beyond 4 ml/min. No positive apical pressures were generated, even when the needles were placed at 1 mm from working length at the higher range of flow rates used in this study. Therefore, in order to gain maximum clearance of dye, knowing that no positive apical pressures are generated at any flow rate used in this study, a blunt open-ended needle would be the most effective needle design for use with negative pressure irrigation. Due to the apparent difficulty in achieving higher flow rates with certain needle designs, such as the 30 ga side-vented closed-ended needle used in this study during negative pressure irrigation, it may not be a practical needle design for use.

The current study has limitations in its generalizability to all root canals, as this study used a single apical preparation size and taper for the entire study. An apical preparation size of ISO 35 (0.35 mm) and a 6% taper was chosen, as this represents a common preparation end point for many practitioners and enables the placement of certain needles very close to the apical foramen. Sources of error include challenges in maintaining a system sealed against the leakage of air despite the use of adhesive sealants to seal connections between irrigation needle tips and tubing. There is also an inherent ebbing that exists in the delivery of irrigant through a peristaltic pump. This was addressed by using a peristaltic pump with multiple

rollers in an attempt to achieve a smooth flow of irrigant. The side of the side vent in the various sizes of side-vented closed-ended needles will also necessarily vary due to differences in the size of the needle barrel. Future studies should include a variety of preparations, to investigate the effect of apical preparation size and canal taper on apical pressure and irrigant replenishment. Other factors possibly influencing apical pressure and irrigant replenishment such as anastomoses between canals and severe canal curvature should also be considered in future research.

## **Chapter 6: Conclusion**

This investigation revealed some interesting and unexpected results, especially compared to the original hypotheses at the start of this study. We hypothesized that during positive pressure irrigation, the larger blunt open-ended needles without safety mechanisms incorporated into the design would yield the highest apical pressures and the greatest clearance of dye. It was an important finding of this study that the irrigation needles designed to laterally shunt the irrigant for increased safety were able to provide comparable dye clearance, in addition to the lower apical pressures as we had predicted. We can conclude that very little sacrifice in irrigation efficacy will result from the use of safe irrigation needle tips. During negative pressure irrigation, we hypothesized correctly that all of the needles would not generate positive apical pressures, but to our surprise, certain needle designs were able to clear dye ahead of the needle tip to a considerable extent, comparable to even positive pressure irrigation conditions. The ability of a needle tip to exchange irrigant for some distance beyond the end of the needle tip represents an advantage in moderate to severely curved canals. We had originally hypothesized that dye clearance would be limited to the end of the needle tip regardless of needle design. Thus, if certain needle designs used during negative pressure irrigation are able to achieve irrigation effectiveness comparable to that achieved with positive pressure irrigation, but without the generation of any positive apical pressures, negative pressure irrigation represents an extremely safe and comparably effective method of endodontic irrigation.

The model described provides a reproducible assessment of apical pressure during irrigation. Increasing positive or negative apical pressure is dependent upon increasing flow rate, needle

design, and depth of needle placement. The apical pressure at high irrigation flow rates during positive pressure irrigation can be several times higher than at low flow rates, yet there is no further clearance of dye above 4 ml/min. If apical clearance of dye beyond the needle tip is a measure of irrigation effectiveness, the results show that maximum effectiveness during positive pressure irrigation can be gained at specifically determined flow rates and with safe apical pressures. During negative pressure irrigation, there is also no further clearance of dye above 4 ml/min, but no positive apical pressures are generated, which confers a great safety benefit for the patient. Maximum effectiveness during negative pressure irrigation can also be gained at specifically determined flow rates, but irrigation needle tip design has a significant influence on apical clearance of dye.

For the endodontic clinician, positive pressure irrigation should be performed with a small gauge needle, such as a 30 gauge needle, with a design that is side-vented and closed-ended. Based on the results of this study, there is no requirement to irrigate at a very high flow rate, and a gentle irrigation pressure yielding approximately 4 ml/min will achieve the maximum length of irrigant exchange. This will allow clinicians to feel more confidence when irrigating in the apical third of the root canal, but the clinician must still be wary of unpredictable oscillations in apical pressure. A clinician should be forward thinking in adopting negative pressure irrigation into their practice, which has as its benefits the generation of only negative apical pressures even when the needle is placed very close to the apical foramen, and replenishment of irrigant comparable to positive pressure irrigation. A blunt open-ended needle design would be most effective for this purpose.

## References

1. Abou-Rass, M., & Piccinino, M. V. (1982). The effectiveness of four clinical irrigation methods on the removal of root canal debris. *Oral surgery, oral medicine, and oral pathology*, 54(3), 323–328.
2. Ahmad, M., & Ford, T. P. (1987). Ultrasonic debridement of root canals: acoustic streaming and its possible role. *Journal of endodontics*.10(13), 490-499.
3. Al-Jadaa, A., Paqué, F., Attin, T., & Zehnder, M. (2009). Acoustic hypochlorite activation in simulated curved canals. *Journal of endodontics*, 35(10), 1408–1411.
4. Alves, F. R. F., Almeida, B. M., Neves, M. A. S., Moreno, J. O., Rôças, I. N., & Siqueira, J. F. (2011). Disinfecting oval-shaped root canals: effectiveness of different supplementary approaches. *Journal of endodontics*, 37(4), 496–501.
5. Baker, N. A., Eleazer, P. D., Averbach, R. E., & Seltzer, S. (1975). Scanning electron microscopic study of the efficacy of various irrigating solutions. *Journal of endodontics*, 1(4), 127–135.
6. Becker, G. L., Cohen, S., & Borer, R. (1974). The sequelae of accidentally injecting sodium hypochlorite beyond the root apex. Report of a case. *Oral surgery, oral medicine, and oral pathology*, 38(4), 633–638.
7. Bergenholtz, G. (1974). Micro-organisms from necrotic pulp of traumatized teeth. *Odontologisk revy*, 25(4), 347–358.

8. Blank-Gonçalves, L. M., Nabeshima, C. K., Martins, G. H. R., & Machado, M. E. de L. (2011). Qualitative analysis of the removal of the smear layer in the apical third of curved roots: conventional irrigation versus activation systems. *Journal of endodontics*, 37(9), 1268–1271.
9. Boutsoukis, C., Lambrianidis, T., & Kastrinakis, E. (2009). Irrigant flow within a prepared root canal using various flow rates: a Computational Fluid Dynamics study. *International endodontic journal*, 42(2), 144–155. doi:10.1111/j.1365-2591.2008.01503.
10. Boutsoukis, C., Lambrianidis, T., Kastrinakis, E., & Bekiaroglou, P. (2007). Measurement of pressure and flow rates during irrigation of a root canal ex vivo with three endodontic needles. *International endodontic journal*, 40(7), 504–513.
11. Boutsoukis, C., Lambrianidis, T., Verhaagen, B., Versluis, M., Kastrinakis, E., Wesselink, P. R., & van der Sluis, L. W. M. (2010a). The effect of needle-insertion depth on the irrigant flow in the root canal: evaluation using an unsteady computational fluid dynamics model. *Journal of endodontics*, 36(10), 1664–1668.
12. Boutsoukis, C., Verhaagen, B., Versluis, M., Kastrinakis, E., & Van der Sluis, L. W. M. (2010b). Irrigant flow in the root canal: experimental validation of an unsteady Computational Fluid Dynamics model using high-speed imaging. *International endodontic journal*, 43(5), 393–403.

13. Boutsoukis, C., Verhaagen, B., Versluis, M., Kastrinakis, E., Wesselink, P. R., & van der Sluis, L. W. M. (2010c). Evaluation of irrigant flow in the root canal using different needle types by an unsteady computational fluid dynamics model. *Journal of endodontics*, 36(5), 875–879.
14. Bowden, J. R., Ethunandan, M., & Brennan, P. A. (2006). Life-threatening airway obstruction secondary to hypochlorite extrusion during root canal treatment. *Oral surgery, oral medicine, oral pathology, oral radiology, and endodontics*, 101(3), 402–404.
15. Bradford, C. E., Eleazer, P. D., Downs, K. E., & Scheetz, J. P. (2002). Apical pressures developed by needles for canal irrigation. *Journal of endodontics*, 28(4), 333–335.
16. Brito, P. R. R., Souza, L. C., Machado de Oliveira, J. C., Alves, F. R. F., De-Deus, G., Lopes, H. P., & Siqueira, J. F. (2009). Comparison of the effectiveness of three irrigation techniques in reducing intracanal *Enterococcus faecalis* populations: an in vitro study. *Journal of endodontics*, 35(10), 1422–1427.
17. Bronnec, F., Bouillaguet, S., & Machtou, P. (2010). Ex vivo assessment of irrigant penetration and renewal during the final irrigation regimen. *International endodontic journal*, 43(8), 663–672.
18. Brown, D. C., Moore, B. K., Brown, C. E., & Newton, C. W. (1995). An in vitro study of apical extrusion of sodium hypochlorite during endodontic canal preparation. *Journal of endodontics*, 21(12), 587–591.

19. Byström, A., & Sundqvist, G. (1981). Bacteriologic evaluation of the efficacy of mechanical root canal instrumentation in endodontic therapy. *Scandinavian journal of dental research*, 89(4), 321–328.
20. Byström, A., & Sundqvist, G. (1983). Bacteriologic evaluation of the effect of 0.5 percent sodium hypochlorite in endodontic therapy. *Oral surgery, oral medicine, and oral pathology*, 55(3), 307–312.
21. Chow, T. W. (1983). Mechanical effectiveness of root canal irrigation. *Journal of endodontics*, 9(11), 475–479.
22. Dalton, B. C., Ørstavik, D., Phillips, C., Pettiette, M., & Trope, M. (1998). Bacterial reduction with nickel-titanium rotary instrumentation. *Journal of endodontics*, 24(11), 763–767.
23. de Gregorio, C., Estevez, R., Cisneros, R., Heilborn, C., & Cohenca, N. (2009). Effect of EDTA, sonic, and ultrasonic activation on the penetration of sodium hypochlorite into simulated lateral canals: an in vitro study. *Journal of endodontics*, 35(6), 891–895.
24. de Gregorio, C., Estevez, R., Cisneros, R., Paranjpe, A., & Cohenca, N. (2010). Efficacy of different irrigation and activation systems on the penetration of sodium hypochlorite into simulated lateral canals and up to working length: an in vitro study. *Journal of endodontics*, 36(7), 1216–1221.
25. Desai, P., & Himel, V. (2009). Comparative safety of various intracanal irrigation systems. *Journal of endodontics*, 35(4), 545–549.

26. Druttman, A. C., & Stock, C. J. (1989). An in vitro comparison of ultrasonic and conventional methods of irrigant replacement. *International endodontic journal*, 22(4), 174–178.
27. Endal, U., Shen, Y., Knut, A., Gao, Y., & Haapasalo, M. (2011). A high-resolution computed tomographic study of changes in root canal isthmus area by instrumentation and root filling. *Journal of endodontics*, 37(2), 223–227.
28. Fukumoto, Y., Kikuchi, I., Yoshioka, T., Kobayashi, C., & Suda, H. (2006). An ex vivo evaluation of a new root canal irrigation technique with intracanal aspiration. *International endodontic journal*, 39(2), 93–99.
29. Gao, Y., Haapasalo, M., Shen, Y., Wu, H., Li, B., Ruse, N. D., & Zhou, X. (2009). Development and validation of a three-dimensional computational fluid dynamics model of root canal irrigation. *Journal of endodontics*, 35(9), 1282–1287.
30. Gondim, E., Setzer, F. C., Carmo, Dos, C. B., & Kim, S. (2010). Postoperative pain after the application of two different irrigation devices in a prospective randomized clinical trial. *Journal of endodontics*, 36(8), 1295–1301.
31. Grossman, L. (1982). Solution of pulp tissue by chemical agents. *Journal of endodontics*.
32. Gulabivala, K., Ng, Y.-L., Gilbertson, M., & Eames, I. (2010). The fluid mechanics of root canal irrigation. *Physiological measurement*, 31(12), R49–84.
33. Gulabivala, K., Patel, B., & Evans, G. (2005). Effects of mechanical and chemical procedures on root canal surfaces. *Endodontic topics*. 10(1), 103-122.
34. Guyton, A.C., Hall, J.E. (2006). *Textbook of medical physiology* (11<sup>th</sup> ed.). Philadelphia, PA: Elsevier Inc.

35. Haapasalo, M., Shen, Y., Qian, W., & Gao, Y. (2010). Irrigation in endodontics. *Dental clinics of North America*, 54(2), 291–312.
36. Hockett, J. L., Dommisch, J. K., Johnson, J. D., & Cohenca, N. (2008). Antimicrobial efficacy of two irrigation techniques in tapered and nontapered canal preparations: an in vitro study. *Journal of endodontics*, 34(11), 1374–1377.
37. Hsieh, Y. D., Gau, C. H., Kung Wu, S. F., Shen, E. C., Hsu, P. W., & Fu, E. (2007). Dynamic recording of irrigating fluid distribution in root canals using thermal image analysis. *International endodontic journal*, 40(1), 11–17.
38. Huang, T., & Gulabivala, K. (2008). A bio-molecular film ex-vivo model to evaluate the influence of canal dimensions and irrigation variables on the efficacy of irrigation. *International endodontic journal*, 41(1), 60-71.
39. Hülsmann, M., & Hahn, W. (2000). Complications during root canal irrigation--literature review and case reports. *International endodontic journal*, 33(3), 186–193.
40. Jiang, L.-M., Verhaagen, B., Versluis, M., & van der Sluis, L. W. M. (2010). Evaluation of a Sonic Device Designed to Activate Irrigant in the Root Canal. *Journal of endodontics*, 36(1), 143–146.
41. Kahn, F. H., Rosenberg, P. A., & Gliksberg, J. (1995). An in vitro evaluation of the irrigating characteristics of ultrasonic and subsonic handpieces and irrigating needles and probes. *Journal of endodontics*, 21(5), 277–280.
42. Kakehasi, S., Stanley, H. R., & Fitzgerald R. J. (1965). The effects of surgical exposures of dental pulps in germ-free and conventional laboratory rats. *Oral surgery, oral medicine, and oral pathology*, 20, 340–349.

43. Kanter, V., Weldon, E., Nair, U., Varella, C., Kanter, K., Anusavice, K., & Pileggi, R. (2011). A quantitative and qualitative analysis of ultrasonic versus sonic endodontic systems on canal cleanliness and obturation. *Oral Surgery Oral Medicine Oral Pathology Oral Radiology and Endodontology*, *112*(6), 809–813.
44. Kleier, D. J., Averbach, R. E., & Mehdipour, O. (2008). The sodium hypochlorite accident: experience of diplomates of the American Board of Endodontics. *Journal of endodontics*, *34*(11), 1346–1350.
45. Marshall, F., & Rosen, S. (1970). The bactericidal efficiency of sodium hypochlorite as an endodontic irrigant. *Oral surgery*. *29*(4), 613-619.
46. Metzger, Z., Zary, R., Cohen, R., Teperovich, E., & Paqué, F. (2010). The quality of root canal preparation and root canal obturation in canals treated with rotary versus self-adjusting files: a three-dimensional micro-computed tomographic study. *Journal of endodontics*, *36*(9), 1569–1573.
47. Miller, T. A., & Baumgartner, J. C. (2010). Comparison of the antimicrobial efficacy of irrigation using the EndoVac to endodontic needle delivery. *Journal of endodontics*, *36*(3), 509–511.
48. Mitchell, R. P., Baumgartner, J. C., & Sedgley, C. M. (2011). Apical extrusion of sodium hypochlorite using different root canal irrigation systems. *Journal of endodontics*, *37*(12), 1677–1681.
49. Mitchell, R. P., Yang, S.-E., & Baumgartner, J. C. (2010). Comparison of apical extrusion of NaOCl using the EndoVac or needle irrigation of root canals. *Journal of endodontics*, *36*(2), 338–341.

50. Naenni, N., Thoma, K., & Zehnder, M. (2004). Soft Tissue Dissolution Capacity of Currently Used and Potential Endodontic Irrigants. *Journal of endodontics*, 30(11), 785–787.
51. Nair, P., Cano, V., & Vera, J. (2005). Microbial status of apical root canal system of human mandibular first molars with primary apical periodontitis after. *Oral surgery*. 99 (2), 231-252.
52. Nguy, D., & Sedgley, C. (2006). The influence of canal curvature on the mechanical efficacy of root canal irrigation in vitro using real-time imaging of bioluminescent bacteria. *Journal of endodontics*, 32(11), 1077–1080.
53. Nielsen, B. A., & Craig Baumgartner, J. (2007). Comparison of the EndoVac system to needle irrigation of root canals. *Journal of endodontics*, 33(5), 611–615.
54. Paqué, F., Balmer, M., Attin, T., & Peters, O. A. (2010). Preparation of oval-shaped root canals in mandibular molars using nickel-titanium rotary instruments: a micro-computed tomography study. *Journal of endodontics*, 36(4), 703–707.
55. Paragliola, R., Franco, V., Fabiani, C., Mazzone, A., Nato, F., Tay, F. R., Breschi, L., et al. (2010). Final rinse optimization: influence of different agitation protocols. *Journal of endodontics*, 36(2), 282–285.
56. Peters, O. A., Bardsley, S., Fong, J., Pandher, G., & Divito, E. (2011). Disinfection of root canals with photon-initiated photoacoustic streaming. *Journal of endodontics*, 37(7), 1008–1012.

57. Peters, O. A., Boessler, C., & Paqué, F. (2010). Root canal preparation with a novel nickel-titanium instrument evaluated with micro-computed tomography: canal surface preparation over time. *Journal of endodontics*, *36*(6), 1068–1072.
58. Peters, O., & Barbakow, F. (2000). Effects of Irrigation on Debris and Smear Layer on Canal Walls Prepared by Two Rotary Techniques: A Scanning Electron Microscopic Study. *Journal of endodontics*, *26*(1), 6–10.
59. Hulsmann, M., Peters, O., & Dummer, P. (2005). Mechanical preparation of root canals: shaping goals, techniques and means. *Endodontic topics*, *10*(1), 30-76.
60. Ram, Z. (1977). Effectiveness of root canal irrigation. *Oral surgery, oral medicine, and oral pathology*, *44*(2), 306–312.
61. Reynolds, M. A., Madison, S., Walton, R. E., Krell, K. V., & Rittman, B. R. (1987). An in vitro histological comparison of the step-back, sonic, and ultrasonic instrumentation techniques in small, curved root canals. *Journal of endodontics*, *13*(7), 307–314.
62. Rôças, I. N., & Siqueira, J. F. (2011). Comparison of the in vivo antimicrobial effectiveness of sodium hypochlorite and chlorhexidine used as root canal irrigants: a molecular microbiology study. *Journal of endodontics*, *37*(2), 143–150.
63. Salzgeber, R. M., & Brilliant, J. D. (1977). An in vivo evaluation of the penetration of an irrigating solution in root canals. *Journal of endodontics*, *3*(10), 394–398.
64. Schoeffel, G. J. (2007). The EndoVac method of endodontic irrigation: safety first. *Dentistry today*, *26*(10), 92, 94, 96 passim.
65. Sedgley, C. (2004). Root canal irrigation--a historical perspective. *Journal of the history of dentistry*, *52*(2), 61–65.

66. Sedgley, C. M., Nagel, A. C., Hall, D., & Applegate, B. (2005). Influence of irrigant needle depth in removing bioluminescent bacteria inoculated into instrumented root canals using real-time imaging in vitro. *International endodontic journal*, *38*(2), 97–104.
67. Senia, E. S., Marshall, F. J., & Rosen, S. (1971). The solvent action of sodium hypochlorite on pulp tissue of extracted teeth. *Oral surgery, oral medicine, and oral pathology*, *31*(1), 96–103.
68. Shen, Y., Gao, Y., Qian, W., Ruse, N. D., Zhou, X., Wu, H., & Haapasalo, M. (2010). Three-dimensional numeric simulation of root canal irrigant flow with different irrigation needles. *Journal of endodontics*, *36*(5), 884–889.
69. Shen, Y., Stojicic, S., & Haapasalo, M. (2011). Antimicrobial efficacy of chlorhexidine against bacteria in biofilms at different stages of development. *Journal of endodontics*, *37*(5), 657–661.
70. Shin, S.-J., Kim, H.-K., Jung, I.-Y., Lee, C.-Y., Lee, S.-J., & Kim, E. (2010). Comparison of the cleaning efficacy of a new apical negative pressure irrigating system with conventional irrigation needles in the root canals. *Oral surgery, oral medicine, oral pathology, oral radiology, and endodontics*, *109*(3), 479–484.
71. Shuping, G. B., Ørstavik, D., Sigurdsson, A., & Trope, M. (2000). Reduction of intracanal bacteria using nickel-titanium rotary instrumentation and various medications. *Journal of endodontics*, *26*(12), 751–755.
72. Sinanan, S.K., Marshall, F.J., Quinton-Cox, R. (1983). The effectiveness of irrigation in endodontics. *Journal of the Canadian Dental Association*, *49*(11), 771-776.

73. Siqueira, J. F., & Rôças, I. N. (2008). Clinical implications and microbiology of bacterial persistence after treatment procedures. *Journal of endodontics*, 34(11), 1291–1301.e3.
74. Sirén, E. K., Haapasalo, M. P. P., Waltimo, T. M. T., & Ørstavik, D. (2004). In vitro antibacterial effect of calcium hydroxide combined with chlorhexidine or iodine potassium iodide on *Enterococcus faecalis*. *European journal of oral sciences*, 112(4), 326–331.
75. Siu, C., & Baumgartner, J. C. (2010). Comparison of the debridement efficacy of the EndoVac irrigation system and conventional needle root canal irrigation in vivo. *Journal of endodontics*, 36(11), 1782–1785.
76. Sjögren, U., Figdor, D., Persson, S., & Sundqvist, G. (1997). Influence of infection at the time of root filling on the outcome of endodontic treatment of teeth with apical periodontitis. *International endodontic journal*, 30(5), 297–306.
77. Stamos, D. E., Sadeghi, E. M., Haasch, G. C., & Gerstein, H. (1987). An in vitro comparison study to quantitate the debridement ability of hand, sonic, and ultrasonic instrumentation. *Journal of endodontics*, 13(9), 434–440.
78. Stojicic, S., Shen, Y., & Qian, W. (2011). Antibacterial and smear layer removal ability of a novel irrigant, QMiX. *International endodontic journal*, 45(4), 363-371.
79. Stojicic, S., Zivkovic, S., Qian, W., Zhang, H., & Haapasalo, M. (2010). Tissue dissolution by sodium hypochlorite: effect of concentration, temperature, agitation, and surfactant. *Journal of endodontics*, 36(9), 1558–1562.

80. Susin, L., Liu, Y., Yoon, J. C., Parente, J. M., Loushine, R. J., Ricucci, D., Bryan, T., et al. (2010). Canal and isthmus debridement efficacies of two irrigant agitation techniques in a closed system. *International endodontic journal*, 43(12), 1077–1090.
81. Svec, T. A., & Harrison, J. W. (1977). Chemomechanical removal of pulpal and dentinal debris with sodium hypochlorite and hydrogen peroxide vs normal saline solution. *Journal of endodontics*, 3(2), 49–53.
82. Tardivo, D., Pommel, L., La Scola, B., About, I., & Camps, J. (2010). Antibacterial efficiency of passive ultrasonic versus sonic irrigation. Ultrasonic root canal irrigation. *Odonto-stomatologie tropicale = Tropical dental journal*, 33(129), 29–35.
83. Tay, F. R., Gu, L.-S., Schoeffel, G. J., Wimmer, C., Susin, L., Zhang, K., Arun, S. N., et al. (2010). Effect of vapor lock on root canal debridement by using a side-vented needle for positive-pressure irrigant delivery. *Journal of endodontics*, 36(4), 745–750.
84. Teplitsky, P., Chenail, B., & Mack, B. (1987). Endodontic irrigation—a comparison of endosonic and syringe delivery systems. *International endodontic journal*, 20(5), 233-241.
85. Trepagnier, C. M., Madden, R. M., & Lazzari, E. P. (1977). Quantitative study of sodium hypochlorite as an in vitro endodontic irrigant. *Journal of endodontics*, 3(5), 194–196.
86. Usman, N., Baumgartner, J. C., & Marshall, J. G. (2004). Influence of instrument size on root canal debridement. *Journal of endodontics*, 30(2), 110–112.
87. Vertucci, F. (1984). Root canal anatomy of the human permanent teeth. *Oral surgery, oral medicine, oral pathology*. 58(5), 589-599.

88. Walia, H., & Brantley, W. (1988). An initial investigation of the bending and torsional properties of Nitinol root canal files. *Journal of endodontics*, 14(7), 346-351.
89. Wesselink, P. (2001). A primary observation on the preparation and obturation of oval canals. *International endodontic journal*, 34(2), 137-141.
90. Witton, R., Henthorn, K., Ethunandan, M., Harmer, S., & Brennan, P. A. (2005). Neurological complications following extrusion of sodium hypochlorite solution during root canal treatment. *International endodontic journal*, 38(11), 843–848.
91. Zaugg-Vesti, B., Dorffler-Melly, J., Spiegel, M., Wen, S., Franzeck, U.K., Bollinger, A. (1993). Lymphatic capillary pressure in patients with primary lymphedema. *Microvascular research*, 46(2), 128-134.
92. Zehnder, M. (2006). Root canal irrigants. *Journal of endodontics*, 32(5), 389–398.